

**Development of Alternative Protocols for Antimicrobial Efficacy
Testing of Antimicrobial Surfaces**

by

Joseph Nwaiwu

A thesis

presented to the University of Waterloo

in fulfillment of the

thesis requirement for the degree of

Master of Applied Science

in

Chemical Engineering

Waterloo, Ontario, Canada, 2020

© Joseph Nwaiwu 2020

AUTHOR'S DECLARATION

I hereby declare that I am the sole author of this thesis. This is a true copy of the thesis, including any required final revisions, as accepted by my examiners.

I understand that my thesis may be made electronically available to the public.

Abstract

Self-disinfecting surfaces have been studied for a long time for use in reducing the occurrence of infections. Several industries are focused on manufacturing antimicrobial products with high toxicity to microbes for contact killing. However, when these products are manufactured, they need to be tested to determine their antimicrobial efficacy before they can be sold for public use. This study focuses on developing fast and accurate protocols to determine the antimicrobial efficacy of antimicrobial products and can be useful for irregular or larger surfaces where some regulatory protocols based on small coupons cannot be applied.

Three different protocols were developed and their results for testing antimicrobial products using industrially manufactured samples against *E. coli* and *P. aeruginosa* were compared to results obtained from a coupon-based method which is similar to the EPA protocol. Protocol 1 (modified EPA protocol) was used as the control, for comparison with other protocols and this protocol involved applying bacteria solution on a test surface coupon for 1-hour contact time, the test surface was then placed in a beaker containing phosphate buffered saline (20 μ l), sonicated for 5 minutes, then bacteria solution was plated on agar plates and incubated. Protocol 2 involved applying bacteria solution on a test surface for 1 hour, then the bacteria solution was retrieved using a pipette, dilutions were made, plated and incubated. Protocol 3 involved applying bacteria onto the test surface, then the test surface was inverted onto an agar plate surface, left for 1-hour contact time, then surface was removed, and plate incubated. Protocol 4 involved applying bacteria onto test surface and left in contact for 1 hour, then stamped onto an

agar surface for 30 seconds, removed and incubated. The results from comparing the log reductions and killing percentages from these protocols show that protocol 4 show the best comparison for both microorganisms, compared to results from protocol 1 and possesses less coefficient of variation calculations in all cases. Protocol 2 shows good comparison with results from the Protocol 1 however, there is higher coefficient of variation while protocol 3 did not correlate with results from the Protocol 1 when bacteria is applied on a pure copper surface.

Plate counting techniques are the widely used for enumeration of live bacteria. It involves plating microorganisms on an agar plate, incubation for 24 – 48 hours then counting of colonies formed. Obtaining results using this technique takes time and can be inaccurate sometimes depending on the concentration of plated microorganism. An accurate flow cytometry FCM technique was developed to determine the antimicrobial efficacy of test samples. Microbial solution (*E. coli*, *P. aeruginosa* and *Saccharomyces cerevisiae*) stained with calcein am dye was analysed with a flow cytometer. FCM results showed correlation with plate count results when the microbial solution was diluted to 10^4 CFU/ml without application on a copper surface but failed to correlate with plate count results when bacterial solution was exposed to copper, due to the interaction between calcein AM and copper. So, another technique involving staining 10^6 CFU/ml yeast solution with propidium iodide after exposure to copper surface and comparing with plate count results was studied. This technique was used to accurately predict the log reduction of yeast applied on some industrially manufactured antimicrobial samples with a maximum underestimation and overestimation range of -0.33 and 0.48.

Acknowledgments

Firstly, I would like to specially thank my supervisor, Prof. William A. Anderson, for his guidance and constant support throughout my graduate career. His constructive comments and suggestions were invaluable and encouraged me to conduct this research and finalize the thesis, from which I have acquired a great deal of knowledge.

Furthermore, I would like to thank my Co-supervisor Prof. Boxin Zhao for all his assistance and Dr. Shazia Tanvir, for her training, help and encouragement that led to this work. I also want to extend my appreciation to Professor Brian Ingalls and his research team for providing me with all the necessary assistance that I needed.

Special thanks go to the Ontario Centers of Excellence, the Natural Science and Engineering Research Council of Canada and Mitacs Accelerate. Sincere thanks for the support of Aereus Inc.

Finally, a whole-hearted appreciation to my parents for their love and continuous support.

Table of Contents

Author's Declaration	-----	ii
Abstract	-----	iii
Acknowledgements	-----	v
List of Figures	-----	xi
List of Tables	-----	xiv
List of Abbreviations	-----	xvi
Chapter 1 Introduction	-----	1
1.1 Motivation	-----	1
1.2 Research Objectives	-----	3
Chapter 2 Literature review	-----	4
2.1 Copper Chemistry	-----	4
2.1.1 Oxidation	-----	4
2.1.2 Copper Ions	-----	5
2.2 Contact Killing mechanism of Copper	-----	7
2.3 CuNPs Synthesis and Size Effects on Antimicrobial Property	-----	10
2.3.1 Copper Alloys	-----	12
2.4 Testing Protocols for Antimicrobial Surfaces	-----	15

2.4.1 EPA Protocol	17
2.4.2 Agar disk-diffusion method	18
2.4.3 TLC Bioautographic method Direct Variant	19
2.4.4 Agar Dilution Method	19
2.4.5 Broth Dilution Method	20
2.4.6 ATP bioluminescence assay	21
2.5 Flow cytometry	22
2.5.1 General Principles of a Flow Cytometer	23
2.5.2 Fluorochromes used in Flow Cytometry	25
2.5.3 Flow Cytometry Data Analysis	28
2.6 Summary	30
Chapter 3 Standardization of Antimicrobial solid surface testing Protocols	32
3.1 Overview	32
3.2 Introduction	33
3.3 Materials and Sample Preparation	35
3.3.1 Reagents and Materials	35
3.3.2 Sample Preparation	36
3.3.3 Bacteria Strains	36

3.4 Protocols Investigated	-----	36
3.4.1 EPA Protocol	-----	37
3.4.2 Protocol 2	-----	38
3.4.3 Stamping Protocol	-----	39
3.4.4 Antimicrobial Powder Particles	-----	40
3.4.5 Log Reduction and Percentage of Killing	-----	40
3.4.6 Coefficient of Variation	-----	41
3.5 Results and Discussion	-----	41
3.5.1 Characterization of Antimicrobial Samples	-----	42
3.5.2 EPA Protocol – Protocol 1	-----	43
3.5.3 Protocol 2	-----	45
3.5.4 Stamping Protocols	-----	46
3.5.4.1 “Straight stamping”- Protocol 3	-----	46
3.5.4.2 “1-hour contact”- Protocol 4	-----	48
3.5.5 Comparison Between different Protocols	-----	49
3.5.5.1 Comparison between EPA protocol results and Protocol 2 results	-----	49
3.5.5.2 Comparison between EPA protocol results and Protocol 3 results	-----	52

3.5.5.3	Comparison between EPA protocol results and Protocol 4 results	55
3.5.6	Antimicrobial Powder Particles	57
3.6	Summary and Conclusions	59
Chapter 4 Development of rapid test method for antimicrobial surfaces with flow cytometry		
		61
4.1	Overview	61
4.2	Introduction	62
4.3	Materials and Methods	64
4.3.1	Reagents and Materials	64
4.3.2	Sample Preparation	65
4.3.3	Microorganism Investigated	65
4.4	Standardization of protocol using Calcein AM dye	66
4.4.1	Experimental Procedure	66
4.5	Results and Discussion	67
4.5.1	<i>Escherichia coli</i>	67
4.5.2	<i>Pseudomonas aeruginosa</i>	70
4.5.3	<i>Saccharomyces cerevisiae</i>	72
4.5.4	Calibration Curve of FCM and Plate Count results after exposure to pure copper surface	74

4.6 Standardization of protocol using Propidium iodide	78
4.6.1 Experimental Procedure	78
4.6.2 Predicting Log Reduction of Yeast on Industrial Antimicrobial samples using FCM	81
4.7 Summary and Conclusions	83
Chapter 5 Conclusions and Recommendations	85
5.1 Conclusions	85
5.2 Recommendations for Future Work	86
References	88
Appendix	109

List of Figures

Figure 2.0: Hydrodynamic focusing	P23
Figure 2.1: Schematic of a flow cytometer	P25
Figure 2.2: Spectral profiles. Light absorbance and light emission of fluorescein isothiocyanate (FITC)	P26
Figure 3.0: Killing percentage of <i>E. coli</i> pure copper, nickel and zinc surfaces	P41
Figure 3.1: (a) SEM image of sample A at a 200µm scale bar (b) EDS spectrum for sample A	P42
Figure 3.2: (a) SEM image of sample B at a 200µm scale bar (b) EDS spectrum for sample B	P43
Figure 3.3: Killing percentage of <i>E. coli</i> calculated on samples using EPA protocol	P44
Figure 3.4: Killing percentage of <i>P. aeruginosa</i> calculated on samples using EPA protocol	P44
Figure 3.5: Killing percentage of <i>E. coli</i> calculated on samples using Protocol 2	P45
Figure 3.6: Killing percentage of <i>P. aeruginosa</i> calculated on samples using Protocol 2	P46
Figure 3.7: Killing percentage of <i>E. coli</i> calculated on samples using Protocol 3	P47
Figure 3.8: Killing percentage of <i>P. aeruginosa</i> calculated on samples using Protocol 3	P47
Figure 3.9: Killing percentage of <i>E. coli</i> calculated on samples using Protocol 4	P48
Figure 3.10: Killing percentage of <i>P. aeruginosa</i> calculated on samples using Protocol 3	P49
Figure 3.11: Comparison of killing percentage of <i>E. coli</i> between EPA protocol and Protocol 2	P50
Figure 3.12: Comparison of killing percentage of <i>P. aeruginosa</i> between EPA protocol and Protocol 2	P50
Figure 3.13: Comparison of killing percentage of <i>E. coli</i> between EPA protocol and Protocol 3	P52
Figure 3.14: Comparison of killing percentage of <i>P. aeruginosa</i> between EPA protocol and Protocol 3	P53
Figure 3.15: Comparison of killing percentage of <i>E. coli</i> between EPA protocol and Protocol 4	P55

Figure 3.16: Comparison of killing percentage of <i>P. aeruginosa</i> between EPA protocol and Protocol 4	P55
Figure 3.17: Qualitative results of Antimicrobial powder particles efficacy against <i>E. coli</i>	P57
Figure 3.18: (a) Antimicrobial efficacy of Aereus shield powder at a loading of 0.13mg/cm ² (b) Antimicrobial efficacy of Aereus shield powder at a loading of 0.25mg/cm ² (c) Antimicrobial efficacy of Aereus shield powder at a loading of 0.38mg/cm ² (d) Antimicrobial efficacy of Aereus shield powder at a loading of 0.45mg/cm ²	P58
Figure 3.19: Antifungal efficacy of Aereus shield powder applied at different concentrations	P59
Figure 4.0: Correlation between PC results and FCM results for <i>E. coli</i>	P69
Figure 4.1: Correlation between PC results and FCM results for <i>P. aeruginosa</i>	P72
Figure 4.2: Correlation between PC results and FCM results for yeast	P74
Figure 4.3: Comparison between PC and FCM results for <i>E. coli</i> on copper surface	P76
Figure 4.4: Calibration curve for FCM and plate count results	P80
Figure 4.26: Comparison between PC and FCM results	P83
Figure 6.0: FCM results of Log 6 <i>E. coli</i> stained with calcein AM	P112
Figure 6.1: FCM results of Log 5 <i>E. coli</i> stained with calcein AM	P113
Figure 6.2: FCM results of Log 4 <i>E. coli</i> stained with calcein AM	P114
Figure 6.3: FCM results of Log 3 <i>E. coli</i> stained with calcein AM	P115
Figure 6.4: FCM results of Log 6 <i>P. aeruginosa</i> stained with calcein AM	P116
Figure 6.5: FCM results of Log 5 <i>P. aeruginosa</i> stained with calcein AM	P116
Figure 6.6: FCM results of Log 4 <i>P. aeruginosa</i> stained with calcein AM	P117
Figure 6.7: FCM results of Log 3 <i>P. aeruginosa</i> stained with calcein AM	P118
Figure 6.8: FCM results of Log 6 yeast stained with calcein AM	P119
Figure 6.9: FCM results of Log 5 yeast stained with calcein AM	P120
Figure 6.10: FCM results of Log 4 yeast stained with calcein AM	P120
Figure 6.11: FCM results of Log 3 yeast stained with calcein AM	P121

Figure 6.12: (a) FCM results of Log 4 *E. coli* applied on plastic control and stained with calcein AM

(b) FCM results of Log 4 *E. coli* applied on copper surface and stained with calcein AM
P122

Figure 6.13: Intensity plot of Log 4 *E. coli* applied on copper surface for 5 minutes and stained with Calcein AM
P122

Figure 6.14: Intensity plot of Log 4 *E. coli* applied on copper surface for 120 minutes and stained with Calcein AM
P123

Figure 6.15: FCM results of yeast on Cu surface after 10 minutes, stained with propidium iodide
P123

Figure 6.16: FCM results of yeast on Cu surface after 30 minutes, stained with propidium iodide
P124

Figure 6.17: FCM results of yeast on Cu surface after 60 minutes, stained with propidium iodide
P125

Figure 6.18: FCM results of yeast on Cu surface after 120 minutes, stained with propidium iodide
P125

Figure 6.19: FCM results of yeast on Control after (a=120 minutes, b= 10 minutes, c= 30 minutes d= 60minutes) stained with propidium iodide
P126

Figure 6.20: FCM results of yeast applied on surfaces for 2 hours then stained with propidium iodide (a=control, b= A1-sample, c= B1-sample d= F1-sample, e= G1-sample, f= X-sample, g= Z-sample)
P127

List of Tables

Table 2.0: Composition of some common Copper Alloys	P13
Table 2.1: Fluorochromes commonly used in flow cytometry and emission spectrum	P27
Table 3.0: Summary of antimicrobial efficacy results for <i>E. coli</i> between EPA protocol and protocol 2	P51
Table 3.1: Summary of antimicrobial efficacy results for <i>P. aeruginosa</i> between EPA protocol and protocol 2	P52
Table 3.2: Summary of antimicrobial efficacy results for <i>E. coli</i> between EPA protocol and protocol 3	P54
Table 3.3: Summary of antimicrobial efficacy results for <i>P. aeruginosa</i> between EPA protocol and protocol 3	P54
Table 3.4: Summary of antimicrobial efficacy results for <i>E. coli</i> between EPA protocol and protocol 4	P56
Table 3.5: Summary of antimicrobial efficacy results for <i>P. aeruginosa</i> between EPA protocol and protocol 4	P56
Table 4.0: FCM results of Log 6 <i>E. coli</i> stained with calcein AM	P68
Table 4.1: FCM results of Log 5 <i>E. coli</i> stained with calcein AM	P68
Table 4.2: FCM results of Log 4 <i>E. coli</i> stained with calcein AM	P69
Table 4.3: FCM results of Log 3 <i>E. coli</i> stained with calcein AM	P69
Table 4.4: FCM results of Log 6 <i>P. aeruginosa</i> stained with calcein AM	P70
Table 4.5: FCM results of Log 5 <i>P. aeruginosa</i> stained with calcein AM	P71
Table 4.6: FCM results of Log 4 <i>P. aeruginosa</i> stained with calcein AM	P71
Table 4.7: FCM results of Log 3 <i>P. aeruginosa</i> stained with calcein AM	P71
Table 4.8: FCM results of Log 6 yeast stained with calcein AM	P73
Table 4.9: FCM results of Log 5 yeast stained with calcein AM	P73
Table 4.10: FCM results of Log 4 yeast stained with calcein AM	P73
Table 4.11: FCM results of Log 5 yeast stained with calcein AM	P73
Table 4.12: FCM data for <i>E. coli</i> applied on plastic control and copper surface, stained with calcein AM	

Table 4.13: Comparison between PC and FCM results for <i>E. coli</i> on antimicrobial surface	P75
Table 4.14: <i>E. coli</i> applied on copper surface for 5 and 120 minutes, stained with Calcein AM	P75
Table 4.15: FCM results of yeast on Control after contact time, stained with propidium iodide	P77
Table 4.16: FCM results of yeast on Cu surface after contact time, stained with propidium iodide	P79
Table 4.17: Comparison between PC results and FCM gate percentages for yeast	P80
Table 4.18: FCM results of yeast applied on surfaces for 2 hours then stained with propidium iodide	P81
Table 4.19: Comparison between PC and FCM log reduction for yeast	P82
Table 6.0: Antimicrobial efficacy of samples against <i>E. coli</i> using EPA protocol	P110
Table 6.1: Antimicrobial efficacy of samples on <i>Pseudomonas aeruginosa</i> using EPA protocol	P110
Table 6.2: Antimicrobial efficacy of samples on <i>E. coli</i> using Protocol 2	P110
Table 6.3: Antimicrobial efficacy of samples on <i>Pseudomonas aeruginosa</i> using Protocol 2	P110
Table 6.4: Antimicrobial efficacy of samples on <i>E. coli</i> using Protocol 3	P111
Table 6.5: Antimicrobial efficacy of samples on <i>Pseudomonas aeruginosa</i> using Protocol 3	P111
Table 6.6: Antimicrobial efficacy of samples on <i>E. coli</i> using Protocol 4	P111
Table 6.7: Antimicrobial efficacy of samples on <i>Pseudomonas aeruginosa</i> using Protocol 4	P111
Table 6.8: Comparison between Plate count and Flow cytometry results of <i>E. coli</i> stained with calcein AM	P115
Table 6.9: Comparison between Plate count and Flow cytometry results of <i>P. aeruginosa</i> stained with calcein AM	P118
Table 6.10: Comparison between Plate count and Flow cytometry results of yeast stained with calcein AM	P122

List of Abbreviations

HAIs	Hospital-acquired infections
CDC	Centers for Disease Control
EPA	Environmental protection agency
CuNPs	Copper nanoparticles
FCM	Flow cytometry
FSC	Forward scatter channel
SSC	Side scatter channel
LR	Log Reduction
PK	Percentage of Killing
PI	Propidium Iodide
PC	Plate count
CFU	Colony forming units
PBS	Phosphate buffered saline
MIC	Minimum inhibitory concentration
DI water	Deionized water
SEM	Scanning electron microscope
Cu	Copper
Zn	Zinc
Ni	Nickel

CHAPTER 1

Introduction

1.1 Motivation

Hospital-acquired infections (HAIs) have caused a heavy toll worldwide (Monk et al., 2014). In Canada alone, over 200,000 patients are infected when receiving healthcare (Health Canada and Public Health Agency of Canada, 2018). In the United States over 2 million patients annually contract an infection with HAI being one of the leading causes of deaths behind cancer and stroke (Klevens et al., 2007) (Monk et al., 2014). The Centers for Disease Control (CDC) reported that in 1995 there were 1.9 million HAIs in hospitals in the United States and an estimated 1.7 million HAIs were contracted in 2002 (Klevens et al., 2007). More than 177,000 HAIs occur in Australia each year (Monk et al., 2014). The World Health Organization defines HAIs as "infections occurring in a patient during the treatment process in a hospital or other healthcare facility that were not present or incubated at the time of admission" (Health Canada and Public Health Agency of Canada, 2018) (World Health Organization. (2017). The prevalent microbial species that cause HAI include *Staphylococcus aureus*, *Pseudomonas aeruginosa* and *Enterobacter* species, according to the United States Center for Disease Control (Hidron, 2008) (Monk et al., 2014).

Nevertheless, HAIs are preventable. HAIs should be minimized as they present a significant threat to patient health (Centers for Disease Control and Prevention, 2018). If infection prevention and control methods were pursued, about 70 per cent of all forms of HAIs could be avoided (Health Canada and Public Health Agency of Canada, 2018). To

minimize HAI rates, several action initiatives have been put in place. Some of which includes, enhancing regional monitoring, use of active antibiotic prevention programmes, preparing health staff for better hygiene, separating sick patients, use of disposable devices, washing and disinfecting external surfaces (Monk et al., 2014). Nonetheless, reports show that only 25-50 percent of all hospital surfaces are regularly washed and increased surface maintenance procedures in health care facilities are difficult to manage (Sifri et al., 2016) (Carling et al, 2008) (Carling et al, 2010) (Hess et al, 2018). However, besides from hospital surfaces, there is a need for antimicrobial surfaces in other applications like consumer appliances or in food processing to minimize growth of microbes and infections.

Several gram-negative bacteria such as *Escherichia coli*, *Pseudomonas aeruginosa* and gram-positive bacteria, like *Staphylococcus aureus* can survive for months on inanimate surfaces (Kramer et al., 2006). Self-disinfecting surfaces have been suggested as a way of reducing new infections and reducing the occurrence of HAIs. Copper has a high antimicrobial activity and is attracting growing exposure to possible applications in the healthcare environment (Sifri et al., 2016) (O’Gorman and Humphreys, 2012) (Humphreys, 2014). Composites impregnated with copper oxide have been developed which can be deposited onto hard surface countertops and even woven into fabrics (Sifri et al., 2016) (Lazary et al., 2014). It has been reported that copper oxide-containing surfaces kill more than 99.9 percent of a broad selection of bacteria within two hours of exposure and continue to do so even after repeated contamination (Monk et al., 2014). When composites coated with copper are manufactured, a testing protocol by the United States Environmental Protection Agency (herein simply referred to as the EPA) is

recommended before approval is granted for the registration of surface products with antimicrobial claims (Sifri et al., 2016). However, there are some limitations of the EPA protocol. Experiments conducted following the EPA protocol takes several days and this does not allow for rapid analysis of test surfaces. Also, the scope of the EPA protocol is defined for bacterial species but does not include other microbial species like fungi. Finally, the EPA protocol is specific to copper and copper alloy technologies for hard non-porous surfaces with sample dimensions of 2.5 x 2.5 cm square, and yet there are porous materials that are of interest and not all materials can be formed in the specified sample dimensions.

1.2 Research Hypothesis and Objectives

The driving hypothesis is that a more generic method can be developed to assess the anti-microbial properties of a material that is not limited to non-porous copper or copper-alloy materials having specific dimensions, using flow cytometry.

To attack this hypothesis, two objectives were set. The first objective sought to develop a rapid protocol (faster than the EPA protocol) that could accommodate dimensions that were different than those stated in the EPA protocol. The second objective aimed to specifically quantify anti-fungal properties of materials using flow cytometry.

Chapter 2

Literature Review

2.1 Copper Chemistry on Surfaces

2.1.1 Oxidation

Copper (II) oxide (CuO) and/or copper (I) oxide (Cu₂O) are formed on the surface of pure copper, depending on factors like time and temperature for atmospheric oxidation (Walkowicz et al. 2018) (Horton et al. 2015) (Payer, 1990). Oxidation of copper begins with a Cu₂O layer being formed. It has been reported that with sustained and frequent contact with sweat from the human palm, a Cu₂O film with a thickness of approximately 50–230 nm developed on copper surfaces (Fredj et al. 2013) (Walkowicz et al. 2018). At temperatures above 200°C, the Cu₂O layer reacts with oxygen, creating a CuO layer (Hans et al., 2013) (Rönquist and Fischmeister 1960) (Cocke et al., 1995). For CuO to form at room temperature, moisture is required as reported by Platzman et al., who observed the formation of a 2-5nm CuO layer after 112 days at about ~60% relative humidity. In ambient conditions (room temperature and about ~60% relative humidity), metastable Cu(OH)₂ was observed as an intermediate step of CuO formation on Cu₂O (Platzman et al., 2008) (Hans et al. 2013).

Copper existing in different forms (Cu, CuO and Cu₂O) has been found to have antimicrobial properties, meaning that it possesses the ability to inhibit the growth of microbes (bacteriostatic) and at high concentrations, kill microbes (bactericidal) so that they cannot grow under any conditions (Wiegand et al., 2008). Hans et al. suggested that

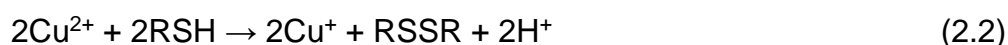
oxidation of dry pure metallic copper surfaces exposed at ambient temperatures does not affect its antimicrobial properties. Under conditions where bacteria suspension in buffer solution is applied on a dry pure copper coupon, CuO was formed on the copper surface and it significantly inhibited killing.

2.1.2 Copper Ions

Copper is a transition metal with two stable and nine radioactive isotopes. It occurs mainly as one of two stable oxidation states: the oxidized cupric form, Cu^{2+} and the reduced cuprous form, Cu^+ . Cu^+ is a closed shell 3D^{10} transition metal ion that is diamagnetic (Chaturvedi and Henderson, 2014) (Frausto da Silva and Williams, 1993). Cu^{2+} is paramagnetic with a 3D^9 structure and is considered an intermediate Lewis acid. Cu^{2+} forms square planar complexes with sulphates, nitrates, nitrogen donors such as histidine, and oxygen donors such as glutamate and aspartate in addition to ligands bound by Cu^+ (Bertini et al., 2007) (Chaturvedi and Henderson, 2014). It has been explained that Cu^+ can form insoluble cuprite (Cu_2O), even under anaerobic conditions (Matocha et al. 2005), which is toxic to bacteria. When cells are exposed to metallic iron supplemented with Cu^{2+} , iron solubilization and copper reduction to Cu^+ occurs, which causes rapid bacteria killing. Matthews et al., determined the presence of Cu^+ ions in contact killing experiments of bacteria on iron. They found that in the presence of CuSO_4 , significant generation of Cu^+ ions was observed within the shortest measurable times when cells were exposed to metallic iron (Mathews et al., 2015).

Oxidative damage of biological structures involving reduced, transition metal cations is well known. The widely recognized damage mechanism includes Fenton

reactions, in which the reduced cations react with an oxidant to create radical hydroxyl, OH•, the agent commonly believed to cause the greatest damage to nucleic acids, proteins, and lipids (Dunning et al., 1998). Copper may propagate toxic hydroxyl radical formation by Fenton-like chemistry in environments like the phagosome, which is rich in hydrogen peroxide and superoxide (Liochev, 1999), as illustrated in equations 2.1 and 2.2.



Hydroxyl radicals are very reactive and cannot be scavenged by enzymatic reactions. They show a diffusion-controlled half-life of 10^{-9} s prior to *in vivo* reactions with organic molecules (Freinbichler et al. 2011), suggesting that the radical hydroxyl damage would be in proximity to the copper ions (Chaturvedi and Henderson, 2014).

The exact mechanism in microorganisms has been reported to be organism dependent if not disputed. The two most convincing studies have involved either phagocytes or *Escherichia coli*. One should note that the overall structure of these two organisms/cell types is significantly different, thus the mechanisms may indeed be expected to be different.

Solioz reviewed the redox state of copper in phagosomes and mycobacterial infections during infection, noting that the first line of defence against a microbial infection is phagocytic immune cells in the phagosome where copper and iron also accumulates after infection by mycobacteria. It has been reported that copper transferred to the phagosomes is in the reduced Cu^+ form, which is more toxic to bacteria than Cu^{2+} (Abicht

et al. 2013). Due to spontaneous oxidation in the phagosome, significant Cu^{2+} can generate and in principle, this Cu^{2+} could be re-reduced by non-enzymatic reduction of copper through menaquinones in the membranes of Mycobacteria, which restores the more toxic Cu^+ necessary to fight off infections (Solioz, 2016). Attempts to understand copper toxicity through classic copper-catalyzed Fenton chemistry by Macomber et al. have produced contrary results. Their findings suggest that circumstances might exist where copper propagates cytotoxic Fenton chemistry *in vivo*, but an alternative copper toxicity mechanism exists in *E. coli* (Macomber et al. ,2007) (Chaturvedi and Henderson, 2014).

Copper is found in the form of cupric ions, Cu^{2+} , in an oxidizing, extracellular environment. It was recognized more than 30 years ago that cultures of *Escherichia coli* reduced Cu^{2+} to Cu^+ due mostly to menaquinones and NADH dehydrogenase activity. The reduced Cu^+ was five to ten times more toxic than Cu^{2+} (Beswick et al., 1976). The Cu^+ produced in aerobic cultures was steadily re-oxidized to less toxic Cu^{2+} by oxygen, whereas the accumulating Cu^+ seriously affected anaerobic cultures (Abicht et al. 2013). Cu^+ has been reported to be considerably more toxic to bacteria than Cu^{2+} , presumably because it possesses greater membrane permeability than Cu^{2+} (Matocha et al. 2005) (Chaturvedi and Henderson JP. 2014). Dunning et al. reported lethal damage due to several factors ultimately leading to death of oral Streptococci that was caused by Cu^+ and Fe^{2+} , which included mechanisms that appeared to be oxygen independent, since it occurred in anaerobic conditions. They suggested that the addition of transition metal ions at a 10 mM level, could enhance the bactericidal effect since it favored the reduction of copper and iron to Cu^+ and Fe^{2+} (Dunning et al. 1998).

2.2 Contact Killing Mechanism of Copper

On metallic copper surfaces, microbes like bacteria and some fungi are quickly killed and the word "contact killing" has been coined for this mechanism, which destroys microbes causing reductions of up to 7 to 8 logs, and no live microorganisms have usually been retrieved from copper surfaces after extended incubation (Grass et al. 2011). It is however important to understand how copper works and the mechanism of killing microbes on contact. Laboratory studies have shown that bacteria on copper surfaces experience rapid damage to their membrane, DNA, and other cellular damage, with release of copper ions from the metal surface (Mathews et al. 2015). Living organisms require copper for some of their proteins, as electron donors/acceptors by alternating between redox states Cu (I) and Cu (II) (Karlin, 1993). But with excess copper present, this oxidation state cycling can lead to cell damage due to the generation of reactive hydroxyl radicals, which can be involved in reactions such as oxidizing proteins and lipids, to the detriment of cellular molecules (Yoshida et al. 1993). Another antimicrobial mechanism for copper is the displacement of iron from iron-sulfur clusters (Macomber and Imlay, 2009). Iron-sulfur clusters (Fe-S) are iron and inorganic sulphur cofactors, essentially needed for the functioning of proteins in a broad array of activities, such as electron transport in respiratory complexes, photosynthesis and DNA repair (Rouault, 2012). Macomber and Imlay reported that copper treatment rapidly inactivated isopropylmalate dehydrase, which is an iron-sulfur cluster enzyme, blocking biosynthesis in *E. coli* (Macomber and Imlay, 2009).

Santo et al. investigated the mode of action of dry metallic copper surfaces against *E. coli* and other bacterial model organisms. By applying *E. coli* cells suspended in buffer

solution, then plating on copper coupons, they reported a marked increase in copper ion concentrations over time in the buffer in which the cells were suspended, compared to concentrations in buffer alone. The structural integrity of copper-surface-exposed cells was also investigated, and after 1 minute of exposure of *E. coli* and *Bacillus cereus* cells on copper coupons, followed by observation using a microscope, cells had started to disintegrate, and cell debris was detected. Their results demonstrated that exposed cells accumulated copper ions and exhibited membrane and cell envelope damage, which was likely a result of copper targeting membrane proteins or the membrane lipids. However, they stated that contact killing did not involve lethal damage to the cellular DNA through mutations and lesions (Santo et al. 2011).

Another study by Santo et al. focused on the molecular mechanisms by which the Gram-positive *Staphylococcus haemolyticus* is inactivated by metallic Cu. Using Coppersensor-1 which is a membrane permeable dye, for *in vivo* staining with a live/dead staining technique and inductively coupled plasma mass spectroscopy (ICP-MS) for analyzing kinetics of uptake of Cu ion into cells from copper surfaces within 10 minutes, indicated that cells accumulated large amounts of Cu ions from metallic Cu surfaces contributing to lethal damage. Cells that were immediately removed from Cu surfaces had accumulated about 1×10^{10} Cu atoms. Their results demonstrated that death of *S. haemolyticus* after contact with Cu surfaces was due to membrane damage, not genotoxicity, because the organisms experienced significant membrane damage, but their genetic material remained intact (Santo et al. 2012).

Warnes et al investigated the mechanism of copper surface toxicity in *E. coli* O157:H7 and *Salmonella*. They observed immediate cytoplasmic membrane

depolarization, by assessing the electrical potential difference between the inside and outside of the cell using ionophore carbonylcyanide m-chlorophenylhydrazone (CCCP) and Rhodamine 123 (RH123). The cells on Cu surfaces were depolarized on contact, while there was no depolarization on cells that were applied on stainless steel for the duration of 10 minutes. Using the carboxylated, fluorinated derivative of fluorescein, H2DFFDA (5-(and-6)-carboxy-2',7'- difluorodihydrofluorescein diacetate), reactive oxygen species (ROS), which were generated *in situ* on copper surface throughout contact, were detected, which suggested that generation of ROS and hydroxyl radicals were important to the killing mechanism. They also observed extensive DNA degradation of *E. coli* on Cu surfaces after 30 minutes by *in situ* assessment of the DNA of cells. Therefore, the copper killing mechanism for *E. coli* involved Cu ionic species and generation of reactive oxygen species that cause immediate cytoplasmic membrane depolarization, inhibition of respiration, DNA degradation and cell death (Warnes et al. 2012).

In another study by Macomber and Imlay, mutants of *E. coli* without Cu homeostatic systems (*copA*, *cueO*, *cus*) were used to test the hypothesis that toxicity involves the action of reactive oxygen species and to identify intracellular targets. They discovered that Cu-stressed cells produced endogenous H₂O₂ at a rate that was higher than untreated cells. Excess amounts of superoxide (O₂⁻) and H₂O₂ can disrupt several biosynthetic amino acid pathways (Jang and Imlay, 2007) (Carlioz and Touati 1986) (Imlay and Fridovich, 1992). They also stated that copper inactivated iron-sulfur cluster dehydratases inside aerobic cells (Macomber and Imlay, 2009).

Based on the existing information, contact killing begins by successive damage to the cell membrane, copper inflow into the cells, oxidative disruption, cell death and DNA deterioration (Grass, 2011). However, there appears to be differences in the relative role of each mechanism, and there are conflicting reports on copper effects on DNA deterioration.

2.3 CuNPs Synthesis and Size Effects on Antimicrobial Properties

Copper nanoparticles (CuNPs) like most nanoparticles (NPs) can be synthesized using two different methods, i.e. the bottom up and top down approaches (Umer et al. 2012). The bottom up or chemical method is the most common method used because it offers better scope and control over resulting shapes and size of NPs (Gawande et al. 2016). The rapid oxidation of Cu on exposure to air causes oxidation to CuO and Cu₂O, and conversion to Cu²⁺ during preparation and storage, makes it difficult to synthesize copper nanoparticles at ambient conditions (Usman et al. 2013) but allows for the formation of more stable copper oxide NPs in many cases. Cu and Cu oxide NPs synthesis basically revolves around four forms of chemical reaction, namely, reduction, hydrolysis, condensation, and oxidation.

The major methods for synthesizing NPs are through chemical reductions, microemulsion (colloidal) processes, sonochemical reduction, electrochemical synthesis, microwave synthesis, biological synthesis and hydrothermal synthesis. Physical methods of synthesis of NPs include laser ablation (pulse), vacuum vapor deposition, pulse wire discharge and mechanical milling (Umer et al. 2012).

Usman et al. prepared NPs from pure Cu in the presence of a chitosan stabilizer through chemical means, and the antibacterial as well as antifungal activity of the NPs were investigated, with NPs in the range of 2–350 nm. They suggested that the size of the NPs is important for antimicrobial activity, and found that chitosan-Cu NPs with a concentration of 0.2 wt% and a size range of 5–50 nm with standard deviation of 18.29 ± 7.75 nm proved to be optimal due to a higher activity against microbial species tested (Usman et al. 2013).

Azam et al. synthesized different sized CuO NPs using a gel combustion method and explored the size-dependent antibacterial activity of each CuO NP preparation (Azam et al. 2012). Their results indicate that the smallest CuO NPs with a particle size of 20 ± 1.24 nm that were synthesized at the lowest temperature (400°C), showed a significant inhibitory effect against both gram-negative and gram-positive bacteria due to their smaller particle size as compared to other samples that were prepared. It has also been suggested that CuNPs' antibacterial efficacy is based on NP concentration levels; low levels lead to delays in the lag phase, demonstrating the micronutritional role of Cu for bacteria, while higher concentrations inhibited bacteria growth (Raffi et al. 2010) (Mahmoodi et al. 2018).

In another study by Theivasanthi and Alagar, CuNPs were synthesized by electrolysis and compared with CuNPs synthesized by chemical methods. Their results indicated that CuNPs synthesized using the electrolysis method showed better antimicrobial activity against *E. coli* compared to NPs obtained from chemical method, and they suggested the possibility of this technique being used in water purification, air

filtration, air quality management and antibacterial packaging (Theivasanthi and Alagar, 2011).

2.3.1 Copper Alloys

About 500 types of Cu and Cu alloys have been approved as products for antimicrobial surfaces by the EPA on the basis of laboratory testing and clinical studies (Walkowicz et al. 2018). However, Cu alloys have been preferred for use as high touch surfaces because of their aesthetic appeal and due to better corrosion resistance compared (Mikolay et al. 2010) (Walkowicz et al. 2018).

Cu and Cu alloys can be classified into three classes, according to the chemical composition; Cu and high Cu alloys (mainly composed of pure Cu), brass (which is mainly composed of Cu, zinc (Zn) and other alloy elements), bronze (which is mainly composed of Cu and other elements except Zn) (Collini, 2012). Some common types of brasses are, Tin (Sn) brass, Nickel (Ni) Silver, Cartridge Brass and Red Brass. Common types of bronzes include Aluminum (Al) Bronzes, Silicon Bronzes, and Phosphor Bronzes (Association, 2007). The nominal composition of common Cu alloys are shown in Table 2.0.

Table 2.0: Composition of some common Copper Alloys (Association, 2007)

ALLOY UNS No.	COMMON NAME	NOMINAL COMPOSITION Wt%
C11000	Copper	99 min Cu
C12200	Phosphorus Deoxidized Copper	0.025 P
C17200	Beryllium Copper	1.90 Be

C23000	Red Brass	15 Zn
C26000	Cartridge Brass	30 Zn
C28000	Muntz Metal	40 Zn
C42500	Tin Brass	10 Zn – 2 Sn
C51000	Phosphor Bronze A	5 Sn – 0.2 P
C52400	Phosphor Bronze D	10 Sn – 0.2 P
C65500	High Silicon Bronze A	3.3 Si – 1.0 Mn
C70600	Copper Nickel, 10%	10 Ni – 1.4 Fe
C71500	Copper Nickel, 30%	30 Ni – 0.7 Fe
C74500	Nickel Silver, 65-10	25 Zn – 10 Ni
C75200	Nickel Silver, 65-18	17 Zn – 18 Ni

Research has been conducted on some of the commercially available Cu alloy surfaces investigating antimicrobial and other properties. Michels and Anderson conducted antimicrobial tests using the EPA Good Laboratory Practice (GLP) protocol on a range of commercially used Cu alloys which included Cu (C110), brass (C260), bronze (C510), (C706) and Cu-nickel-Zn (C752) with each of the five alloys representing a major family of alloys. The results showed over 99% reduction in 2 hours and 24 hours of *S. aureus* (including methicillin-resistant *S. aureus* aka MRSA), *Enterbacter aerogenes*, *P. aeruginosa* and *E. coli* O157:H7 on all test surfaces (Michels and Anderson, 2008).

Walkowicz et al. investigated the tarnishing of Cu and various Cu alloys by oxidation at elevated temperatures and the impact of oxidation on antimicrobial efficacy of the Cu alloys. Superficial layers of copper oxide (I) were created on pure Cu (Cu-ETP), Yellow Brass (CuZn37), Tin Bronze (CuSn6) and Nickel Silver (CuNi18Zn20) to mimic the layers of Cu oxide that are formed on Cu and Cu alloys due to contact with human palm sweat in real life conditions for high touch surfaces. They concluded that there was very little to no effect of oxidation on the antimicrobial efficacy of test samples except for Tin Bronze which showed visible improvement in antimicrobial efficacy for oxidized samples compared to unoxidized samples (Walkowicz et al, 2018).

Noyce et al. evaluated seven cast Cu alloys (61 to 95% Cu) for their ability to reduce the viability of *E. coli* O157, mixed with or without ground beef, comparing results with stainless steel. The Cu alloys included Silicon Bronze (C87300), Red Brass (C83300), Brass (C83600), Ni-Al Bronze (C95800), Al Bronze (C95500), Ni Silver (C97600), Yellow Brass (C85700). They suggested that the viability of *E. coli* O157 depended applied on test surface depended on the concentration of substrate alloy (i.e. Cu, Zn and Ni content) that microbial culture is applied on, ambient temperature and presence of beef juice. They found that the alloys tested showed varying levels of antimicrobial activity in different conditions and suggested that alloys with over 90% copper should be used in chill temperatures (below 4°C) for greater antimicrobial performance (Noyce et al. 2006).

In another study conducted by Róžańska et al, three clinical *Acinetobacter baumannii* strains, one *A. Iwoffii* strain and an *A. pittii* strain isolated from a hospital environment, were tested for their susceptibility to Cu alloys. Test surfaces used for this

study included: Cu (99% pure Cu), Yellow Brass (CuZn37), Phosphor Bronze (CuSn6), Nickel Silver (CuNi18Zn20) and Stainless Steel. It was reported that although all copper alloy test surfaces investigated showed antimicrobial properties, the most effective antibacterial activity was found for copper, followed by tin bronze, while the weakest was found in brass and nickel silver (Rózańska et al. 2018). This is in line with suggestions that the antimicrobial efficacy of copper alloys depends proportionally on the copper content in a given alloy (Rózańska et al. 2017).

2.4 Testing Protocols for Antimicrobial Surfaces

Different protocols have been used by researchers for conducting antimicrobial test on Cu and Cu alloy surfaces in the past. Mehtar et al. conducted tests on copper alloys (1cm x 1cm) with *Candida albicans*, *P. aeruginosa*, *Klebsiella pneumoniae* and MRSA isolated from blood cultures, by inoculating each surface with 20 µl of culture (2.5×10^7 CFU/ml) and incubating at room temperature for different time periods. After the incubation period, the surfaces were placed in sterile bottles with screw caps that contained sterile phosphate buffered saline (10 ml) and twenty 2 mm glass beads before centrifuging for 30 seconds. Dilutions were then made, and samples were collected from each dilution and inoculated on agar plate at 37°C for 18 hours (Mehtar et al., 2008).

Koseoglu et al. conducted tests on Cu alloy surfaces (1 cm x 1 cm) by applying 10 µl of microbial suspension (5×10^6 CFU/ml) and incubating at room temperature for different time periods. After the incubation period, surface was placed in aliquots of phosphate buffered saline (5 ml) with twenty glass beads, before vortexing. Dilutions were

then made, and samples were collected from each dilution and inoculated on agar plate at 37°C for 18 hours (Koseoglu et al., 2015).

Hassan et al. conducted tests on Cu and Cu(I) oxide films (1 cm x 1 cm) using *E. coli* and *S. aureus* by applying 25 µl of bacterial suspension (10⁶ CFU/ml) and spreading on the surface before incubation for different time periods at room temperature. After the incubation period, the surfaces were placed in 225 ml of phosphate buffered saline and vortexed for 30 seconds. Dilutions were then made, and samples were collected from each dilution and inoculated on agar plate at 37°C for 24 hours (Hassan et al., 2014).

The steps involved in the protocols summarized above follow a similar pattern. First, bacteria suspension is prepared, then a determined amount and concentration is applied onto a test surface and allowed to sit for a contact time period. Then, surfaces are placed in phosphate buffered saline medium and vortexed, centrifuged or sonicated for a period of time to release bacteria into solution before dilutions are made and applied on agar surface for incubation. This generally follows the steps outlined by the environmental protection agency (EPA) for determining antimicrobial efficacy of copper and copper alloy surfaces.

2.4.1 EPA Protocol

The approval of the EPA is required before making antimicrobial claims related to public health for Cu and Cu alloy surfaces in the USA, so products must be approved and registered by the EPA before they are legally permitted to make antimicrobial claims (Michels and Anderson, 2008). Harold and Douglas mentioned that the three EPA approved GLP test dealing with antimicrobial claims include:

- Efficacy as a sanitizer, which measures surviving bacteria on Cu and Cu alloy surfaces after two hours.
- Residual self-sanitizing activity, which measures surviving bacteria on Cu or Cu alloy surfaces before and after six wet and dry wear cycles over 24 hours in a standard wear apparatus, and
- Continuous reduction of bacterial contamination, which measures surviving bacteria after repeatedly inoculating surfaces eight times in a 24-hour period without intermediate cleaning and wiping (Michels and Anderson, 2008).

However, several other laboratory techniques are available to determine susceptibility of microorganisms to antimicrobial agents. Some of these techniques includes, Diffusion methods, Dilution methods, Thin Layer Chromatography (TLC) Bioautography, Adenosine triphosphate (ATP) Bioluminescence assay and Flow cytometric methods (Balouiri et al. 2016). The bioautographic and diffusion methods are referred to as qualitative methods because they only give an indication of the existence or lack of antimicrobial substances, dilution methods are considered quantitative assays once the minimum inhibitory concentration has been determined (Valgas et al, 2007).

2.4.2 Agar disk-diffusion method

The agar disk-diffusion method is the standard procedure for routine antimicrobial susceptibility measures used in many clinical microbiology laboratories. In this procedure, the agar plate is inoculated with a standardized microorganism inoculum, followed by placing a paper disc (about 6 mm in diameter), containing the test compound on the surface of the agar. The petri dishes are incubated under suitable conditions for the

microbe of interest. The antimicrobial agent generally diffuses into the agar inhibiting microbial growth and then diameters of inhibition growth zones are measured. The diameter of inhibition is proportional to the strength of the antimicrobial effect on that organism (Balouir et al 2016) (Heatley, 1944). The agar disk- diffusion method is one of the various types of diffusion methods. Some other types of diffusion methods include: the antimicrobial gradient method (Etest), the well diffusion method, the agar plug diffusion method, the cross-streak method, and the poisoned food method (Magaldi et al. 2004) (Balouir et al 2016). This method is not applicable for a typical antimicrobial hard surface, where the antimicrobial activity and effect is localized on the surface and not in a material than can readily diffuse.

2.4.3 TLC Bioautographic Method Direct Variant

The measures involved in the direct version of the bioautographic process include: the preparation and application of natural antimicrobial products on thin layer chromatographic plates (TLC), followed by the preparation and application of bacterial inoculum on the TLC plates, then incubation; and colorimetric assay (INT) growth detection and measurement of growth inhibition diameters (Valgas et al. 2007). This method incorporates chromatographic separation and *in situ* determination of activity, which enables targeted isolation and localization of the active ingredients in a mixture (Suleiman et al., 2010) and can be utilized for either fungi or bacteria. It is also a simple technique for detecting antifungal substances, which gives consistent results for spore-producing fungi like *Aspergillus*, *Penicillium* and *Cladosporium* (Balouiri et al. 2016). Other types of TLC bioautographic method include agar diffusion (indirect variant) and the agar overlay bioassay.

2.4.4 Agar Dilution Method

This is a type of dilution method which involves injecting different concentrations of the antimicrobial agent into the molten agar medium, typically using serial double dilutions, followed by inoculation of the specified microbial inoculum onto the agar plate surface. The purpose of the agar dilution method is to determine the lowest concentration of the assayed antimicrobial agent that inhibits the visible growth of the bacteria being tested (typically expressed in $\mu\text{g} / \text{ml}$ or mg / litre) (O.I.E. 2012). The minimum inhibitory concentration (MIC) end point is reported as the lowest antimicrobial agent concentration that completely inhibits growth under acceptable incubation conditions (Ali-Shtayeh et al. 1999) (Balouiri et al. 2016). However, growth inhibition (bacteriostatic activity) differs from killing of microbes (bactericidal activity), and the MIC value does not give any indication of the latter. This is because there might still be viable cells that exist within the determined MIC value which shows no visible growth on agar plates (i.e. alive but non-culturable). Hence, growth could resume afterwards if the antimicrobial agent is removed (Wiegand et al., 2008). Another type of dilution method is the broth dilution method.

2.4.5 Broth Dilution Method

This type of dilution method involves inoculating a defined number of microbial cells in liquid growth medium which contains geometrically increasing concentration of antimicrobial agents and the presence of sediment or turbidity of solution after incubation indicates growth of organism. Two methods described for broth dilution, based on final volume of mixtures are, macrodilution (when using up to 2 ml) and microdilution (when using is less than 500 μl). MIC value is recorded (Wiegand et al., 2008).

The dilution methods are not applicable for measuring antimicrobial efficacy of a typical antimicrobial surface because the antimicrobial activity is associated with the surface and may not be diluted.

2.4.6 ATP bioluminescence assay

The ATP-bioluminescence technique for determining living cells, needs only 2 to 5 h, but is not currently commonly used due to the lack of suitable instrumentation, the prohibitive cost of the reagents and the disagreement with the results obtained compared with the standard methodology (Hattori et al. 1998). Adenosine triphosphate (ATP) is the chemical form of energy of all living cells, present in a cell. The ATP bioluminescence assay is based on the ability to measure adenosine triphosphate (ATP) produced by bacteria or fungi, the quantification of which is used to estimate the microbial population in the sample. The amount of light produced from the conversion of D-luciferin in the presence of ATP by luciferase to oxyluciferin is determined by a luminometer and expressed as a relative light unit (RLU) which can then be converted to an ATP RLU / mole. Care must be taken because the presence of ATP does not directly relate to the ability of cells to reproduce or be viable, since ATP is an indicator of the presence of organic material (Sanna et al., 2018) and cells could be recently killed with the ATP still available. Linear relationships have been observed between cell viability and luminescence by some authors (Balouiri et al. 2016) (Amodio and Dino, 2014).

2.5 Flow cytometry

Flow cytometry (FCM) is a method used to analyze the physical and chemical properties of suspended microscopic particles in a liquid medium using an optical-electronic detection device (Errante et al. 2016). It provides rapid analysis of multiple cell characteristics and provides qualitative as well as quantitative information. Cell size, cytoplasmic complexity, DNA or RNA levels as well as a broad range of membrane-bound and intracellular proteins are characteristics that can be measured by flow cytometry, using appropriate fluorescent labels for features of interest (Brown and Wittwer, 2000). FCM has become an increasingly important technique for microbiologists to study cells at the individual and population levels in the last few decades and is a reliable technique based on its optical detection of scattered light and fluorescence, which can identify cells with interesting characteristics (Ou et al. 2017).

The principal components of a flow cytometer include the flow chamber; a light source; a detector and a digital analogical converter that generates the size, complexity, signal and fluorescence; a linear or logarithmic signal amplification system and a computer for analysis of the signal (Errante et al. 2016) (Kurec, 2014). Although the high cost of equipment and reagents involved, added to the requirement for training qualified personnel to use it, due to its high potential, flow cytometry has been extended to various fields in the biological sciences, used in clinical diagnostics, biotechnology, basic and applied research (Errante et al. 2016).

2.5.1 General Principles of a Flow Cytometer

When a sample enters a flow cytometer, single particles of the sample are investigated by the detection system of the instrument through a process where sample is ordered into a single particle stream (Bio-Rad Laboratories Inc. 2015). A pneumatic pump propels particles and cells suspended in a continuous flow into a hydrodynamic focusing chamber (flow cell) which, due to its conical shape, forces the capillary or nozzle of 250 μm in diameter to accommodate particles or cells, producing a thin jet of fluid at an average rate of 10 m/s (Errante et al. 2016). Hydrodynamic focusing of the flow of cells in a single stream that passes through the point of illumination, allows for single cell analysis and this process is shown in Figure 2.0 below.

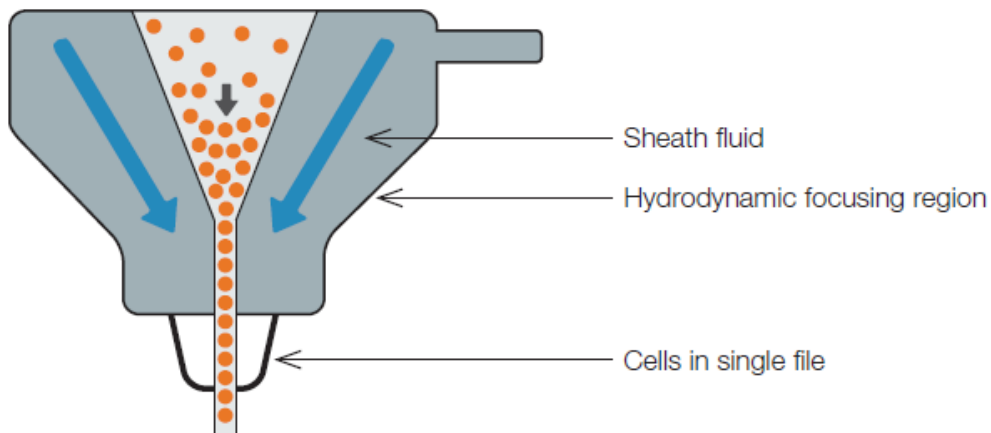


Figure 2.0: Hydrodynamic focusing (Bio-Rad Laboratories Inc. 2015)

At the interrogation point the cells are intersected by a beam of monochromatic light, usually from a laser. The light emitted is collected in all directions via optics and is directed into several filters and dichroic mirrors that isolate particular wavelengths (Brown and Wittwer, 2000). The lasers produce light of a single wavelength known as the laser

line at a specific frequency (typically specified in mW as photon output / time) (Bio-Rad Laboratories Inc. 2015).

A photomultiplier tube (PMT) or photodiode collects light dispersed in the forward direction from interaction with a particle (up to 20° offset from the angle of the beam) and is known as the forward scatter (FSC). FSC measurements can estimate the size of particles that refract more light than smaller particles, although this can be dependent on various factors, like, laser wavelengths, the collection angle and the refractive index of the sample and sheath. However, light measured at an angle of 90° to the excitation line is called the Side Scatter (SSC) which provides information on relative complexity, such as granularity and internal cell or particle structures. For each individual particle, both FSC and SSC are unique and a combination of the two can be used to differentiate cell types in a heterogeneous population (Bio-Rad Laboratories Inc. 2015). A schematic representation of a typical flow cytometer is shown in Figure 2.1 below.

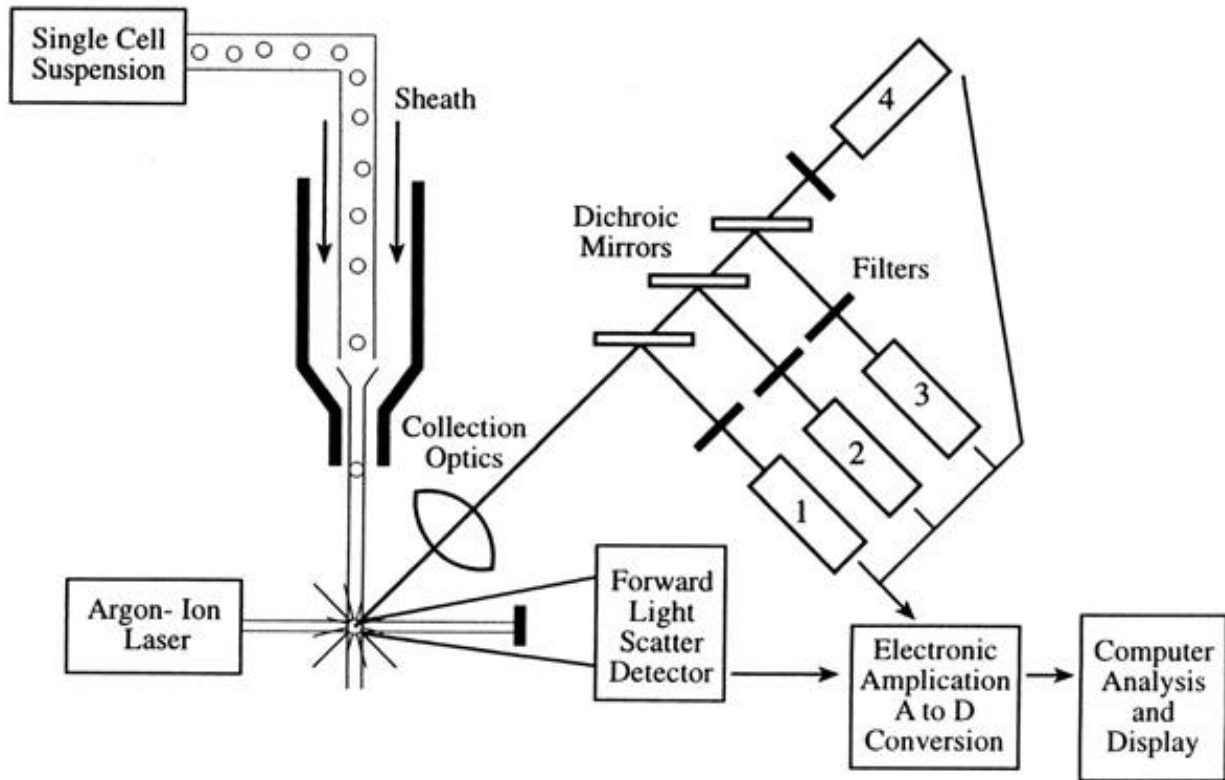


Figure 2.1: Schematic of a flow cytometer (Brown and Wittwer, 2000).

A single cell suspension is hydrodynamically focused with sheath fluid to intersect an argon-ion laser. Signals are collected by a forward angle light scatter detector, a side-scatter detector (1), and multiple fluorescence emission detectors (2–4). The signals are amplified and converted to digital form for analysis and display on a computer screen. (Brown and Wittwer, 2000)

2.5.2 Fluorochromes used in Flow Cytometry

Fluorophores are fluorescent markers that are used to detect expression of cellular molecules like proteins or nucleic acids (Bio-Rad Laboratories Inc. 2015). Fluorochromes absorb the luminous energy of a specific wavelength and then emit light in a longer

wavelength with lower energy (Errante et al. 2016). These processes are referred to as excitation and emission. Emission follows extremely rapid excitation, commonly in nanoseconds, and is known as fluorescence. The wavelength of excitation is critical to the total light photons absorbed by the fluorophore. For example, fluorescein isothiocyanates (FITC) absorbs light from 400-530 nm; however, its excitation maximum or peak is 490 nm, which is the most efficient wavelength for excitation. Fluorophores should be excited as much as possible at their excitation maximum because as more photons are absorbed, the more intense the fluorescence emission will be (Bio-Rad Laboratories Inc. 2015). Figure 2.2 below shows the spectral profile of FITC.

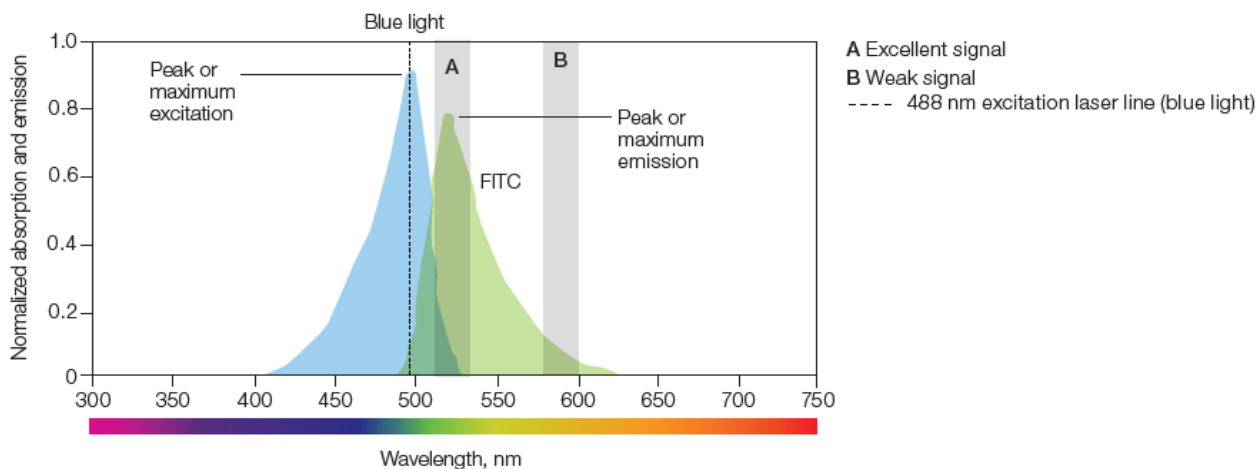


Figure 2.2: Spectral profiles, light absorbance and emission of fluorescein isothiocyanate (FITC) (Bio-Rad Laboratories Inc. 2015).

In the case illustrated above, the maximum absorbance of FITC falls within the blue spectrum, so the blue 488 nm laser, which is close to the absorbance peak of FITC at 490 nm, is commonly used to excite this fluorophore. FITC emits fluorescence from 475 to 650 nm, peaking at 525 nm, which falls within the green spectrum (Bio-Rad

Laboratories Inc. 2015). Some other fluorochromes and their emission spectrum which are commonly used in flow cytometry is shown in Table 2.1 below.

Table 2.1: Fluorochromes commonly used in flow cytometry and emission spectrum (Errante et al. 2016)

Fluorochrome	Laser (nm)	Emission (nm)	References
FITC	488	519 – 525	IBÁÑEZ-PERAL et al., 2008
Alexa Flúor	488	519	DAVIS et al., 2013b
R-PE (PE)	488	575 – 578	DAVIS et al., 2013a
PE -Cy5 (TC1)	488	667	KALINA et al., 2012
PerCP (BD2)	488	675 – 678	DAVIS et al., 2013a
PerCP/Cy5.5 (BD)	488	695	DEGHEIDY et al., 2015
PE – Cy7	488	795	PREIJERS et al., 2011
7 – AAD	488	655 (620 – 675)	DAVIS et al., 2013b
HOECHST 3342	488	461	BARNETT et al., 2013
Propidium Iodide	488	570 – 617	DE ROSA et al., 2001
Rodamine 123	488	528	ADLER; SCHMITT-JANSEN; ALTENBURGER 2007
Texas Red	595	615	KAPOOR et al., 2008
APC	633, 635, 640	660	TJIOE et al., 2001
Cy5	633, 635	667	KALINA et al., 2012

DAPI	488	461 (DNA), 500 (RNA)	DARZYNKIEWICZ et al., 2011.
------	-----	-------------------------	--------------------------------

2.5.3 Flow Cytometry Data Analysis

Typical analysis of FCM data can be carried out through the process of gating and interpretation (Brown and Wittwer, 2000). Gating is a highly subjective process in which the researchers determine the regions within multiparametric spaces containing "interesting" data based on their knowledge of experimental factors and experience (Bashashati and Brinkman, 2009).

Gating methods can be divided in two main categories. Sequential or manual gating is the application of software to manually draw gates around regions in the data plots representing two parameters along two axes based on researchers' expertise. The other, automated gating is based on the mathematical modeling of the fluorescence intensity distribution of cell populations and can be performed using two different approaches namely, supervised and unsupervised analysis (Montante and Brinkman, 2019). The goal is to identify events within the same cluster in the automated gating of FCM data. The clusters contain groups of events more like each other than that from other clusters (Bashashati and Brinkman 2009).

Interpretation involves the use of correlations between certain characteristics of the cell populations identified (e.g., percentages of cells in a cell population, mean or median fluorescent intensity of a cell population for different markers) and clinical outcomes (e.g. diagnosis, survival) (Bashashati and Brinkman, 2009). A number of

computational methods may be used to determine the association between FCM samples and the class of interest or to identify clusters of patients with similar FCM data, depending on the purpose of the study, supervised or unsupervised learning (Montante and Brinkman 2019).

Various research has been carried out on FCM data analysis, with the purpose of facilitating and automating the review and reporting process. Bashashati and Brinkman reviewed state-of-the-art FCM data analysis approaches using a framework introduced to report each of the components in a data analysis pipeline (Bashashati and Brinkman, 2009). Montante and Brinkman summarized the main steps of FCM data analysis, focusing on the use of the most recent bioinformatic tools developed for an R-based programming environment. They listed libraries and packages for each stage of the data analysis, including descriptions of their functioning (Montante and Brinkman, 2019).

A great deal of research has occurred using flow cytometry techniques by various researchers in different fields. Ou et al. investigated the use of flow cytometry protocols for the enumeration of live and dead bacteria present in a mixture, by staining mixtures of live and dead *E. coli* with SYTO 9 and Propidium Iodide (PI) at concentration ratios varying from 0 to 100% (Ou et al. 2017). They found this protocol to be accurate and reliable when compared with traditional plate counting methods.

Another study was carried out by Prigione et al., to develop a reliable method of analysis based on FCM for the detection and rapid enumeration of airborne spore-forming and filamentous fungi by combining light scatter and propidium iodide red fluorescence parameters. Direct counting with epifluorescence microscopy was used as the standard

for comparison using pure suspensions of *Aspergillus fumigatus* and *Penicillium brevicompactum* conidia at different concentrations (Prigione et al. 2004).

Wenisch et al conducted a study for antifungal susceptibility testing by measuring the impairment of fungal metabolic activity with FCM, using nine *Candida albicans* strains and staining with FUN-1 as a fluorescent probe, which emits red fluorescence due to metabolic activity of fungi (Wenisch et al. 1997). Another study by Vanhauteghem et al. developed a flow cytometry method for the assessment of the viability of fungal Conidia in Metalworking Fluids using *Fusarium solani* as the model organism and staining with SYTO 9 and PI, then validating results by comparing with microscopic analysis and plating experiments (Vanhauteghem et al. 2017).

2.6 Summary

In this review, Cu as an antimicrobial surface was discussed, its chemistry, oxidation and ion effects on antimicrobial efficacy. The antimicrobial mechanism, synthesis and size effects on antimicrobial activity was also discussed, with some common alloys of Cu listed. Some antimicrobial testing protocols were reviewed, and flow cytometry was introduced.

Since most of the testing protocols discussed were developed to test for antimicrobial agents like drugs, antibiotics, preservatives, and disinfectants, they are not applicable for testing hard solid antimicrobial surfaces. The EPA protocol, which is the standard protocol for testing the antimicrobial efficacy of solid Cu surfaces has some limitations including a slow evaluation and determination of results. This thesis focuses

on developing alternative methods that are more rapid, while still correlating to results from the EPA protocol.

Furthermore, since the EPA protocol does not address testing with fungi, and typical plate counting techniques are rather slow due to the incubation time required (48 hours), a rapid flow cytometry technique was developed and compared to plate count results.

Chapter 3

Standardization of Protocols for Antimicrobial Efficacy Testing

3.1 Overview

Antimicrobial efficacy testing is important for determining the efficiency of industrially manufactured products against microbes. The testing protocol widely recommended and used for antimicrobial products containing Cu or Cu alloys has been proposed by the EPA. In this study, 4 separate protocols were developed, studied and the results compared with results obtained from a coupon-based method similar to the EPA protocol, when *E. coli* and *P. aeruginosa* were separately applied to industrially manufactured antimicrobial products. Protocol 1 (modified EPA protocol) involved applying bacteria solution on a test surface for 1-hour contact time, the test surface was then placed in a beaker containing phosphate buffered saline (20 µl), sonicated for 5 minutes, then bacteria solution was plated on agar plates and incubated. Protocol 1 was used as the control, for comparison with other protocols. Protocol 2 involved applying bacteria solution on a test surface for 1 hour, then the bacteria solution was retrieved using a pipette, dilutions were made, plated and incubated. Protocol 3 involved applying bacteria onto the test surface, then the test surface was inverted onto an agar plate surface, left for 1 hour contact time, then surface was removed and plate incubated. Protocol 4 involved applying bacteria onto test surface and left in contact for 1 hour, then stamped onto an agar surface for 30 seconds, removed and incubated. The coefficient of variation calculation of results from all protocols indicate that Protocol 3 showed the highest variation relative to its mean value for both log reduction and killing percentage

calculations, making it the least reliable technique. Protocol 2 also showed a high coefficient of variation calculation compared to the modified EPA protocol while Protocol 4 showed a low coefficient of variation and the results correlated well with results obtained from the modified EPA protocol. These developed protocols involved traditional plate counting techniques but are accurate, since the results obtained from each protocol was correlated with results obtained from the EPA protocol. Protocol 3 and 4 allowed for more rapid testing of antimicrobial surfaces compared to the modified EPA protocol, saving up to 30 minutes per sample. A technique for the efficacy testing of antimicrobial powder particles was also studied, which showed that the antimicrobial powder particles investigated totally inhibited bacterial growth on agar plates when the powder particles covered an area with a density of 0.45 mg/cm^2 on the plate surface.

3.2 Introduction

More than 50 percent of the HAIs are caused by the presence of bacteria that are resistant to at least one type of antibiotic, and there are fewer new antibiotics that are being developed by pharmaceutical companies (Mauldin et al. 2010) (Canadian agency for drugs and technologies in health, 2015). Multi-drug resistant (MDR) infections are thus a growing concern and, in combination with the lack of new antimicrobial products, there are limited options for effective antimicrobial therapy. In this struggle, the use of biocidal surfaces has proved effective as continuous killing surfaces for bacteria, fungi and viruses on contact, hence helping to reduce the transmission of MDR infections between people (Warnes et al. 2012). A wide range of components, including bed rails, overbed tables, intra-venous poles, laundry components and working surfaces, can be used as substrates for antimicrobial Cu. The Cu antimicrobial activity also suggests that it can be used as a

food-processing surface to reduce microbial load in the presence of a food matrix (Parra et al. 2018) (Canadian agency for drugs and technologies in health, 2015).

The EPA approved the use of Cu alloy surfaces as clinical contact surfaces in 2008, due to their antimicrobial properties (Parra et al. 2018), and they have been approving even more Cu alloys for use as antimicrobial surfaces in high touch areas. Therefore, it is important to use quantitative methods which provide accurate assessment of how effective Cu is at killing microbes in different conditions. The EPA recommended a testing protocol to support the registration of hard non-porous copper containing surface products with non-food contact surface sanitizer claims (Environmental Protection Agency, 2016), which has been used by various researchers and laboratories as the standard protocol for investigation of antimicrobial efficacy of Cu and Cu alloy surfaces under different conditions and for different applications.

A great deal of attention has also been paid to antimicrobial activity screening and evaluation methods to help quantify the antimicrobial effects of various antimicrobial compounds and agents. Several bioassays, such as disc diffusion and broth or agar dilution methods are well known and commonly used, although comparisons between different methods and results are often difficult due to the variety of available methods and variations in experimental design (Bankier et al. 2018) (Balouiri et al. 2016). In the USA, the National Committee for Clinical Laboratory Standards (NCCLS) has an approved standard procedure for performing disc diffusion antibiotic susceptibility tests that is updated every three years and new techniques for assessing antimicrobial activity have been described, with the aim of decreasing the time taken for the testing protocols.

However, most protocols have been developed to assess *in vivo* or *in vitro* antimicrobial activity of extracts, pure compounds or drugs, which can be applied as a liquid onto a test strip or disc (Kempe and Heinzl-Wieland, 2018) (Pidcock, 1990) (De Castillo et al. 1998). There are no existing standard alternative protocols to the EPA protocol that can be used to accurately determine the antimicrobial efficacy of solid hard non-porous copper and copper alloys, as well as copper particles. In addition, since bacterial growth inhibition does not mean bacterial death, it is important to have standard protocols which can accurately test for bactericidal and bacteriostatic effects of Cu and Cu alloy surfaces under different conditions. However, the test conditions and conditions for the actual use of the Cu materials should be similar to be relevant.

One of the biggest challenges with employing the EPA protocol in laboratory testing of Cu and Cu alloys antimicrobial efficacy is that it is quite rigorous and a time-consuming procedure, taking up to 2 hours to complete the experimental procedure per sample set, followed by 1 to 2 days for growth incubation. The procedure is quite tedious when multiple test surfaces are to be screened. The development of accurate alternative protocols would be beneficial in this instance.

3.3 Materials and Sample Preparation

3.3.1 Reagents and Materials

Phosphate buffered saline (PBS) tablets were purchased from Sigma-Aldrich (Saint Louis, USA). One tablet dissolved in 200 ml of deionized water to yield 0.01 M phosphate buffer. Plate count agar (PCA) and Potato dextrose agar (PDA) were purchased from Difco Laboratories (Sparks Glencoe, USA). Lauryl sulfate broth (LSB) was purchased

from Sigma-Aldrich. Potato dextrose broth (PCB) and Cetrimide broth (CB) were both purchased from the Himedia Company (Nashik, India). All the bacterial species in the study were purchased from Cedarlane Laboratories (Burlington, Ontario). The diode array spectrophotometer is a product of Hewlett Packard, HP 8452A (East Oshawa, Ontario). Ethanol (95%) was purchased from Anachemia, a VWR company (Rochester, New York). Liquinox was used as the liquid detergent for cleaning, purchased from Alconox (White Plains, New York). Scanning electron microscopy and Energy dispersive X-ray spectroscopy (SEM/EDS) analysis was conducted with FEI Quanta Feg 250 ESEM (with EDX) at low pressure (~0 bar). Ni (95%), Zn (99%) and Cu (99%) were purchased from Alfa Aesar (Massachusetts, USA). Plastic surfaces (1" x 1"), copper alloy metal antimicrobial samples (1" x 1") and powder were provided by Aereus Technologies Inc (Rosemont, Ontario).

3.3.2 Sample Preparation

Samples of plastic, Cu, Zn, Ni, and industrially manufactured antimicrobial surfaces were soaked in Liquinox solution for 2 hours to degrease them, then rinsed with deionized water and allowed to dry at room temperature (~22°C). After drying, samples were soaked in 95% ethanol for 15 minutes to sterilize and left to dry in a beaker for up to 24 hours at room temperature.

3.3.3 Bacteria Strains

The Gram-negative bacteria *E. coli* (ATCC PTA-4752) and *P. aeruginosa* (ATCC 15442) were chosen to test the antibacterial properties of the test surfaces.

1) Agar plates and Cetrinide broth preparation: For plate count agar, 23.5 g was suspended in 1000 ml DI water, and heated to boiling to dissolve the medium completely. Nutrient broth (25.3 g) was dissolved in 1000 ml deionized water. Both were then sterilized by autoclaving at 15 lbs pressure (121°C) for 20 minutes. After autoclaving, hot agar solution was poured into sterile Petri plates in a sterile environment.

2) Bacterial cultures: Bacteria were cultured in flasks with 50 ml Cetrinide Broth (for *P. aeruginosa*) and Plate Count Broth (for *E. coli*) at 37°C for 24 hours. To prepare the diluted bacterial solution, 1 ml of the culture was pipetted from the cultured flask into a 1.5 ml microcentrifuge tube. After washing twice with sterile PBS water, the bacteria solution was calibrated to 10^8 CFU/ml by analyzing with UV spectrophotometer, where the absorbance reading was adjusted to 0.2 at a wavelength of 600 nm. Then a serial dilution method was used to prepare 5 dilutions from this solution (10^7 , 10^6 , 10^5 , 10^4 , 10^3 CFU/ml).

3.4 Protocols Investigated

3.4.1 Modified EPA Protocol (Protocol 1)

The standard EPA protocol was modified by excluding the use of soiling agents in the test solution, which would have otherwise been mixed with microbial solution before applying final solution on the test surface. The importance of soiling agents is to ensure that antimicrobial action is carried out in a nutrient rich environment for bacteria, hence ensuring that the test surfaces seeking EPA approval are very effective and properly simulates real life applications. However, introduction of soiling agents would create more variability in results especially for test samples with low antimicrobial activity (Noyce et al., 2006). This work is focused on comparing results obtained from the different

developed protocols, and test samples with low antimicrobial efficacy were used, to ensure more accurate comparison. The detailed steps for this protocol are outlined below.

- After sample preparation was carried out, 20 μl from 10^8 CFU/ml of prepared culture was applied onto the 1 x 1-inch test surface and allowed for a contact time of 60 minutes
- After contact time, the test surface was rinsed with PBS by placing the 1 x 1-inch test sample in a beaker containing 20 ml of PBS, then the beaker was placed in an ultrasonic bath for 5 minutes.
- Serial dilutions were prepared for each test sample rinse (10^1 to 10^4) and 100 μl of each dilution were plated using appropriate agar plates.
- Agar plates were incubated for 24 hours for bacteria and 48 hours for fungi at 37°C.
- All colony growth observed on agar plates were counted after incubation. Samples were rejected if the count was above 500 or contamination was observed

3.4.2 Pipette Retrieval (Protocol 2)

- After sample preparation was carried out, 60 μl from 10^8 CFU/ml of prepared culture was applied onto the test surface and allowed for a contact time of 60 minutes.
- After the contact time, the culture was carefully retrieved using a pipette, and 20 μl was collected and diluted in 20 ml of PBS.
- Serial dilutions were prepared for each test sample (10^1 to 10^4) and 100 μl of each dilution were plated using appropriate agar plates.
- Agar plates were incubated for 24 hours for bacteria and 48 hours for fungi at 37°C.

- All colony growth observed on agar plates was counted after incubation. Samples were rejected if the count was above 500 or contamination was observed

3.4.3 Stamping Protocol (Protocol 3)

After sample preparation was carried out, 10 µl from a 10⁴ CFU/ml prepared culture was applied onto the test surface, and a sterile L-shaped spreader was used to evenly spread the culture across the test surface. A stamping protocol was then investigated using two different approaches.

1. “Straight stamping”: This involved stamping the test surface directly onto the agar plates immediately after the bacteria was applied onto the test surface. The test surface was then left on the agar plates for 1 hour before removing. The agar plate was then placed in an incubator at 36°C for 24 to 48 hours and the colony growth observed after incubation was counted.
2. “1-hour contact”: Bacterial culture was applied onto the test surfaces and was left for a contact time of 1 hour before stamping onto agar plates. After the 1-hour contact time, the test surfaces were stamped against the agar plates for 30 seconds before gently removing from the agar plates using sterile forceps. The agar plate was then placed in an incubator at 36°C for 24 to 48 hours and colony growth observed after incubation was counted.

The difference between the two “stamping” procedures was that in the second one (1-hour contact) the applied bacterial culture was more exposed to air during the 1-hour contact period and more desiccation could take place.

3.4.4 Antimicrobial Powder Particles

Aereus Shield powder (a commercial copper alloy sample) of different quantities (10 mg, 20 mg, 30 mg, 35 mg, 45 mg) was measured on a weighing balance and spread out on 100 mm diameter agar plates, by mixing powder with 200 µl of sterile deionized water and evenly spreading paste on agar surface using L-shaped spreaders. Microorganisms (*E. coli* and yeast) of different dilutions (10^8 10^7 10^6 and 10^5 CFU/ml) were added to the agar plates to test the antimicrobial efficacy of the powder.

3.4.5 Log Reduction and Percentage of Killing

The antimicrobial efficacy of test surfaces was determined by calculating the log reduction (LR) and percentage of killing (PK) of test samples with respect to negative control plastic surface. Hence, control samples would always show zero log reductions and killing percentage. Log reduction and percentage of killing are calculated using equation 3.1 and 3.2 respectively.

$$\text{Log Reduction (LR)} = \log(A) - \log(B) \quad \text{equation 3.1}$$

$$\text{Percentage of killing (PK)} = \frac{A-B}{A} \times 100 \quad \text{equation 3.2}$$

Where A is the number of colony growth counted on agar plate for control sample and B is the number of colony growth counted on agar plate for test surface. Values of A and B are in base 10 logarithms.

3.4.6 Coefficient of Variation

The test statistic that was used to compare the investigated protocols to determine their precision and repeatability is the coefficient of variation (CV). The coefficient of variation describes the degree of variation in relation to the calculated mean (Everitt, 1998). This is calculated using equation 3.3 below.

$$\text{Coefficient of variation (CV)} = \frac{\sigma}{\mu} \quad \text{equation 3.3}$$

Where σ is the standard deviation and μ is the calculated mean.

The higher the value of the calculated CV, the higher the variability and lower reliability.

3.5 Results and Discussion

In Figure 3.0 below, the antimicrobial efficacy of pure Cu, Ni and Zn surfaces against *E. coli* using the EPA protocol was observed by calculating the killing percentage of each sample, observed over five separate replicates, and comparing their average killing percentages.

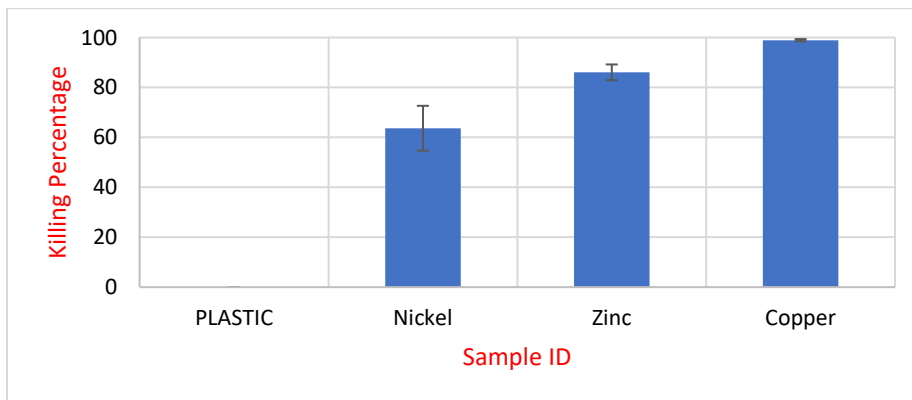


Figure 3.0: Killing percentage of *E. coli* on pure Cu, Ni and Zn surfaces using the EPA protocol.

It was observed that copper showed the highest antimicrobial activity and achieved >98% killing of colony forming units of bacteria, followed by zinc which achieved up to 88% killing, then nickel which achieved 63% killing. Most industrially manufactured alloys of copper contain some amounts of zinc or nickel and in some cases, both. However, pure copper has been reported to be more lethal in inhibiting growth of microbes than these metals (Hrenovic et al., 2012) (Wilks et al., 2005) (Yasuyuki et al., 2010). This fact is observed from figure 3.0.

3.5.1 Characterization of Antimicrobial Samples

Samples A and B are (1" x 1") industrially manufactured antimicrobial samples that were used in this work, to investigate the developed antimicrobial protocols. These samples were characterized using SEM-EDS analysis to determine their morphology and active elements.

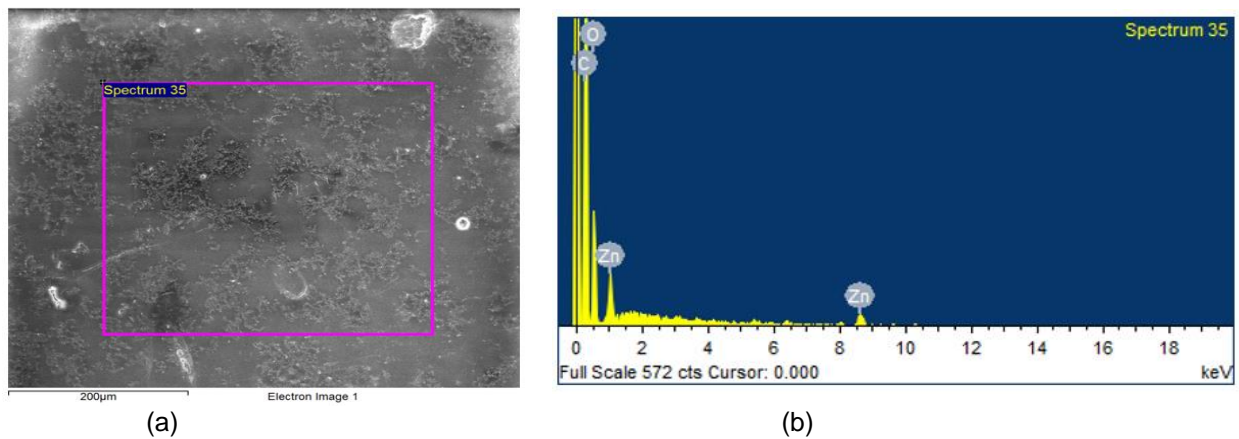


Figure 3.1: (a) SEM image of sample A at a 200 μm scale bar
(b) EDS spectrum for sample A.

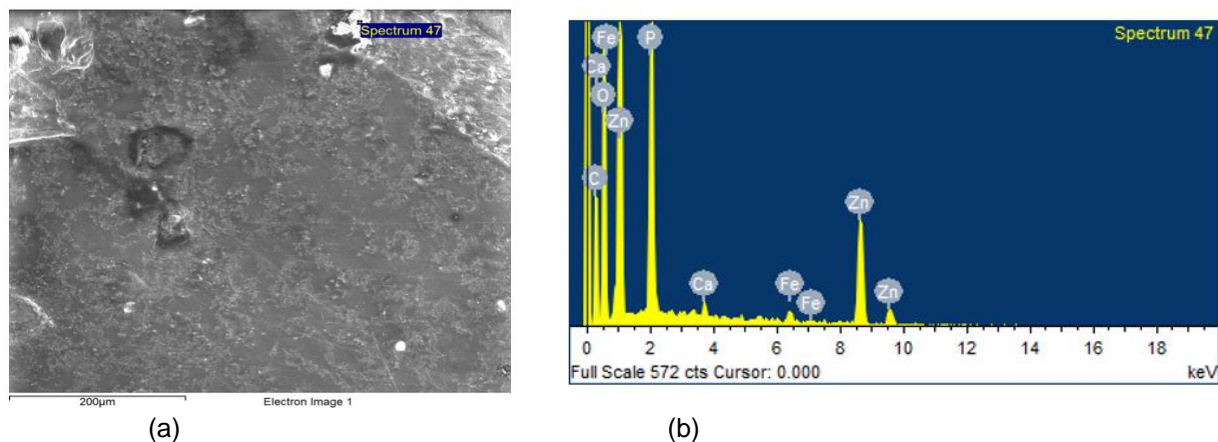


Figure 3.2: (a) SEM image of sample B at a 200µm scale bar
 (b) EDS spectrum for sample B

According to the EDS analysis illustrated in Figure 3.1b, it is observed that for Sample A, zinc was found on the sample after analyzing up to three spots on the sample surface. It is also observed from Figure 3.2b, that on Sample B, zinc and iron were found after analyzing three different spots on the sample surface

3.5.2 EPA Protocol – Protocol 1

The antimicrobial efficacy of both samples A and B against *E. coli* and *Pseudomonas aeruginosa* was determined using the EPA protocol. A plastic surface was used as the negative control and a pure copper surface was used as a positive control for this experiment. Five different experiments were done to obtain replicates. The average log reduction and killing percentages were calculated and compared as shown in Figure 3.3 for *E. coli* and Figure 3.4 for *Pseudomonas aeruginosa*.

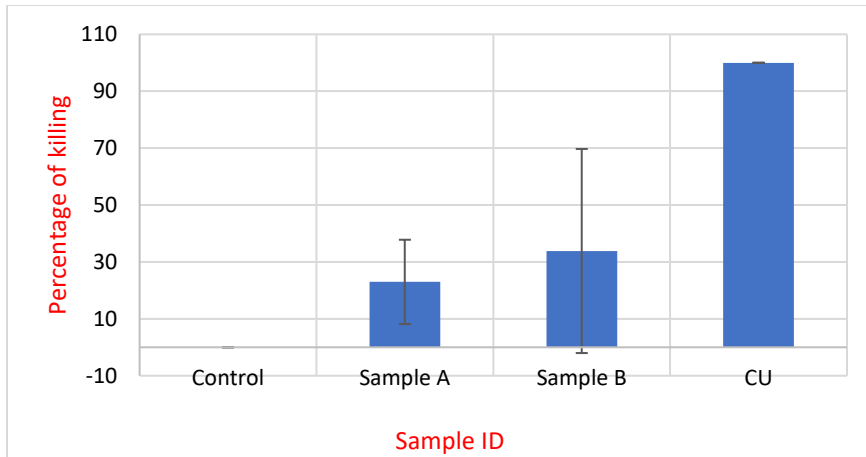


Figure 3.3: Killing percentage of *E. coli* calculated on samples using EPA protocol

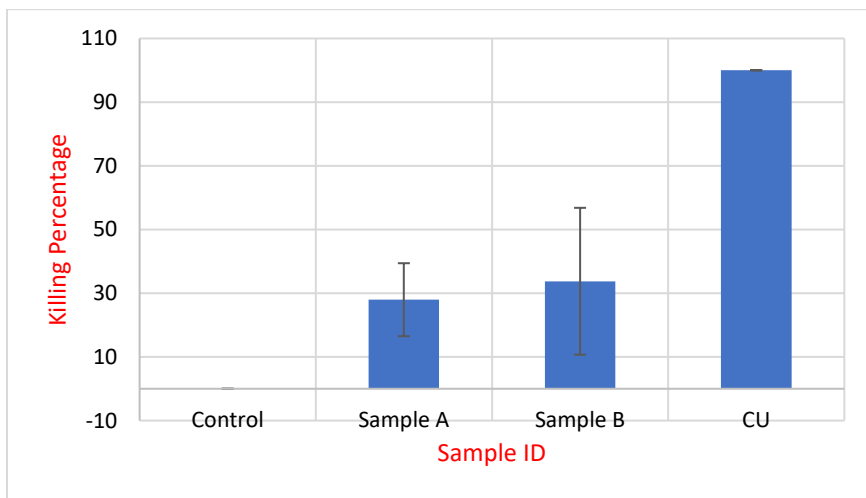


Figure 3.4: Killing percentage of *P. aeruginosa* calculated on samples using EPA protocol

It is observed that sample B showed slightly higher antimicrobial efficacy compared to sample A for both *E. coli* and *Pseudomonas aeruginosa* with mean killing percentage of 33.8% for *E. coli* on sample B compared to the mean killing percentage of 22.9% for *E. coli* on sample A. Also, the mean killing percentage for *Pseudomonas aeruginosa* is recorded as 33.8% for sample B and 22.9% for sample A.

3.5.3 Protocol 2

An alternative protocol to the EPA protocol called Protocol 2 was developed, like the EPA protocol but without the sonication step (see methodology, Section 3.4 for reference), to allow for antimicrobial testing of specific spots within the test surface. This is useful for its potential to determine if antimicrobial particles on industrially manufactured surfaces are evenly distributed or exposed for antimicrobial action. It also avoids the EPA requirement for samples to be 2.5 x 2.5 cm dimensions so that they fit within a beaker and sonicator.

The antimicrobial efficacy of Samples A and B against *E. coli* and *Pseudomonas aeruginosa* was determined using the Protocol 2. For this experiment, a plastic surface was used as the negative control and a pure copper surface was used as positive control. Five separate replicates were obtained. The average killing percentages were calculated and compared as shown in Figure 3.5 for *E. coli* and Figure 3.6 for *Pseudomonas aeruginosa*.

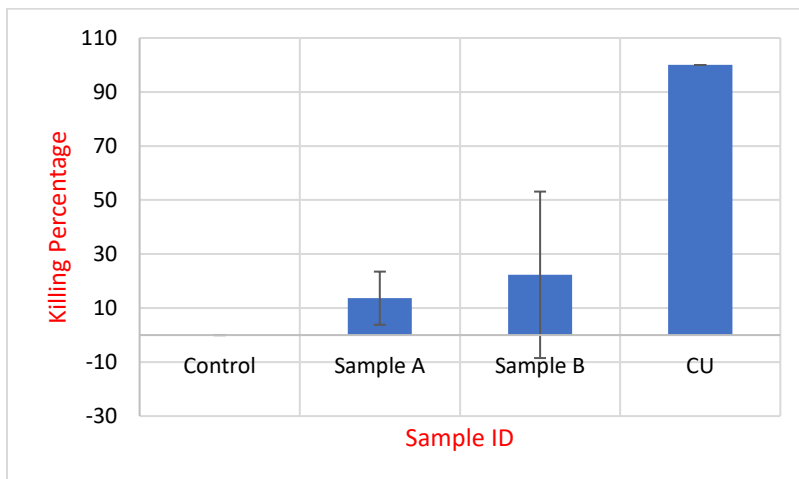


Figure 3.5: Killing percentage of *E. coli* calculated on samples using Protocol 2

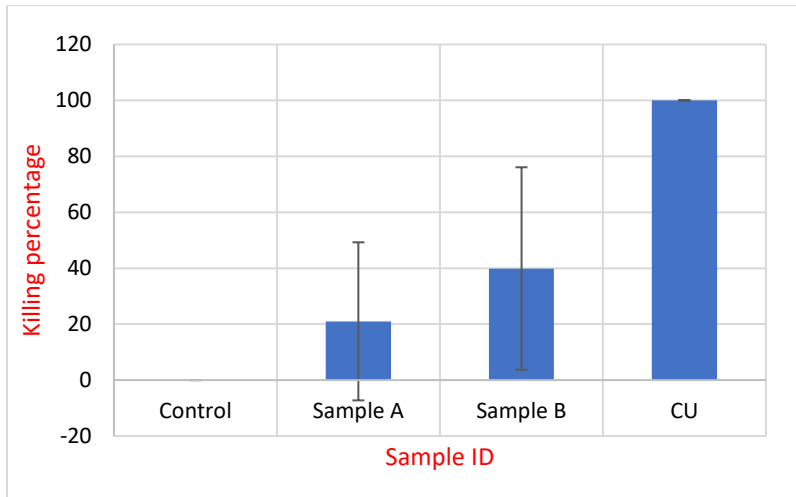


Figure 3.6: Killing percentage of *P. aeruginosa* calculated on samples using Protocol 2

Similar to the EPA protocol, it is observed that Sample B showed slightly higher antimicrobial efficacy compared to sample A for both *E. coli* and *Pseudomonas aeruginosa* with mean killing percentage of 22.3% or *E. coli* on sample B compared to the mean killing percentage of 13.7% for *E. coli* on sample A. Also, the mean killing percentage for *Pseudomonas aeruginosa* is recorded as 39.9% for sample B and 21.0% for sample A.

3.5.4 Stamping Protocols

A “stamping technique” was developed to provide a consistent comparison between the surfaces, under controlled conditions. Surfaces are contaminated with a microbial culture, then gently “stamped” onto an agar plate surface for a period of time.

3.5.4.1 “Straight stamping”- Protocol 3

After applying bacteria onto the surfaces, the samples were inverted onto the agar plate surface, left for 1 hour contact time, then surface is removed and plate incubated overnight. This represents a nutrient-rich/soiled environment.

The antimicrobial efficacy of sample A and B against *E. coli* and *Pseudomonas aeruginosa* was determined using the Protocol 3. Five replicates were obtained with plastic used as the negative control and pure copper surface used as positive control. The average killing percentages were calculated and compared as shown in Figure 3.7 for *E. coli* and Figure 3.8 for *Pseudomonas aeruginosa*.

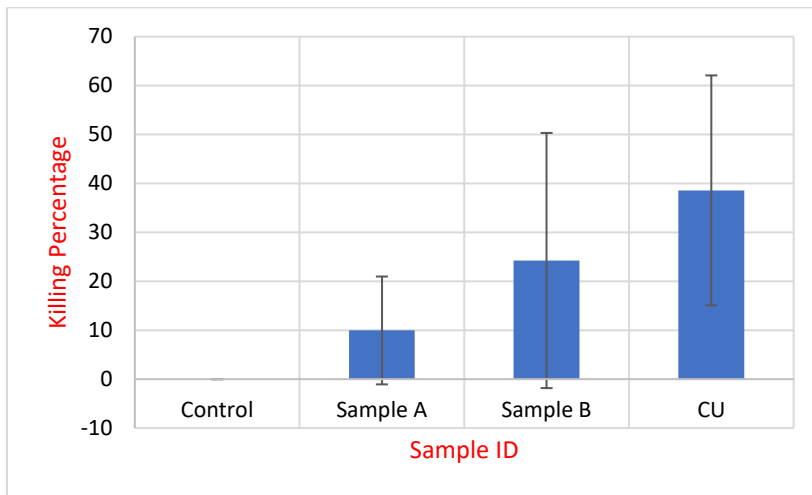


Figure 3.7: Killing percentage of *E. coli* calculated on samples using Protocol 3

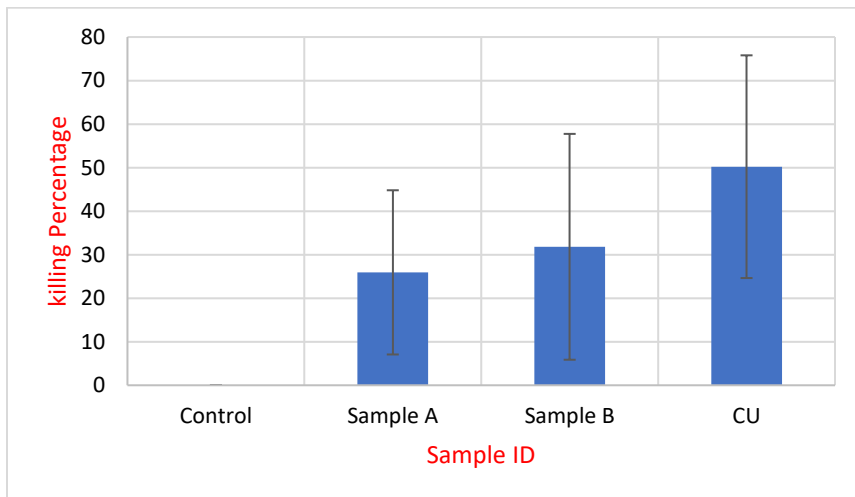


Figure 3.8: Killing percentage of *P. aeruginosa* calculated on samples using Protocol 3

Similar to the EPA protocol and protocol 2, it is observed that sample B showed slightly higher antimicrobial efficacy compared to sample A for both *E. coli* and

Pseudomonas aeruginosa with mean killing percentage of 24.2% for *E. coli* on sample B compared to the mean killing percentage of 9.95% for *E. coli* on sample A. Also, the mean killing percentage for *Pseudomonas aeruginosa* is recorded as 31.8% for sample B and 25.9% for sample A. However, copper does totally exhibit the growth of bacteria when this protocol is applied and shows a mean killing percentage of 38.6% for *E. coli* and 50.2% for *Pseudomonas aeruginosa*.

3.5.4.2 “1-hour contact”- Protocol 4

Bacteria was applied to surfaces and left in contact for 1 hour, then stamped onto the agar surface, and grown overnight. This represents a harsher, unsoiled environment. The antimicrobial efficacy of sample A and B against *E. coli* and *Pseudomonas aeruginosa* was determined using the Protocol 4.

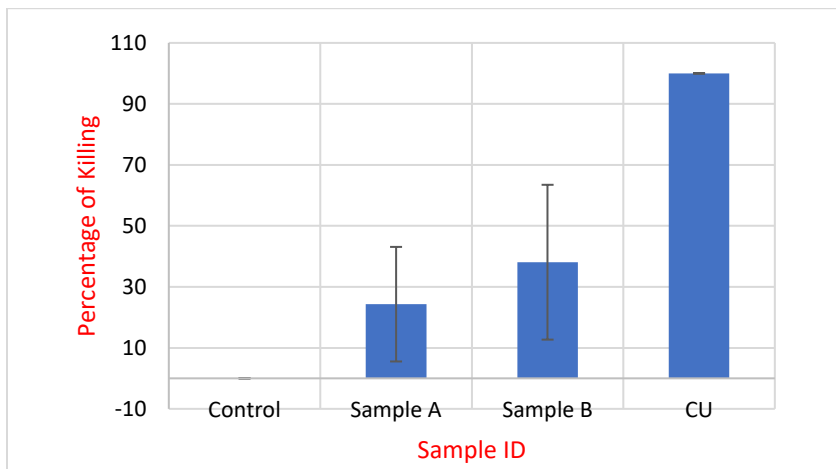


Figure 3.9: Killing percentage of *E. coli* calculated on samples using Protocol 4

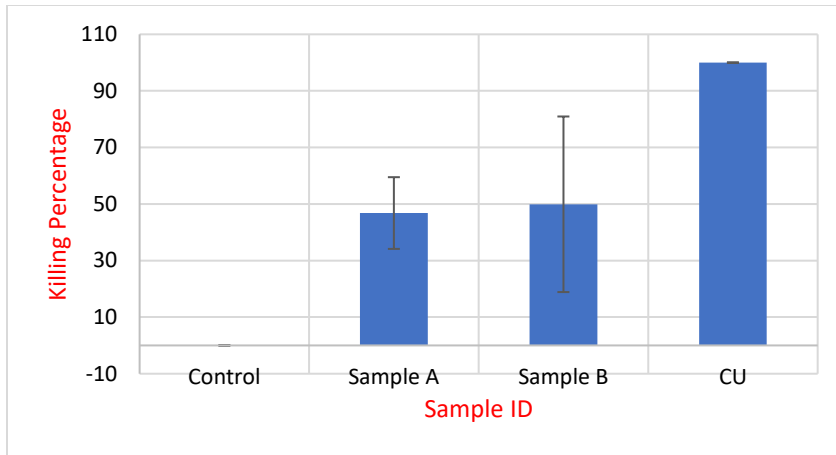


Figure 3.10: Killing percentage of *P. aeruginosa* calculated on samples using Protocol 3

Similar to the previously investigated protocols, it is observed that sample B showed slightly higher antimicrobial efficacy compared to sample A for both *E. coli* and *Pseudomonas aeruginosa* with mean killing percentage of 38.08% for *E. coli* on sample B compared to 24.32% for *E. coli* on sample A. Also, the mean killing percentage for *Pseudomonas aeruginosa* is recorded as 41.91% for sample B and 46.81% for sample A.

3.5.5 Comparison Between different Protocols

3.5.5.1 Comparison between EPA protocol results and Protocol 2 results

The antimicrobial efficacy results of both test samples on *E. coli* and *P. aeruginosa* were compared when protocol 1 (EPA protocol) and protocol 2 was used, as shown in the figures below.

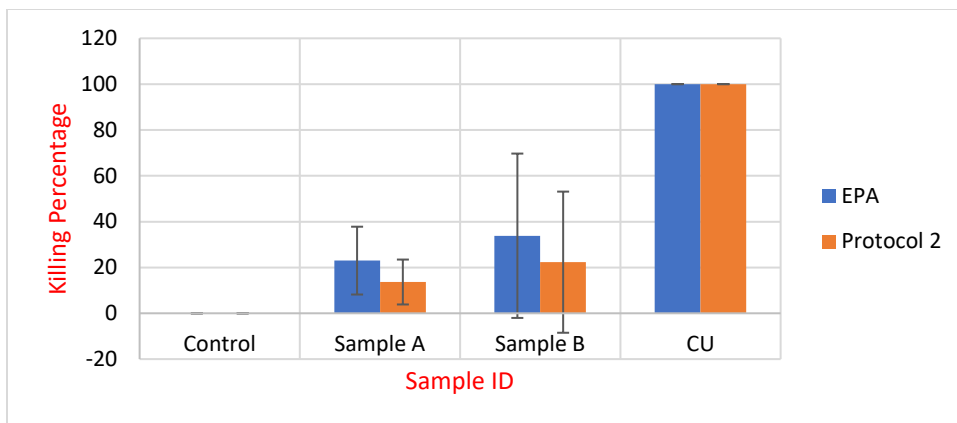


Figure 3.11: Comparison of killing percentage of *E. coli* between EPA protocol and Protocol 2

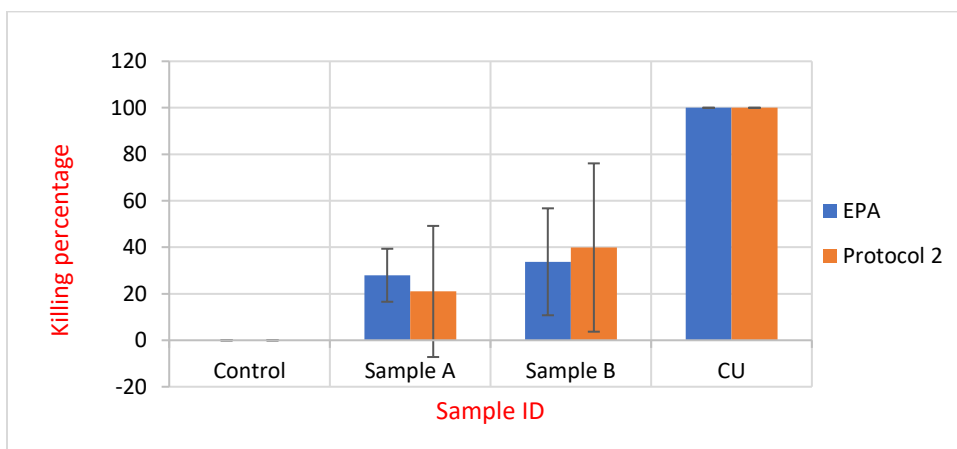


Figure 3.12: Comparison of killing percentage of *P. aeruginosa* between EPA protocol and Protocol 2

In Figure 3.11, a comparison between the results of the EPA protocol and protocol 2 showing the antimicrobial efficacy of samples A and B against *E. coli* is seen. When comparing the mean killing percentages of *E. coli* of both protocols, the EPA protocol has mean killing percentages of 22.9 ± 14.8 and 33.8 ± 35.9 for sample A and sample B respectively, while the protocol 2 has mean killing percentages of 13.7 ± 9.84 and 22.3 ± 30.8 respectively. The coefficient of variation for the killing percentage of the EPA protocol is calculated as 0.64 and 1.06 for sample A and sample B respectively but while using protocol 2, it is calculated as 0.72 and 1.38 respectively.

In Figure 3.12, a comparison between the results of the EPA protocol and protocol 2 showing the antimicrobial efficacy of samples A and B against *Pseudomonas aeruginosa* is seen. When comparing the mean killing percentages of *Pseudomonas aeruginosa* of both protocols, the EPA protocol has mean killing percentages of 27.9 ± 11.5 and 33.8 ± 23.1 for sample A and sample B respectively, while the protocol 2 has mean killing percentages of 21.0 ± 28.3 and 39.9 ± 36.2 respectively. The coefficient of variation for the killing percentage of the EPA protocol is calculated as 0.41 and 0.68 for sample A and sample B respectively but while using protocol 2, it is calculated as 1.35 and 0.91 respectively. This shows that protocol 2 has more variation relative to its mean compared to the EPA protocol for killing percentage evaluation.

This variability could be explained due to inherent variability which would occur from retrieval of bacterial solution with the pipette. This is an indication of why the sonication step is helpful in reproducibly releasing microbes from the surface. Table 3.0 and 3.1 below shows a summary for comparison of the antimicrobial efficacy results between the EPA protocol and protocol 2 for *E. coli* and *P. aeruginosa*, respectively.

Table 3.0: Summary of antimicrobial efficacy results for *E. coli* between EPA protocol and protocol 2

		Killing Percentage		
		Mean	SD	CV
EPA	Control	0	0	0
	Sample A	22.99	14.81	0.64
	Sample B	33.84	35.86	1.06
	Copper	100	0	0
Protocol 2	Control	0	0	0
	Sample A	13.66	9.84	0.72
	Sample B	22.31	30.82	1.38
	Copper	100	0	0

Table 3.1: Summary of antimicrobial efficacy results for *P. aeruginosa* between EPA protocol and protocol 2

		Killing Percentage		
		Mean	SD	CV
EPA	Control	0	0	0
	Sample A	27.97	11.46	0.41
	Sample B	33.75	23.06	0.68
	Copper	100	0	0
Protocol 2	Control	0	0	0
	Sample A	21.0	28.27	1.35
	Sample B	39.9	36.21	0.91
	Copper	100	0	0

3.5.5.2 Comparison between EPA protocol results and Protocol 3 results

The antimicrobial efficacy results of both test samples on *E. coli* and *P. aeruginosa* were compared when protocol 1 (EPA protocol) and protocol 3 (stamped contact with agar surface) was used. Bacteria growth (*E. coli* and *P. aeruginosa*) was observed for the pure copper surface when using protocol 3 and this is attributed to the fact that this protocol is conducted in a ‘nutrient rich’ environment, hence making the copper surface less effective. This is perhaps due to the fact that copper complexes with other organics on contact, thus removing some of the available ions so that biocidal action is reduced.

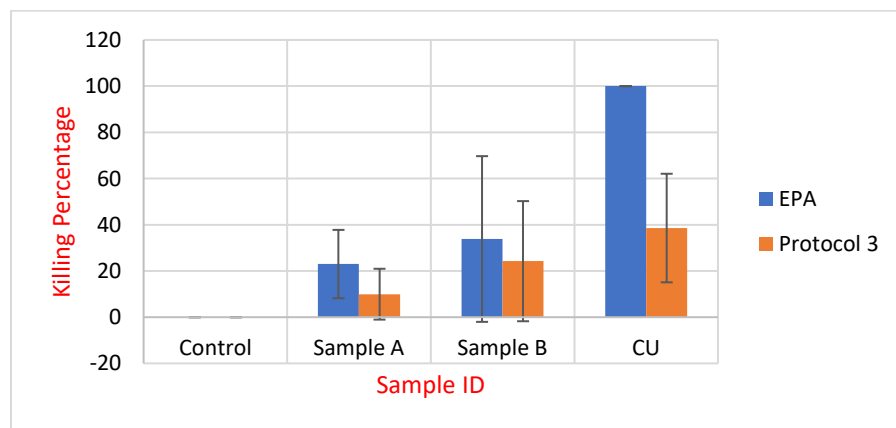


Figure 3.13: Comparison of killing percentage of *E. coli* between EPA protocol and Protocol 3

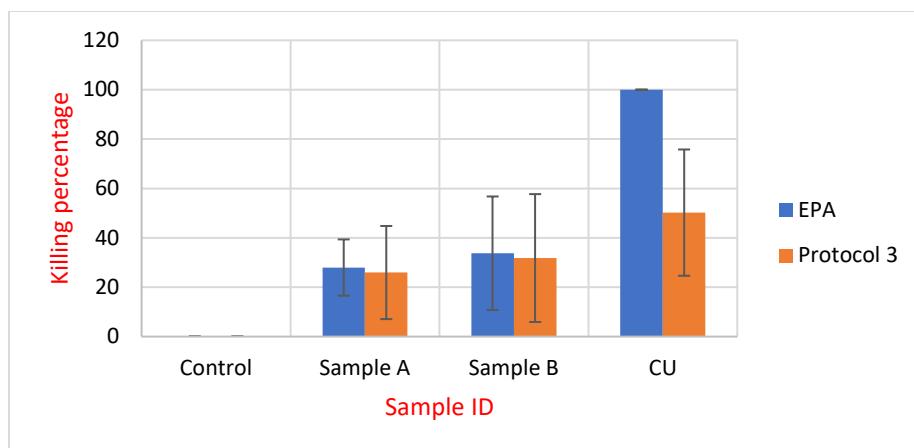


Figure 3.14: Comparison of killing percentage of *P. aeruginosa* between EPA protocol and Protocol 3

In Figure 3.13, a comparison between the results of the EPA protocol and protocol 3 showing the antimicrobial efficacy of Samples A and B against *E. coli* is seen. When comparing the mean killing percentages of *E. coli* of both protocols, the EPA protocol has mean killing percentages of 22.9±14.8, 33.8±35.9 and 100 percent for Sample A, Sample B and copper respectively, while the protocol 3 has mean killing percentages of 9.95±11.0, 24.2±26.1 and 38.6±23.5 respectively. The coefficient of variation for the killing percentage of the EPA protocol is calculated as 0.64, 1.06 and 0 for Sample A, Sample B and copper respectively but while using protocol 3, it is calculated as 1.11, 1.08 and 0.61 respectively.

In Figure 3.14, a comparison between the results of the EPA protocol and protocol 3 showing the antimicrobial efficacy of samples A and B against *Pseudomonas aeruginosa* is seen. When comparing the mean killing percentages of *Pseudomonas aeruginosa* of both protocols, the EPA protocol has mean killing percentages of 27.9±11.5, 33.8±23.1 and 100 percent for Sample A, Sample B and copper respectively, while the protocol 3 has mean killing percentages of 25.9±18.8, 31.8±25.9 and 50.2±25.6

respectively. The coefficient of variation for the killing percentage of the EPA protocol is calculated as 0.41, 0.68 and 0 for Sample A, Sample B and copper respectively but while using protocol 3, it is calculated as 0.73, 0.81 and 0.51 respectively. This shows that protocol 3 has more variation relative to its mean compared to the EPA protocol for killing percentage evaluation. Table 3.2 and 3.3 below shows a summary for comparison of the antimicrobial efficacy results between the EPA protocol and protocol 3 for *E. coli* and *P. aeruginosa*, respectively.

Table 3.2: Summary of antimicrobial efficacy results for *E. coli* between EPA protocol and protocol 3

		Killing Percentage		
		Mean	SD	CV
EPA	Control	0	0	0
	Sample A	22.99	14.81	0.64
	Sample B	33.84	35.86	1.06
	Copper	100	0	0
Protocol 3	Control	0	0	0
	Sample A	9.95	11.02	1.11
	Sample B	24.24	26.07	1.08
	Copper	38.58	23.50	0.61

Table 3.3: Summary of antimicrobial efficacy results for *P. aeruginosa* between EPA protocol and protocol 3

		Killing Percentage		
		Mean	SD	CV
EPA	Control	0	0	0
	Sample A	27.97	11.46	0.41
	Sample B	33.75	23.06	0.68
	Copper	100	0	0
Protocol 3	Control	0	0	0
	Sample A	25.94	18.86	0.73
	Sample B	31.81	25.94	0.82
	Copper	50.21	25.58	0.51

3.5.5.3 Comparison between EPA protocol results and Protocol 4 results

The antimicrobial efficacy results of both test samples on *E. coli* and *P. aeruginosa* were compared when protocol 1 (EPA protocol) and protocol 4 (stamping on agar after 1-hour contact) was used, shown in the figures below.

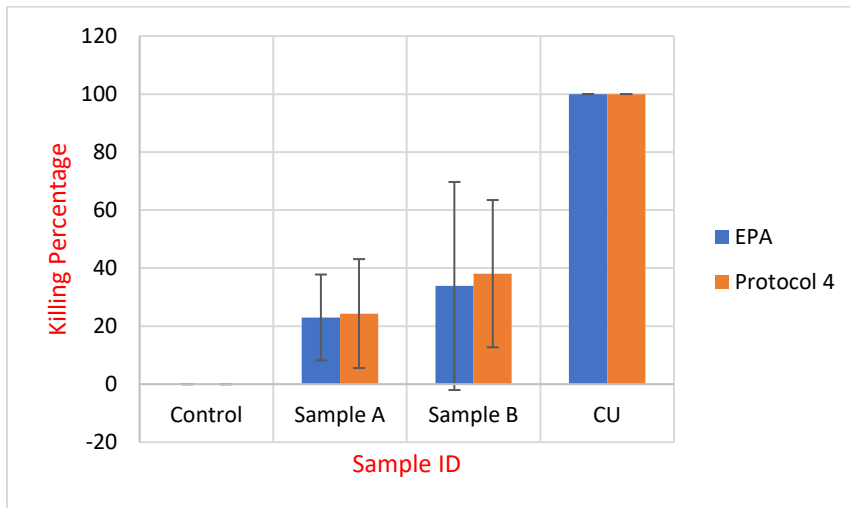


Figure 3.15: Comparison of killing percentage of *E. coli* between EPA protocol and Protocol 4

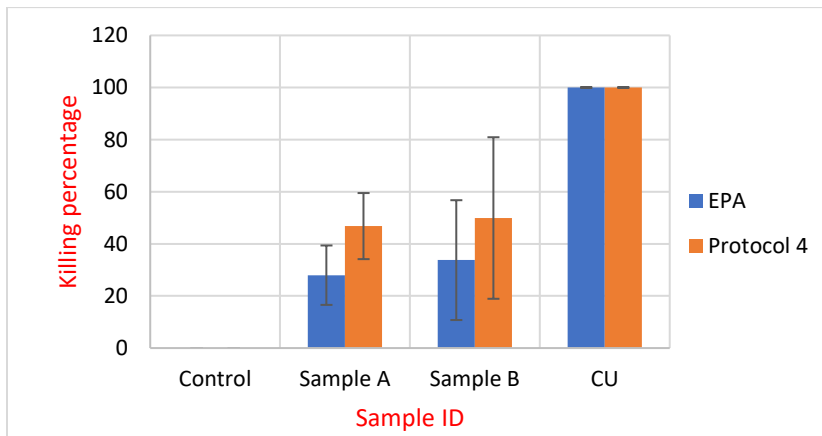


Figure 3.16: Comparison of killing percentage of *P. aeruginosa* between EPA protocol and Protocol 4

In Figure 3.15, a comparison between the results of the EPA protocol and protocol 4 showing the antimicrobial efficacy of samples A and B against *E. coli* is seen. When comparing the mean killing percentages of *E. coli* of both protocols, protocol 4 has mean killing percentages of 24.3±18.8 and 38.1±25.4 for Sample A and Sample B respectively.

The coefficient of variation for the killing percentage using protocol 4 is calculated as 0.78 and 0.67 respectively.

In Figure 3.16, a comparison between the results of the EPA protocol and protocol 4 showing the antimicrobial efficacy of samples A and B against *Pseudomonas aeruginosa* is seen. When comparing the mean killing percentages of *Pseudomonas aeruginosa* of both protocols, protocol 4 has mean killing percentages of 46.8 ± 12.7 and 49.9 ± 31.0 for Sample A and Sample B respectively. The coefficient of variation for the killing percentage using protocol 4 is calculated as 0.27 and 0.62 respectively. Table 3.4 and 3.5 below shows a summary for comparison of the antimicrobial efficacy results between the EPA protocol and protocol 4 for *E. coli* and *P. aeruginosa*, respectively.

Table 3.4: Summary of antimicrobial efficacy results for *E. coli* between EPA protocol and protocol 4

		Killing Percentage		
		Mean	SD	CV
EPA	Control	0	0	0
	Sample A	22.99	14.8	0.64
	Sample B	33.84	35.86	1.06
	Copper	100	0	0
Protocol 4	Control	0	0	0
	Sample A	24.32	18.78	0.77
	Sample B	38.08	25.38	0.67
	Copper	100	0	0

Table 3.5: Summary of antimicrobial efficacy results for *P. aeruginosa* between EPA protocol and protocol 4

		Killing Percentage		
		Mean	SD	CV
EPA	Control	0	0	0
	Sample A	27.97	11.46	0.41
	Sample B	33.75	23.06	0.68
	Copper	100	0	0
Protocol 4	Control	0	0	0

Sample A	46.81	12.68	0.27
Sample B	49.91	31.04	0.62
Copper	100	0	0

3.5.6 Antimicrobial Powder Particles

A technique was developed to evaluate the antimicrobial efficacy of powder particles of copper or copper alloys. Industrially manufactured antimicrobial powder particles were used for this experiment, containing 62% copper and 38% Nickel. The following results were observed for *E. coli*.

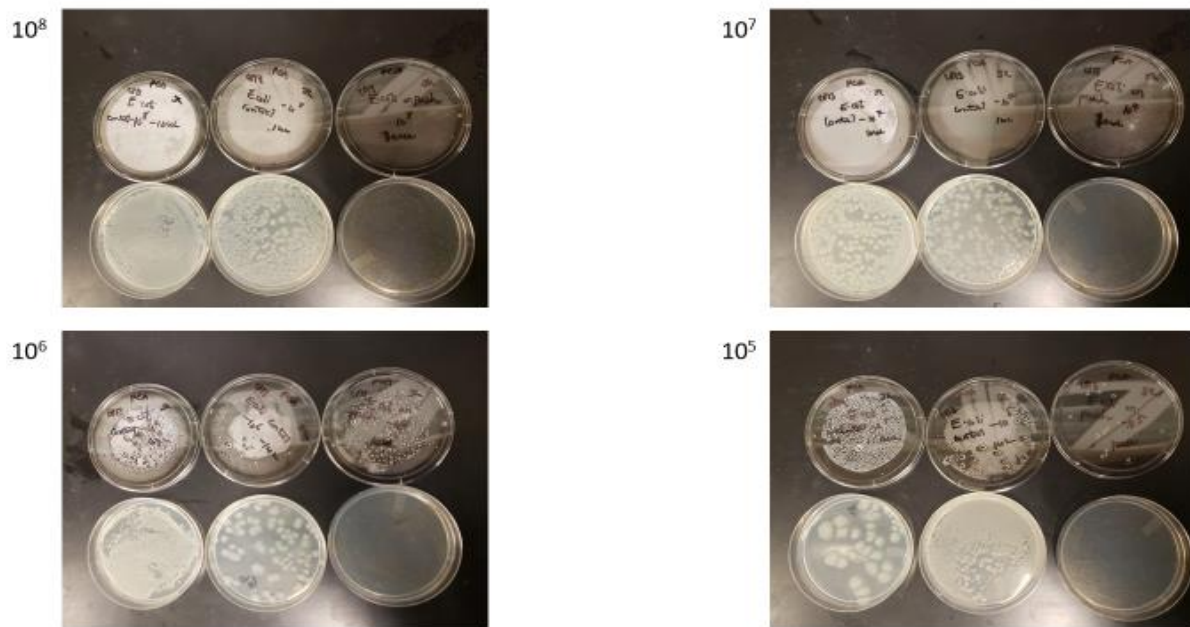
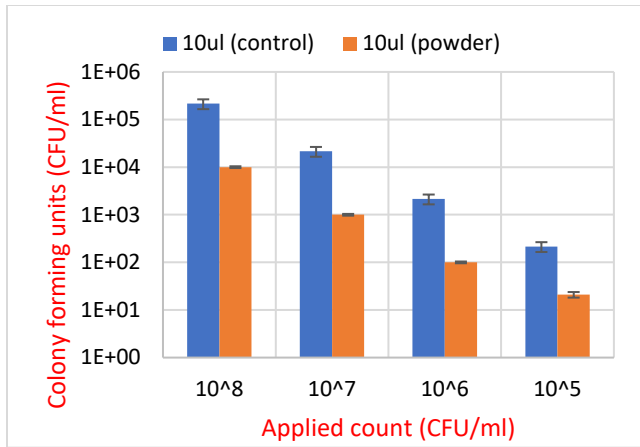
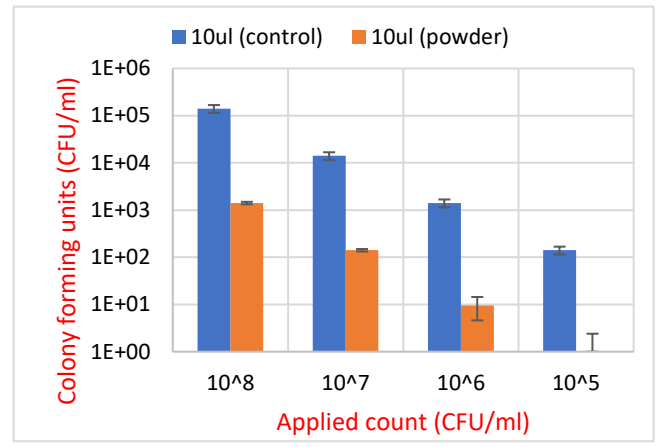


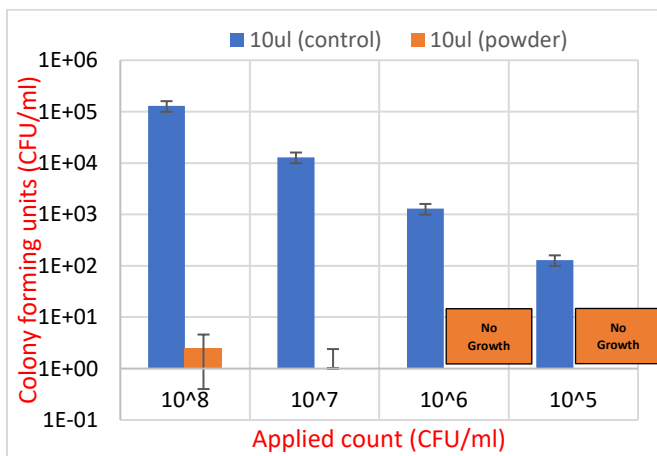
Figure 3.17: Qualitative results of Antimicrobial powder particles efficacy against *E. coli*



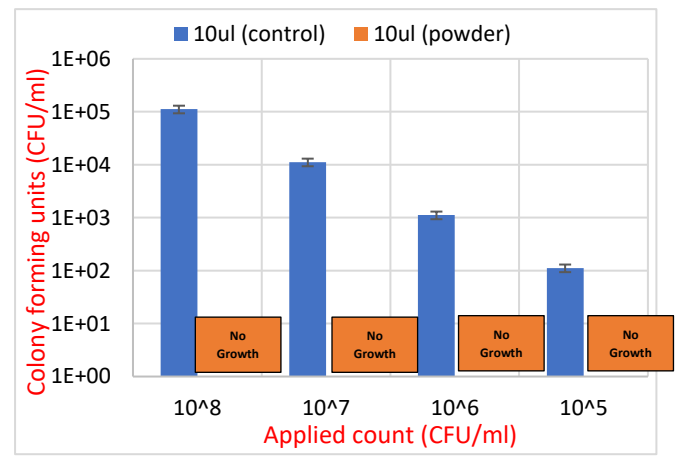
(a)



(b)



(c)



(d)

Figure 3.18: (a) Antimicrobial efficacy of Aereus Shield powder at a loading of 0.13 mg/cm²
 (b) Antimicrobial efficacy of Aereus Shield powder at a loading of 0.25 mg/cm²
 (c) Antimicrobial efficacy of Aereus Shield powder at a loading of 0.38 mg/cm²
 (d) Antimicrobial efficacy of Aereus Shield powder at a loading of 0.45 mg/cm²

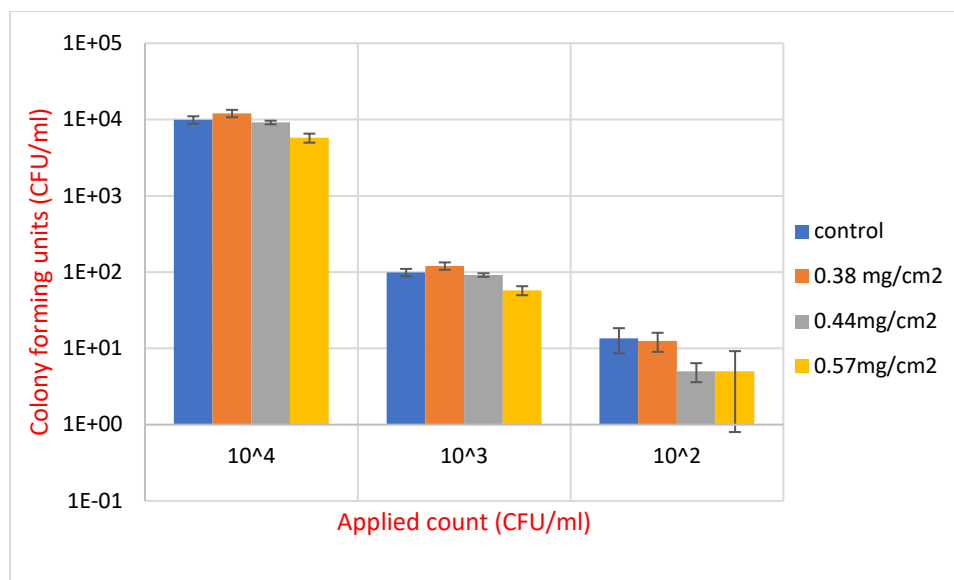


Figure 3.19: Antifungal efficacy of Antimicrobial powder applied at different loadings.

In Figure 3.18, the antimicrobial efficacy of industrially manufactured powder particles against *E. coli* at different concentrations is shown. It was observed that with increasing amount of exposed antimicrobial particles on the agar surface, there was more antimicrobial action on microorganisms. With powder covering about 0.45 mg/cm², it was observed that there was no growth of *E. coli* colony on agar plate even at an initial concentration of 10⁸ CFU/ml. However, for yeast there seems to be little effect on colony growth with increasing amounts of powder as seen in Figure 3.19 suggesting a lack of significant antifungal efficacy of the powder investigated under these conditions.

3.6 Summary and Conclusions

Four different protocols for rapid and accurate determination of antimicrobial efficacy of samples were investigated. Protocol 1, which is similar to the EPA protocol, is a widely used method, which provides consistent results for antimicrobial efficacy testing. When results from the other investigated protocols were compared to the results from the

modified EPA protocol, it was observed that all protocols were accurate in predicting better antimicrobial activity of Sample B over Sample A. However, results from protocol 3 show that a pure copper sample did not achieve 100% killing percentage and maximum log reductions as a result of being conducted in a nutrient rich environment. This means that protocol 3 would not be a very reliable technique to predict the antimicrobial efficacy of samples to correlate with EPA standards. When comparing the coefficient of variation for log reductions and killing percentages for all protocols using *E. coli* and *Pseudomonas aeruginosa*, it is observed that protocol 3 and protocol 2 show the highest variation, meaning that these protocols have a large deviation compared to their mean, suggesting lesser reliability in their results. Protocol 4 has a lower coefficient of variation and accurate comparison with the EPA protocol for both *E. coli* and *Pseudomonas aeruginosa* in log reduction and killing percentage comparison. This suggest that results from obtained from using protocol 4 would be more comparable to the EPA protocol results, reliable and with less variations. The Antimicrobial powder experiment shows that when coating antimicrobial particles on a substrate, depending on the composition of the antimicrobial particles, with greater amount of exposed particle covering the surface area of the substrate, the better the antimicrobial activity of the sample. This approach of sprinkling powder on agar surface can be used to semi-quantitatively determine minimum loadings for good effects and to compare different antimicrobial powders.

Chapter 4

Development of rapid test method for antimicrobial surfaces with flow cytometry

4.1 Overview

The plate counting technique is the most widely used technique for antimicrobial enumeration. It is a reliable protocol, but it is tedious, takes 24 to 48 hours for microbial growth to be observed and depending on the concentration of plated microbial sample, it can be inaccurate for microbial enumeration. In this study, flow cytometry (FCM) techniques were developed which are accurate, faster and allow for rapid antimicrobial efficacy testing of industrially manufactured samples. Results from the developed FCM techniques are compared to plate count results to form a calibration curve, then the developed FCM technique is used to predict log reductions on industrially manufactured antimicrobial surface samples. FCM techniques were developed firstly by staining a microbial solution with calcein AM dye for labelling live cells. Results from this technique showed a correlation with plate count results when the microbial solution used was prepared at 10^4 CFU/ml (for *E. coli* and *P. aeruginosa*) and 10^5 CFU/ml for yeast (*Saccharomyces cerevisiae*) without contact time on an antimicrobial pure copper surface. However, after contact with the surface, the method was significantly affected by copper ion interactions with the dye. Therefore, another technique involving staining with propidium iodide dye, which stains dead cells, after contact with antimicrobial pure copper surfaces at different contact time durations was investigated. Manual gating was applied

to the results for all samples and a correlation was made with plate count results, showing good potential.

4.2 Introduction

Effective evaluation of antimicrobial activity is a serious issue and several methods have been proposed to accurately determine antimicrobial activity. The most common method used by hospitals and in the industry is the agar plate count method for microbial enumeration (Bankier et al. 2018) (Food and Drug Administration, 2014). Agar plate counting allows the determination of bacterial concentrations by the number of colony-forming units (CFUs), assuming that each CFU has grown from one bacterium of the sample (Ou et al. 2017).

This method of enumeration of viable organisms relies entirely on counting visible colonies after spreading enough dilutions of bacterial suspensions on solidified agar media, rather than microscopic counting of individual species (Jepras et al. 1995). One major issue with this method is the long incubation times which can be up to 48 hours, depending on the microorganism being investigated. This technique also does not provide any information on bacterial physiology. The three accepted general parameters for assessing the viability of microbes are intact cell membrane, metabolic activity and reproducibility, but agar-based methods account only for one of those parameters, i.e. reproducibility (Oliver, 2005) (Kumar and Ghosh, 2019).

Agar plate counts include only cells that are culturable under the conditions of the investigation and cannot count dead cells or viable but non-culturable (VBNC) cells, i.e. cells that retain cellular and metabolic activity but are stressed (Bensch et al. 2014) (Ou

et al, 2017). VBNC-state pathogens are known to maintain virulence and can be resuscitated to cause infection under favorable conditions (Amano, 2016).

Cell viability may be determined by morphological changes or by changes in the permeability of the membrane and/or the physiological condition indicated by the exclusion of some dyes or the retention of others (Johnson et al. 2013). Calcein AM is a cell-permeant fluorescent dye that can be used in prokaryotic and eukaryotic cells with an excitation / emission range of 494/517 nm to assess the cell viability. In live cells, calcein AM is converted to green, fluorescent calcein after intracellular ester hydrolysis of acetoxymethyl ester. (SG). Calcein AM is used for distinguishing live cells through the action of intracellular esterase activity (Lilius et al. 1996) (Hendon-Dunn et al. 2016).

Propidium iodide (PI) is a nucleic acid probe that can also be used to determine the viability of microorganisms. PI passes through disrupted cell membranes and intercalates into the RNA and DNA backbone independently of the base pair ratio and the AT-rich region but does not cross through intact cell membranes. (Taylor and Milthorpe 1980) (Crissman et al. 1979) (Chitarra and Van Den Bulk, 2003) (Deere et al 1998). The excitation / emission maxima of propidium iodide is 490/635 nm (Molecular Probes, 2004). A full list of fluorescent dyes can be found in the Molecular probes catalogue (Haugland, 2002) where researchers can find the most appropriate dye for different FCM needs using resources like, the target, the type of cell being studied and the excitation / emission wavelengths of the fluorescent dye (Ambriz-Aviña et al, 2014).

Fluorescent dyes are used in various techniques as a quick way to distinguish between populations and to determine the viability of cells, but results can often be

variable (Berney et al. 2007) (Bankier et al. 2018) (Molecular Probes, 2004). Therefore, it is important to develop an FCM technique for the antimicrobial evaluation of products which is reproducible and correlates with existing plate counting techniques, but with results that are obtained rapidly.

4.3 Materials and Method

4.3.1 Reagents and Materials

Phosphate buffer saline (PBS) tablets were purchased from Sigma-Aldrich (Saint Louis, USA), with one tablet dissolved in 200 ml of deionized water to yield 0.01 M of phosphate buffer. Plate count agar (PCA) and Potato dextrose agar (PDA) were purchased from Difco laboratories (Sparks Glencoe, USA). Lauryl sulfate broth (LSB) was purchased from Sigma-Aldrich (Oakville, Ontario). Potato dextrose broth (PCB) and Cetrimide broth (CB) were both purchased from the Himedia company (Nashik, India). All the microbial species in the study were purchased from Cedarlane Laboratories, Burlington, Ontario. The diode array spectrophotometer is a product of Hewlett Packard, HP 8452A (East Oshawa, Ontario). Ethanol (95%) was purchased from Anachemia, a VWR company (Rochester, New York). Liquinox was used as the liquid detergent for cleaning, purchased from Alconox (White Plains, New York). Propidium Iodide was obtained from the Live/Dead bacteria viability and counting kit containing SYTO9 and PI from Invitrogen by Thermo-Fisher Scientific (Oregon, USA). An Amnis ImageStream flow cytometer was used for flow cytometry analysis for all samples (Texas, USA). Calcein AM was purchased from Invitrogen by Thermo-Fisher Scientific (Oregon, USA). All antimicrobial samples were

produced and provided as non-commercial research samples by Aereus Technologies Inc (Rosemont, Ontario).

4.3.2 Sample Preparation

Samples were soaked in Liquinox solution for 2 hours to degrease them, then rinsed with deionized water and allowed to dry at ambient temperature. After drying, samples were soaked in 95% ethanol for 15 minutes to decontaminate and left to dry in a beaker at room temperature for up to 24 hours.

4.3.3 Microorganism Investigated

The Gram-negative bacteria *Escherichia coli* (ATCC PTA-4752) and *Pseudomonas aeruginosa* (ATCC 15442), and *Saccharomyces cerevisiae* were chosen for investigation.

1) Agar plates and broth preparation: Plate count agar was prepared as stated in Chapter 3 for *E. coli* and *Pseudomonas aeruginosa*. Potato dextrose agar for yeast was prepared by weighing 39 g of powder and suspending in 1000 mL DI water, then heated to boiling to dissolve the medium completely. Potato dextrose broth 24g was dissolved in 1000 ml deionized water. Both were then sterilized by autoclaving at 15 psi pressure (121°C) for 20 minutes. After autoclaving, hot Agar solution was poured into sterile Petri plates in a sterile environment.

2) Microbial cultures: Bacteria were cultured in flasks with 50 ml Cetrimide Broth (for *Pseudomonas aeruginosa*), Plate Count Broth (for *Escherichia coli*) and Potato Dextrose Broth (yeast) at 37°C for 24 hours. To prepare the diluted bacterial solution, 1 ml of the culture was pipetted from the cultured flask into a 1.5 ml microcentrifuge tube. After

washing twice with PBS water, the microbial solution was adjusted to 10^8 (for bacteria) and 10^6 CFU/ml (for yeast) by analyzing with a UV spectrophotometer, where the absorbance reading was measured and recorded at 0.2 (for bacteria) and 0.6 (for yeast) with wavelength at 600 nm. Serial dilutions were made.

4.4 Standardization of protocol using Calcein AM dye

4.4.1 Experimental Procedure

The development of this protocol to correlate with plate counting results was carried out by conducting a series of experiments in a trial-and-error fashion. Different dye staining times and concentrations in bacterial dilutions were investigated to determine the best correlation with plate count results. The final developed procedure for this protocol is reported as follows.

- After microbial cultures had been prepared, serial dilutions of 10^6 , 10^5 , 10^4 and 10^3 CFU/ml were made.
- 100 μ l was collected using a pipette from each dilution and put in a 1.5 ml microcentrifuge tube, then stained with 1 μ l of calcein AM dye representing a 100:1 staining ratio.
- Stained samples were allowed for a staining time of 2 hours and 1.5 hours for bacteria and yeast, respectively, then samples were analysed using the flow cytometer.
- 10 μ l and 100 μ l were collected from unstained samples and plated.
- Agar plates were incubated for 24 to 48 hours and colony growth was counted after incubation

After plate count (PC) results were correlated with flow cytometry (FCM) results, another experimental procedure was developed to compare plate count results with FCM results after the microbial solution has been exposed to an antimicrobial (copper) surface. The protocol investigated is as follows.

- After microbial cultures had been prepared and dilutions made, 300 μl was placed on a prepared pure copper surface for 30 minutes contact time.
- After the contact time, the solution was retrieved using a pipette and 100 μl was collected from the retrieved solution, then put in a 1.5 ml microcentrifuge tube,
- Retrieved microbial solution was stained with 1 μl of calcein AM dye representing a 100:1 staining ratio.
- Stained samples were allowed for a staining time of 2 hours and 1.5 hours for bacteria and yeast respectively, then samples are analysed using the flow cytometer.
- 10 μl and 100 μl were collected from unstained samples and plated.
- Agar plates were incubated for 24 to 48 hours and colony growth was counted after incubation

4.5 Results and Discussion

4.5.1 *Escherichia coli*

During sample analysis of *E. coli* with the flow cytometer, calcein AM is excited by the 488 nm laser line and the emission is recorded in channel 2 with wavelength of 480-560 nm. The brightfield was set at channel 6 and the laser brightness was set at 1.5 mW. Each sample was 'acquired' and stopped after 10 μl had been taken for data analysis.

The emission wavelength of calcein AM (520nm) falls within the band limit for emission on channel 2 (505-560nm). This implies that cells that show calcein AM fluorescence will appear on channel 2. Also, the 'brightfield' for this analysis was set at channel 6. This means that signals from every event which was analysed at the interrogation point by the flow cytometer would appear on channel 6, regardless of fluorescence.

A plot of raw maximum (max) pixel in channel 6 is plotted (on the Y-axis) against raw max pixel in channel 2 (on the X-axis) using the IDEAS v6.2 software (shown in appendix section). Raw max pixel is the intensity value of the brightest pixel in an image with no background-subtraction (Inspire, 2012). Manual gating was then applied to distinguish between live cells (cells that showed calcein AM fluorescence) from other events. This gating method was kept constant for all replicates and the data collected for different *E. coli* concentrations analyzed by FCM with replicates are shown in Table 4.0 – 4.3 below.

Table 4.0: FCM results of Log 6 *E. coli* stained with calcein AM

Population	Replicate 1	Replicate 2	Replicate 3
	Count	Count	Count
All	315	307	315
Live cells <i>E. coli</i> log 6	96	20	96

Table 4.1: FCM results of Log 5 *E. coli* stained with calcein AM

Population	Replicate 1	Replicate 2	Replicate 3
	Count	Count	Count

All	222	83	222
Live cells <i>E. coli</i> log 5	15	13	13

Table 4.2: FCM results of Log 4 *E. coli* stained with calcein AM

Population	Replicate 1	Replicate 2	Replicate 3
	Count	Count	Count
All	146	143	148
Live cells <i>E. coli</i> log 4	15	83	15

Table 4.3: FCM results of Log 3 *E. coli* stained with calcein AM

Population	Replicate 1	Replicate 2	Replicate 3
	Count	Count	Count
All	151	72	151
Live cells <i>E. coli</i> log 3	10	13	10

During sample data analysis, it was determined that cells existing within the defined gate showed fluorescence and were classified as live cells, then used to correlate with plate count results after three replicates were obtained (the FCM results can be found in the appendix section). Figure 4.0 shows a comparison between the results obtained from both FCM and PC techniques for *E. coli*.

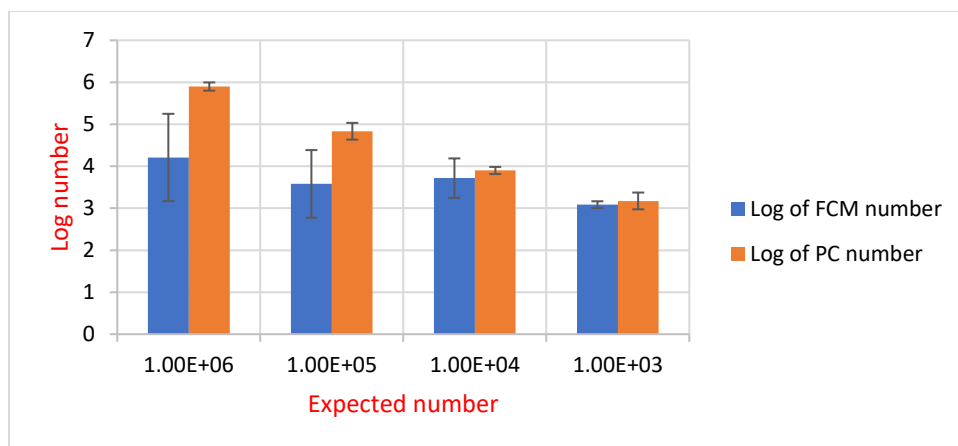


Figure 4.0: Correlation between PC results and FCM results for *E. coli*

Log number for plate count was determined by calculating the logarithm (in base 10) of the colony forming units (CFU/ml) determined from growth on the agar plate, while Log number for FCM was determined by calculating the logarithm (in base 10) of cells that occurred within the defined gate.

As shown in Figure 4.0, it is observed that when comparing results from both techniques, there is underestimation by FCM for log 5 and log 6. However, the values for log 3 and log 4 are comparable for both techniques, with smaller deviation at log 3. This means that the best comparison for both techniques using this technique is recorded when the bacteria concentration is prepared and diluted to 10^3 or 10^4 CFU/ml.

4.5.2 *Pseudomonas aeruginosa*

Sample analysis of *Pseudomonas aeruginosa* with the flow cytometer, was conducted using the same procedure and settings as *E. coli*. Manual gating was applied and kept constant to as previously discussed (see appendix section for all FCM plots for *P. aeruginosa*). The data collected for each bacteria concentration analyzed by FCM for *P. aeruginosa* with replicates are shown in Table 4.4 – 4.7 below.

Table 4.4: FCM results of Log 6 *P. aeruginosa* stained with calcein AM

Population	Replicate 1	Replicate 2
	Count	Count
All	2924	1616
Live cells <i>P. aeruginosa</i> log 6	1758	879

Table 4.5: FCM results of Log 5 *P. aeruginosa* stained with calcein AM

Population	Replicate 1	Replicate 2
	Count	Count
All	1421	901
Live cells <i>P. aeruginosa</i> log 5	220	148

Table 4.6: FCM results of Log 4 *P. aeruginosa* stained with calcein AM

Population	Replicate 1	Replicate 2
	Count	Count
All	669	671
Live cells <i>P. aeruginosa</i> log 4	93	57

Table 4.7: FCM results of Log 3 *P. aeruginosa* stained with calcein AM

Population	Replicate 1	Replicate 2
	Count	Count
All	509	561
Live cells <i>P. aeruginosa</i> log 3	36	12

During sample data analysis, like with the previous case, it was determined that cells existing within the defined gate showed fluorescence and were classified as live

cells, then used to correlate with plate count results. Figure 4.1 shows a comparison between the results obtained from both FCM and PC techniques for *P. aeruginosa*.

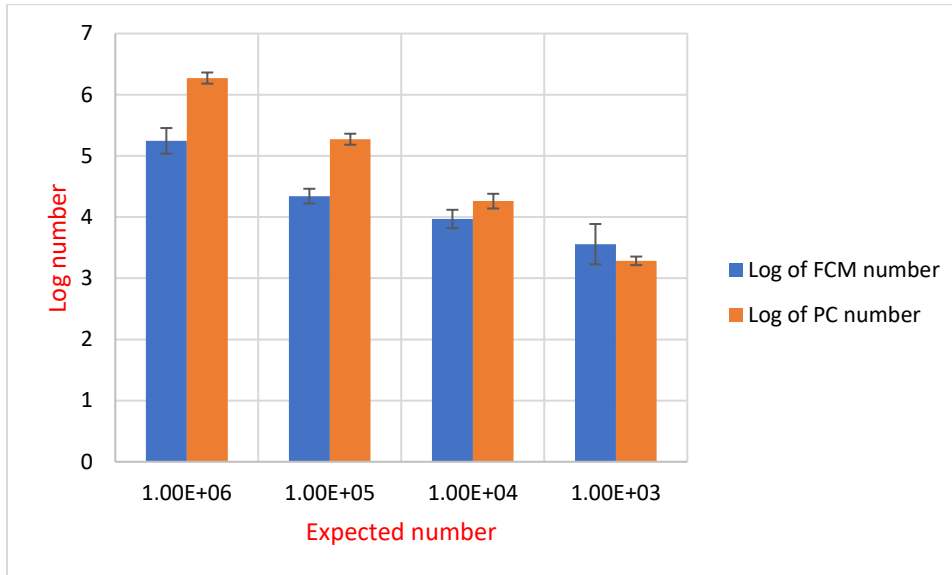


Figure 4.1: Correlation between PC results and FCM results for *P. aeruginosa*

As shown in Figure 4.1, it was observed that when comparing results from both techniques, there is an underestimation by FCM for log 5 and log 6. However, the values for log 3 slightly overestimate and log 4 slightly underestimate, with smaller deviation at Log 4. This means that the best comparison for both techniques using this technique is recorded when bacteria concentration is prepared and diluted to 10^3 or 10^4 CFU/ml.

It is also possible that perhaps a non-linear relationship between FCM and plate count exists using this method. So, deriving a calibration curve to convert FCM to plate count results using a quadratic relationship could be possible. However, there is insufficient data to investigate this assumption and is beyond the scope of this thesis.

4.5.3 *Saccharomyces cerevisiae*

Sample analysis of yeast (*Saccharomyces cerevisiae*) with the flow cytometer, was conducted using the same procedure and settings as the previously investigated microbes. (see appendix section for FCM plots for yeast). The data collected for each culture concentration analyzed by FCM for yeast with replicates are shown in Table 4.8 – 4.11 below.

Table 4.8: FCM results of Log 6 yeast stained with calcein AM

Population	Replicate 1	Replicate 2	Replicate 3
	Count	Count	Count
All	36	10093	41
Live cells yeast log 6	3	724	35

Table 4.9: FCM results of Log 5 yeast stained with calcein AM

Population	Replicate 1	Replicate 2	Replicate 3
	Count	Count	Count
All	48	1950	377
Live cells yeast log 5	4	54	27

Table 4.10: FCM results of Log 4 yeast stained with calcein AM

Population	Replicate 1	Replicate 2	Replicate 3
	Count	Count	Count
All	32	16	76
Live cells yeast log 4	5	13	19

Table 4.11: FCM results of Log 5 yeast stained with calcein AM

Population	Replicate 1	Replicate 2	Replicate 3
	Count	Count	Count
All	44	6	130
Live cells yeast log 3	1	5	17

During sample data analysis, like with previous cases, cells existing within the defined gate showed fluorescence and were classified as live cells, kept constant and then used to correlate with plate count results. Figure 4.2 shows a comparison between the results obtained from both FCM and PC techniques for yeast.

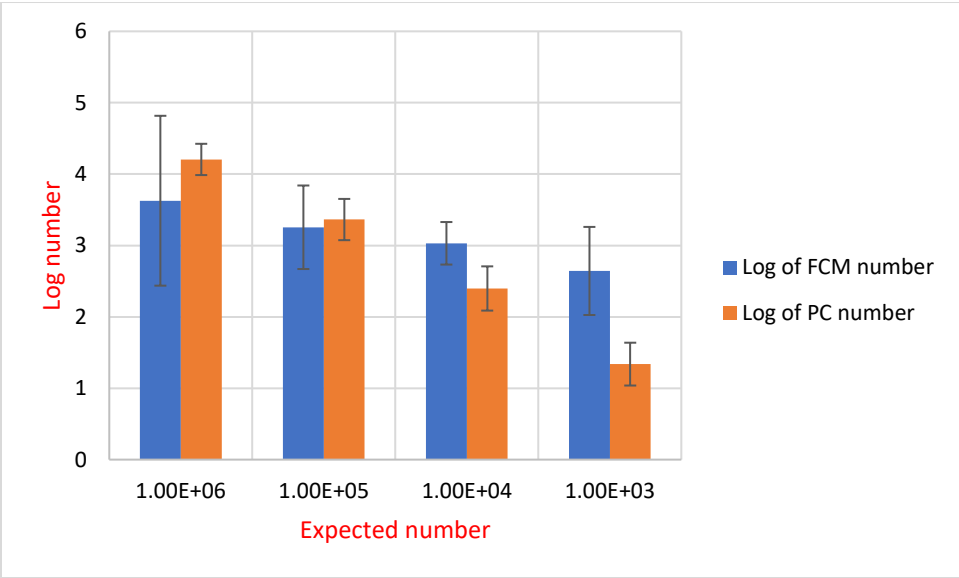


Figure 4.2: Correlation between PC results and FCM results for yeast

As shown in Figure 4.2, it is observed that, there is underestimation by FCM for log 6 but overestimation at log 3 and slightly at log 4. However, the values for log 5 compares favourably with plate count results. This means that the best comparison for both techniques using this technique is recorded when yeast concentration is prepared and diluted to 10⁵ CFU/ml.

4.5.4 Calibration Curve of FCM and Plate Count results after exposure to pure copper surface

To predict the antimicrobial efficacy of samples using FCM, experiments were conducted by applying microbial solution on a test surface (copper) for a certain contact time, then solution was retrieved and stained with calcein AM before flow cytometer analysis. It was determined from previous work that the optimal bacterial concentration that gives the closest correlation between both protocols is at log 4 for all investigated microbial species. So, all prepared microbial solutions were diluted to 10^4 before applying onto a test surface, staining and FCM analysis. Table 4.12 shows the FCM data for *E. coli* applied on both plastic control surface and copper surface after manual gating has been applied to determine live cells.

Table 4.12: FCM data for *E. coli* applied on plastic control and copper surface, stained with calcein AM

Population	Count (control)	Count (copper)
All	35	21
Live <i>E. coli</i> log 4 cells on surface	4	1

These results obtained from the FCM data was then used to compare with plate counting results. This comparison is shown in Table 4.13 and Figure 4.3 below.

Table 4.13: Comparison between PC and FCM results for *E. coli* on antimicrobial surface

	Plastic control	CU surface
flow cytometric number (CFU/ml)	400	100
plate count number (CFU/ml)	6710	270
log of flow cytometry number	2.60	2
Log plate count number	3.83	2.43
FCM log reduction		0.60

PC log reduction		1.39
------------------	--	------

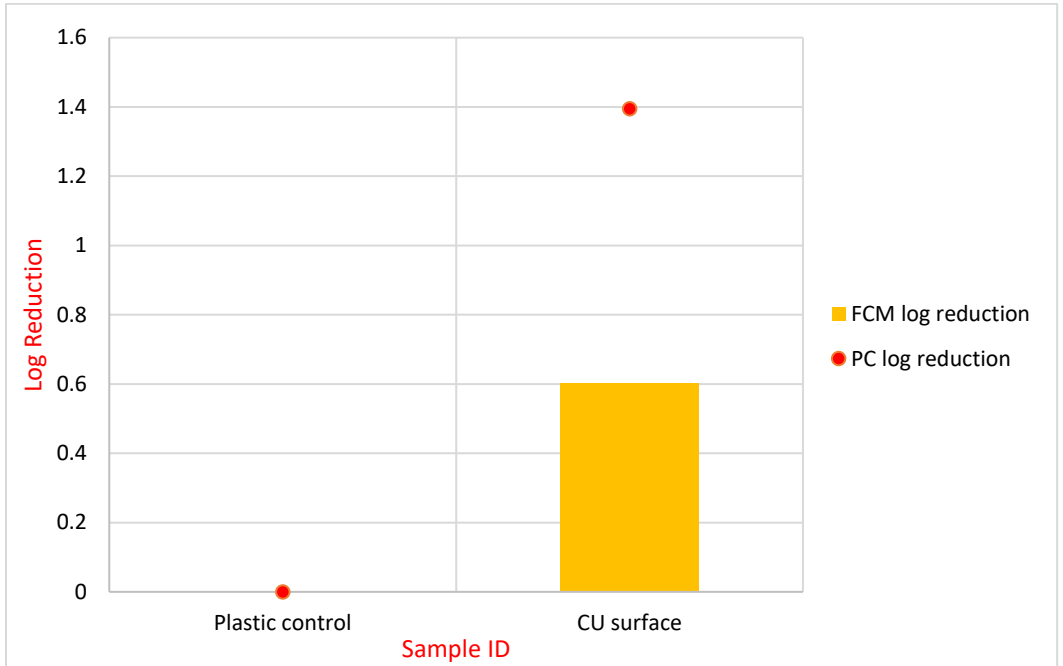


Figure 4.3: Comparison between PC and FCM results for *E. coli* on copper surface

It is observed from Figure 4.3 that the log reduction results of *E. coli* on copper with respect to a plastic control surface using the plate count technique is recorded at 1.395 while FCM techniques is recorded at 0.602, this shows that the FCM technique highly underestimates the results. It was also discovered that Cu^{2+} ions will quench the fluorescence of calcein AM (Invitrogen. Molecular probes: The Handbook).

This phenomenon was briefly investigated by applying *E. coli* solution on pure copper surfaces for 5 minutes and 120 minutes contact times. Samples were then stained with calcein AM at a 100:1 staining ratio and analyzed using flow cytometry. A fluorescent intensity plot against the number of events was made (shown in appendix section) and gate (R1) was made, with fluorescent events occurring within R1. This was done to determine the potential interference of copper ions with calcein AM staining. The data

collected for all analyzed cells and cells occurring within the determined R1 gate is shown in Table 4.14 below.

Table 4.14: *E. coli* applied on copper surface for 5 and 120 minutes, stained with Calcein AM

Population	Count (5 mins)	%Gated (5 mins)	Count (120 mins)	%Gated (120 mins)
All	1000	100	1000	100
R1	13	1.3	4	0.4

In Table 4.14, it is observed that for *E. coli* solution stained with calcein AM after contact with a pure copper surface for 5 minutes, there were just 13 fluorescent events (occurring with the defined R1 region), corresponding to 1300 CFU/ml. After 120 minutes of contact, there were 4 fluorescent events, corresponding to 400 CFU/ml. The corresponding plate counts was recorded as 6400 CFU/ml for 5 minutes and no colony growth recorded after 120 minutes. The lack of calcein AM fluorescence could be because of the copper ions that are present in the solution.

Due to the potential significant interference by copper on calcein AM fluorescence, this protocol might not be applicable for determining the antimicrobial efficacy of industrially manufactured surfaces containing copper but could be potentially used for silver treated surface. There is no evidence from literature that calcein AM fluorescence is interfered with by silver. To avoid the copper interference issue, a protocol involving staining with propidium iodide was tested as it was not believed to be susceptible to copper effects.

4.6 Standardization of protocol using Propidium Iodide

4.6.1 Experimental Procedure

- After a yeast culture was prepared, 300 μl of 10^6 CFU/ml yeast was placed on a prepared pure copper surface and plastic control for contact times of 120 minutes, 60 minutes, 30 minutes and 10 minutes.
- After the contact time, solution was retrieved using a pipette and 100 μl was collected from the retrieved solution, then put into a 1.5 ml microcentrifuge tube,
- Retrieved microbial solution was stained with 2 μl of propidium iodide dye representing a 50:1 staining ratio.
- Stained samples were allowed to sit for a staining time of 30 minutes, then samples were analysed using the flow cytometer.
- 10 μl and 100 μl were collected from unstained samples and plated.
- Agar plates were incubated for 48 hours and colony growth on agar plate was counted after incubation

A protocol using FCM technique was developed to more rapidly predict the antimicrobial efficacy of samples that corresponds to plate count results for yeast. This technique involved applying yeast culture on a copper and a control surface, allowing for contact time then staining with propidium iodide (PI) before analysing with a flow cytometer.

During sample analysis with the flow cytometer, propidium iodide is excited by the 488 nm laser line and emission is recorded in channel 5 with wavelength of 642-745 nm. The brightfield was set at channel 1 and the laser brightness was set at 6.5 mW. The sample was 'acquired' and stopped after 10000 events were taken for data analysis.

PI fluorescence was detected in channel 5 and a plot of events frequency (on the Y-axis) against fluorescence intensity of events in channel 5 (on the X-axis) was made using the IDEAS v6.2 software (see appendix section for FCM plots). This gives information about PI fluorescent events in channel 5 compared to a normalized frequency of all analyzed events. Manual gating was then applied to distinguish cells that showed PI fluorescence and the gate was kept constant for all samples. The data collected for different *E. coli* culture concentration applied on surfaces, stained then analyzed by FCM with replicates are shown in Table 4.15 & 4.16 below.

Table 4.15: FCM results of yeast on Control after contact time, stained with propidium iodide

Time	Gated Population	Count	%Gated
120 minutes	R1	9374	93.7
60 minutes	R1	9024	90.2
30 minutes	R1	8996	89.9
10 minutes	R1	8228	82.3

Table 4.16: FCM results of yeast on Cu surface after contact time, stained with propidium iodide

Gated Population	10 minutes		30 minutes		60 minutes		120 minutes	
	Count	%Gated	Count	%Gated	Count	%Gated	Count	%Gated
Replicate 1- (R1)	2936	29.4	5271	52.7	5323	53.2	3680	36.8
Replicate 2- (R1)	3371	33.7	2507	25.1	4203	42.0	6336	63.4
Replicate 3- (R1)	5787	57.9	5351	53.5	6088	60.9	7387	73.9

A gate (R1) was made and kept constant for all cases. Gating percentages of cells that exist outside R1 gate was used to correlate with plate count results. A comparison

between the FCM gate percentages and PC results is shown in Table 4.17 and a calibration plot is made in Figure 4.4 below.

Table 4.17: Comparison between PC results and FCM gate percentages for yeast

Sample ID	PC Log reduction	FCM gate percent
10min Cu_18	0.46	70.64
10min Cu_23	0.60	66.29
10min Cu_15	0.84	42.13
30min Cu_18	1.60	47.29
30min Cu_23	2.22	74.93
30min Cu_15	1.89	46.49
1hr Cu_18	1.43	46.77
1hr Cu_23	1.79	57.97
1hr Cu_15	2.03	39.12
2h Cu_18	2.28	63.2
2hr Cu_15	2.42	36.64
2hr Cu_23	3.86	26.13
control 2hrs_4	0	93.74
control 10min_6	0	90.24
control 30min_8	0	88.96
control 1hr_7	0	82.28
control 2hr_5	0	77.73

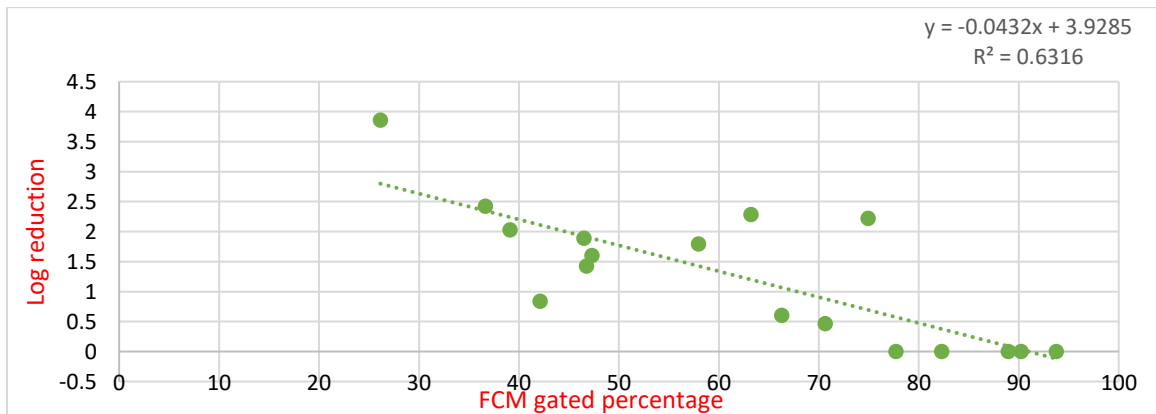


Figure 4.4: Calibration curve for FCM and plate count results

As shown in Figure 4.4, a calibration curve was made between the log reduction of plate count results and the applied flow cytometry gating percentage. FCM gate percent was calculated using the formula:

$$100 - \% \text{ gated (R1)} \qquad \text{equation (4.1)}$$

Equation (4.1) was applicable for all samples applied on copper surface for a contact time period. Gate percentage for the control was taken as the value of ‘% gated (R1)’. This is because samples exposed to copper showed a log reduction for yeast, while the control showed no log reduction. The R-squared value for the regression line was calculated as 0.63 and the equation of the line was given as:

$$y = -0.0432x + 3.9285 \qquad \text{equation (4.2)}$$

4.6.2 Predicting Log Reduction of Yeast on Industrial Antimicrobial samples using FCM

The FCM technique was used to predict the log reduction on industrially manufactured antimicrobial samples by recording the R1 gated percentage and applying equation (4.2) to make predictions. Table 4.18 below shows the FCM data for yeast applied on various industrially manufactured samples with gate applied and gated percentage recorded.

Table 4.18: FCM results of yeast applied on surfaces for 2 hours then stained with propidium iodide

Population	Count	%Gated
All	10000	100
Control- (R1)	9646	96.5
Sample A1- (R1)	9606	96.1

Sample B1- (R1)	9546	95.5
Sample F1- (R1)	6455	64.6
Sample G1- (R1)	6371	63.7
Sample X – (R1)	4572	45.7
Sample Z – (R1)	5139	51.4

Sample analysis with the flow cytometer, was conducted using the same procedure and settings as previously stated when analysing with propidium iodide stain. During sample data analysis, the R1 gate was made from the beginning till point 10000 on the 'intensity on channel 5' axis as seen in Figure 4.25 for all samples. Gating percentages of each sample were used to predict their log reductions by applying equation (4.2) and a comparison between the predicted FCM log reduction number and actual plate count number is seen in Table 4.19 and Figure 4.5 below.

Table 4.19: Comparison between PC and FCM log reduction for yeast

	PC log reduction	FCM log reduction	Error
control	0	-0.2403	-0.2403
A1 sample	0.00629	-0.22302	-0.22931
B1-sample	0.02907	-0.1971	-0.22617
F1-sample	0.65854	1.13778	0.47923
G1-sample	0.81690	1.17666	0.35975
X-sample	1.68545	1.9629	0.27744
Z-sample	2.03915	1.70802	-0.33113

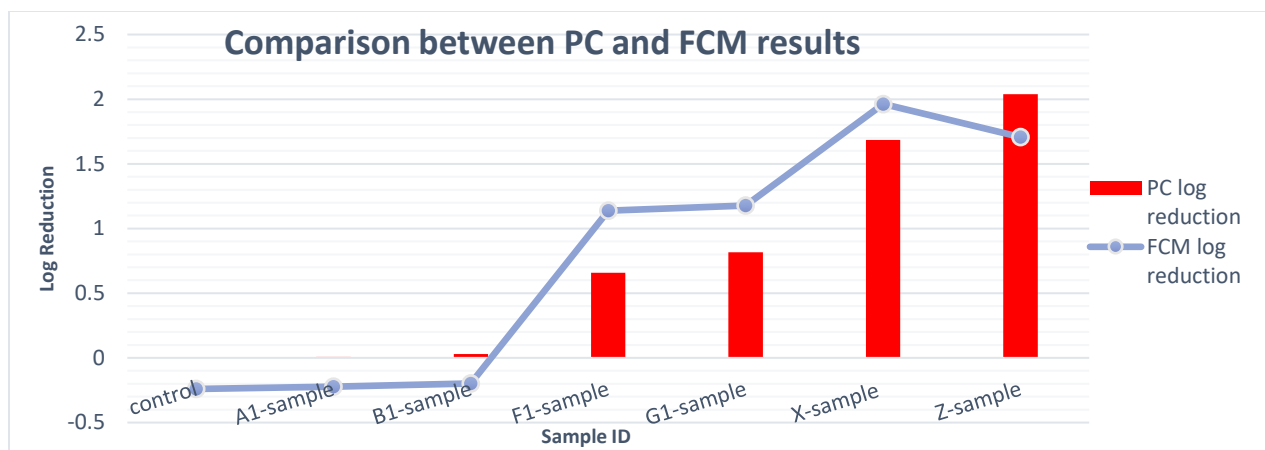


Figure 4.5: Comparison between PC and FCM results

In Figure 4.5, a comparison between plate count log reduction results and flow cytometry predicted log reduction results is seen. It is observed there is underestimation of log reduction values for samples with little or no antifungal efficacy for control, A1 and B1 sample. There is a slight overestimation for samples that show some antifungal efficacy for the F1, G1 and X samples, however, there is underestimation for sample Z even though it shows significant antimicrobial efficacy.

In Table 4.16, the difference in log reductions between results of both techniques is calculated as 'error'. The error calculated based on this study shows that the maximum underestimation and overestimation value for FCM predicted values in correlation with plate count actual values is -0.33 and 0.48.

4.7 Summary and Conclusion

A flow cytometry technique was investigated to determine the antimicrobial efficacy of samples that correlates with plate count results. Firstly, FCM technique involving staining of microbial solution with calcein AM dye was investigated. This technique showed good comparison with plate count results at 10^4 and 10^5 CFU/ml of microbial

solution without exposure to copper. However, on exposure to a copper surface, the technique fails to give accurate and reliable results when compared with results obtained from traditional plate count techniques because of potential interference of calcein AM stain by copper ions. Hence, a second technique was developed involving staining 10^6 CFU/ml of microbial solution with propidium iodide after contact with copper surface. Consistent manual gating techniques were applied to all investigated samples and results compared with plate count results. The results from the developed FCM technique with propidium iodide staining provided good comparison with plate count results and were used to rapidly predict the antimicrobial efficacy of some industrially manufactured antimicrobial samples. This newly developed FCM technique is reliable, quick and ensures rapid analysis of sample with results that can be readily correlated with trends in plate counts.

Chapter 5

Conclusions and Recommendations

Conclusions

The study in this thesis focused on development of alternative protocols to determine the antimicrobial efficacy of industrially manufactured antimicrobial products. The developed protocols are accurate and provide rapid analysis for samples compared to the EPA protocol. This is useful when there is a large batch of samples that need to be analyzed within a short period of time. Furthermore, a flow cytometry technique was developed to correlate traditional plate count results. This technique also shows an accurate comparison with the plate count technique and predicts the antimicrobial efficacy of samples without microbial plating, incubation and growth time. The marked features of this work can be summarized as follows:

- Three different protocols were developed and tested using two industrially manufactured antimicrobial surface samples. The antimicrobial efficacy results against *E. coli* and *P. aeruginosa* by the samples using developed protocols were compared with the EPA protocol by log reduction and killing percentages. The results showed good comparison with the EPA protocol results and the reliability of each protocol was assessed based on coefficient of variation calculations for each case. These alternative protocols may especially be useful on irregular or larger surfaces where the EPA protocol cannot be applied.

- A technique that involves using flow cytometry to correlate with results from traditional plate count techniques that are used during antimicrobial efficacy testing of samples was developed. A protocol involving staining of microbial solution with calcein AM was investigated and found to correlate with plate count results before the microbial solution was applied on a copper surface. Another protocol involving staining a microbial solution with propidium iodide was investigated and compared to plate count results after the microbial solution has been exposed to a copper surface. This FCM technique was used to accurately predict the antimicrobial efficacy of industrially manufactured samples, with same-day results versus the 24 hours or more for the EPA and other plate count methods.

Recommendations for Future Work

The protocol 3, which involved applying bacteria onto the test surface, then inverting the test surface onto an agar plate surface for a 1-hour contact time, removing the surface and incubating agar plate, showed poor correlation with the EPA protocol results especially for pure copper surface. This is likely a result of the nutrient rich environment, which allows bacteria to overcome the toxicity of copper ions. However, further investigation using protocol 3 could reveal the depth to which copper ions from a pure copper or copper alloy surface could reach while maintaining its toxicity and bacterial growth inhibition property. This could be useful information for high touch antimicrobial products like doorknobs or tabletops to determine their toxicity to microbes even if the surface is covered by layers of dust and dirt.

The developed FCM technique using calcein AM dye staining showed good correlation with plate count methods without microbial solution applied on copper plate. However, when the microbial solution was applied to the copper plate and tested with this technique, the results did not compare with plate count results. This was attributed to the presence of copper ions which are reported to quench the fluorescence of calcein AM. This fluorescence quenching action could be further investigated and can be used to detect the presence and amount of copper ions in a microbial solution which can then perhaps be correlated with antimicrobial activity.

Finally, the technique which involves staining microbial samples with propidium iodide showed good prediction capability of antimicrobial efficacy of samples. This is based on the principle of propidium iodide staining dead cells with compromised cell membranes in a sample. Therefore, with the application of double staining techniques using a live/dead kit like SYTO 9 and PI, different properties of the microbial cell culture can be determined, like the number of live cells, number of dead cells, number of live but not culturable cells and much more.

References

- Abicht H. K., Gonskikh, Y., Gerber, S. D., & Solioz, M. (2013). Non-enzymic copper reduction by menaquinone enhances copper toxicity in *Lactococcus lactis* IL1403. *Microbiology (United Kingdom)*, 159(PART 6), 1190–1197. <https://doi.org/10.1099/mic.0.066928-0>
- Adler, N. E., Schmitt-Jansen, M., & Altenburger, R. (2007). Flow cytometry as a tool to study phytotoxic modes of action. *Environmental Toxicology and Chemistry*, 26(2), 297–306. <https://doi.org/10.1897/06-1636R.1>
- Ali-Shtayeh, M. S., & Abu Ghdeib, S. I. (1999). Antifungal activity of plant extracts against dermatophytes. *Mycoses*, 42(11–12), 665–672. <https://doi.org/10.1046/j.1439-0507.1999.00499.x>
- Amano, F. (2016). Differential Resuscitative Effects of Pyruvate and Its Analogs on VBNC (Viable but Nonculturable) Salmonella. In *Stress and Environmental Regulation of Gene Expression and Adaptation in Bacteria* (Vol. 2, pp. 1338–1345). Wiley Blackwell. <https://doi.org/10.1002/9781119004813b.ch131>
- Ambriz-Aviña, V., Contreras-Garduño, J. A., & Pedraza-Reyes, M. (2014). Applications of Flow Cytometry to Characterize Bacterial Physiological Responses. *BioMed Research International*, 2014. <https://doi.org/10.1155/2014/461941>
- Amodio, E., & Dino, C. (2014). Use of ATP bioluminescence for assessing the cleanliness of hospital surfaces: A review of the published literature (1990-2012). *Journal of Infection and Public Health*. Elsevier BV. <https://doi.org/10.1016/j.jiph.2013.09.005>

Association, C. D. (2007). A Guide to Working with Copper and Copper Alloys. *The Copper Advantage*, 5(2), 8. https://doi.org/https://doi.org/10.1007/978-1-4615-3482-2_14

Azam, A., Ahmed, A. S., Oves, M., Khan, M. S., & Memic, A. (2012). Size-dependent antimicrobial properties of CuO nanoparticles against Gram-positive and -negative bacterial strains. *International Journal of Nanomedicine*, 7, 3527–3535. <https://doi.org/10.2147/IJN.S29020>

Balouiri, M., Sadiki, M., & Ibsouda, S. K. (2016, April 1). Methods for in vitro evaluating antimicrobial activity: A review. *Journal of Pharmaceutical Analysis*. Xi'an Jiaotong University. <https://doi.org/10.1016/j.jpha.2015.11.005>

Bankier, C., Cheong, Y., Mahalingam, S., Edirisinghe, M., Ren, G., Cloutman-Green, E., & Ciric, L. (2018). A comparison of methods to assess the antimicrobial activity of nanoparticle combinations on bacterial cells. *PLoS ONE*, 13(2). <https://doi.org/10.1371/journal.pone.0192093>

Barnett, D., Louzao, R., Gambell, P., De, J., Oldaker, T., & Hanson, C. A. (2013, September). Validation of cell-based fluorescence assays: Practice guidelines from the ICSH and ICCS - Part IV - Postanalytic considerations. *Cytometry Part B - Clinical Cytometry*. <https://doi.org/10.1002/cyto.b.21107>

Bashashati, A., & Brinkman, R. R. (2009). A Survey of Flow Cytometry Data Analysis Methods. *Advances in Bioinformatics*, 2009, 1–19. <https://doi.org/10.1155/2009/584603>

Berney, M., Hammes, F., Bosshard, F., Weilenmann, H. U., & Egli, T. (2007). Assessment and interpretation of bacterial viability by using the LIVE/DEAD BacLight kit in

combination with flow cytometry. *Applied and Environmental Microbiology*, 73(10), 3283–3290. <https://doi.org/10.1128/AEM.02750-06>

Bertini I., Gray H., Steifel E., and Valentine J.S. (2007), *Biological Inorganic Chemistry: Structure and Reactivity*, Sausalito, CA: University Science Books.

Beswick, P. H., Hall G. H., Hook A. J., Little K., McBrien D. C. and Lott K. A. (1976), Copper toxicity: evidence for the conversion of cupric to cuprous copper in vivo under anaerobic conditions. *Chem Biol Interact* 14, 347–356.

Bio-Rad Laboratories Inc. (2015). *Flow Cytometry - Basics Guide*. *Bio-Rad Laboratories Inc*, 48.

Brown, M., & Wittwer, C. (2000). Flow cytometry: Principles and clinical applications in hematology. *Clinical Chemistry*, 46(8 II), 1221–1229. <https://doi.org/10.1093/clinchem/46.8.1221>

Canadian agency for drugs and technologies in health, (2015), *Antimicrobial Copper Surfaces for the Reduction of Healthcare–Associated Infections in Intensive Care Settings*, Issue 133.

Carling, P. C., Parry, M. F., Bruno-Murtha, L. A., & Dick, B. (2010). Improving environmental hygiene in 27 intensive care units to decrease multidrug-resistant bacterial transmission. *Critical Care Medicine*, 38(4), 1054–1059. <https://doi.org/10.1097/CCM.0b013e3181cdf705>

Carling, P. C., Parry, M. M., Rupp, M. E., Po, J. L., Dick, B., & Von Beheren, S. (2008). *Improving Cleaning of the Environment Surrounding Patients in 36 Acute Care Hospitals*.

Infection Control & Hospital Epidemiology, 29(11), 1035–1041.
<https://doi.org/10.1086/591940>

Carlioz, A., & Touati, D. (1986). Isolation of superoxide dismutase mutants in *Escherichia coli*: is superoxide dismutase necessary for aerobic life? *The EMBO Journal*, 5(3), 623–630. <https://doi.org/10.1002/j.1460-2075.1986.tb04256.x>

Centers for Disease Control and Prevention. (2018), HAI Data and Statistics. Retrieved from <https://www.cdc.gov/hai/surveillance/index.html>

Champagne, V. K., & Helfritsch, D. J. (2013). A demonstration of the antimicrobial effectiveness of various copper surfaces. *Journal of Biological Engineering*, 7(1). <https://doi.org/10.1186/1754-1611-7-8>

Chandra, S., Kumar, A., & Tomar, P. K. (2014). Synthesis and characterization of copper nanoparticles by reducing agent. *Journal of Saudi Chemical Society*, 18(2), 149–153. <https://doi.org/10.1016/j.jscs.2011.06.009>

Chaturvedi, K. S., & Henderson, J. P. (2014). Pathogenic adaptations to host-derived antibacterial copper. *Frontiers in Cellular and Infection Microbiology*. Frontiers Research Foundation. <https://doi.org/10.3389/fcimb.2014.00003>

Chitarra, L. G., & Van Den Bulk, R. W. (2003). The application of flow cytometry and fluorescent probe technology for detection and assessment of viability of plant pathogenic bacteria. *European Journal of Plant Pathology*. Springer Netherlands. <https://doi.org/10.1023/A:1024275610233>

Cocke, D. L.; Chuah, G. K.; Kruse, N.; Block, J. H. Copper Oxidation and Surface Copper Oxide Stability Investigated by Pulsed Field Desorption Mass Spectrometry. *Appl. Surf. Sci.* 1995, 84, 153–161.

Colin, M., Klingelschmitt, F., Charpentier, E., Josse, J., Kanagaratnam, L., De Champs, C., & Gangloff, S. C. (2018). Copper alloy touch surfaces in healthcare facilities: An effective solution to prevent bacterial spreading. *Materials*, 11(12). <https://doi.org/10.3390/ma11122479>

Collini Luka (2012), Copper Alloys - Early Applications and Current Performance - Enhancing Processes. InTech. <https://doi.org/10.5772/1912>

Crissman, H. A., Orlicky, D. J., & Kissane, R. J. (1979). Fluorescent DNA probes for flow cytometry. Considerations and prospects. *Journal of Histochemistry and Cytochemistry*, 27(12), 1652–1654. <https://doi.org/10.1177/27.12.391999>

Davis, B. H., Dasgupta, A., Kussick, S., Han, J. Y., & Estrellado, A. (2013, September). Validation of cell-based fluorescence assays: Practice guidelines from the ICSH and ICCS - Part II - Preanalytical issues. *Cytometry Part B - Clinical Cytometry*. <https://doi.org/10.1002/cyto.b.21105>

Darzynkiewicz, Z., Traganos, F., Zhao, H., Halicka, H. D., & Li, J. (2011, May). Cytometry of DNA replication and RNA synthesis: Historical perspective and recent advances based on “click chemistry.” *Cytometry Part A*. <https://doi.org/10.1002/cyto.a.21048>

Deere, D., Shen, J., Vesey, G., Bell, P., Bissinger, P., & Veal, D. (1998). Flow cytometry and cell sorting for yeast viability assessment and cell selection. *Yeast*, 14(2), 147–160.

Degheidy, H., Abbasi, F., Mostowski, H., Gaigalas, A. K., Marti, G., Bauer, S., & Wang, L. (2016). Consistent, multi-instrument single tube quantification of CD20 in antibody bound per cell based on CD4 reference. *Cytometry Part B - Clinical Cytometry*, *90*(2), 159–167. <https://doi.org/10.1002/cyto.b.21253>

De Castillo, M. C., De Saab, O. A., De Nader, O. M., & De Ruiz Holgado, A. P. (1998, July). In vitro Comparison of Disk Diffusion and Agar Dilution Antibiotic Susceptibility Test Methods for *Neisseria gonorrhoeae*. *Memorias Do Instituto Oswaldo Cruz*. <https://doi.org/10.1590/s0074-02761998000400019>

De Rosa, S. C., Herzenberg, L. A., Herzenberg, L. A., & Roederer, M. (2001). 11-color, 13-parameter flow cytometry: Identification of human naive T cells by phenotype, function, and T-cell receptor diversity. *Nature Medicine*, *7*(2), 245–248. <https://doi.org/10.1038/84701>

Dunning, J. C., Ma, Y., & Marquis, R. E. (1998). Anaerobic killing of oral Streptococci by reduced, transition metal cations. *Applied and Environmental Microbiology*, *64*(1), 27–33. <https://doi.org/10.1128/aem.64.1.27-33.1998>

Environmental Protection Agency (2016), Protocol for the Evaluation of Bactericidal Activity of Hard, Non-porous Copper Containing Surface Products.

Errante, P. R., Ebbing, P. C. C., Rodrigues, F. S. M., Ferraz, R. R. N., & Da Silva, N. P. (2016). Flow cytometry: a literature review. *Revista de Ciências Médicas e Biológicas*, *14*(2), 221. <https://doi.org/10.9771/cmbio.v14i2.12182>

Everitt, Brian (1998). *The Cambridge Dictionary of Statistics*. Cambridge, UK New York: Cambridge University Press. ISBN 978-0521593465.

Food and Drug Administration. (2014). *Pharmaceutical Microbiology Manual*. *Food and Drug Administration*, 3–30. Retrieved from <http://www.fda.gov/downloads/ScienceResearch/FieldScience/UCM397228.pdf>

Frausto da Silva, J.J.R., and Williams, R. (1993), *The Biological Chemistry of the Elements: The Inorganic Chemistry of Life*. Oxford: Oxford University Press.

Fredj, N., Kolar, J. S., Prichard, D. M., & Burleigh, T. D. (2013). Study of relative color stability and corrosion resistance of commercial copper alloys exposed to hand contact and synthetic hand sweat. *Corrosion Science*, 76, 415–423. <https://doi.org/10.1016/j.corsci.2013.07.015>

Freinbichler W., Colivicchi M.A., Stefanini C., Bianchi L., Ballini C., Misini B., et al. (2011). Highly Reactive Oxygen Species: detection, formation, and possible functions. *Cell. Mol. LifeSci.* 68, 2067–2079. doi:10.1007/s00018-011-0682-x

Gawande, M. B., Goswami, A., Felpin, F. X., Asefa, T., Huang, X., Silva, R., ... Varma, R. S. (2016, March 23). Cu and Cu-Based Nanoparticles: Synthesis and Applications in Catalysis. *Chemical Reviews*. American Chemical Society. <https://doi.org/10.1021/acs.chemrev.5b00482>

Grass, G., Rensing, C., & Solioz, M. (2011), Metallic copper as an antimicrobial surface. *Applied and Environmental Microbiology*. <https://doi.org/10.1128/AEM.02766-10>

Gunasekera, T. S., Attfield, P. V., & Veal, D. A. (2000). A flow cytometry method for rapid detection and enumeration of total bacteria in milk. *Applied and Environmental Microbiology*, 66(3), 1228–1232. <https://doi.org/10.1128/AEM.66.3.1228-1232.2000>

Haddadin Y, Annamaraju P, Regunath H. (2020), Central Line Associated Bloodstream Infections (CLABSI). In: *StatPearls*. Treasure Island (FL): StatPearls Publishing; 2020.

Hans M., Erbe, A., Mathews, S., Chen, Y., Solioz, M., & Mücklich, F. (2013). Role of copper oxides in contact killing of bacteria. *Langmuir*, 29(52), 16160–16166. <https://doi.org/10.1021/la404091z>

Hattori, N., Nakajima, M. O., O'Hara, K., & Sawai, T. (1998). Novel antibiotic susceptibility tests by the ATP-bioluminescence method using filamentous cell treatment. *Antimicrobial Agents and Chemotherapy*, 42(6), 1406–1411. <https://doi.org/10.1128/aac.42.6.1406>

Haugland, R. P. (2002). *Handbook of fluorescent probes and research products*. 9th edition, EU version Eugene (Or.): Molecular probes.

Hassan, I. A., Parkin, I. P., Nair, S. P., & Carmalt, C. J. (2014). Antimicrobial activity of copper and copper(i) oxide thin films deposited via aerosol-assisted CVD. *Journal of Materials Chemistry B*, 2(19), 2855–2860. <https://doi.org/10.1039/c4tb00196f>

Health Canada and Public Health Agency of Canada. (2018). Evaluation of Healthcare Associated Infection Activities at the Public Health Agency of Canada 2012-13 to 2016-17. *Office of Audit and Evaluation Health Canada and Public Health Agency of Canada*.

Heatley, N. G. (1944). A method for the assay of penicillin. *Biochemical Journal*, 38(1), 61–65. <https://doi.org/10.1042/bj0380061>

Hendon-Dunn, C. L., Doris, K. S., Thomas, S. R., Allnutt, J. C., Marriott, A. A. N., Hatch, K. A., ... Bacon, J. (2016). A flow cytometry method for rapidly assessing Mycobacterium tuberculosis responses to antibiotics with different modes of action. *Antimicrobial Agents and Chemotherapy*, 60(7), 3869–3883. <https://doi.org/10.1128/AAC.02712-15>

Hess, A. S., Shardell, M., Johnson, J. K., Thom, K. A., Roghmann, M.-C., Netzer, G., ... Harris, A. D. (2013). A Randomized Controlled Trial of Enhanced Cleaning to Reduce Contamination of Healthcare Worker Gowns and Gloves with Multidrug-Resistant Bacteria. *Infection Control & Hospital Epidemiology*, 34(5), 487–493. <https://doi.org/10.1086/670205>

Hidron, A. I., Edwards, J. R., Patel, J., Horan, T. C., Sievert, D. M., ... Fridkin, S. K. (2008). Antimicrobial-Resistant Pathogens Associated With Healthcare-Associated Infections: Annual Summary of Data Reported to the National Healthcare Safety Network at the Centers for Disease Control and Prevention, 2006–2007. *Infection Control & Hospital Epidemiology*, 29(11), 996–1011. <https://doi.org/10.1086/591861>

Horton, D. J., Ha, H., Foster, L. L., Bindig, H. J., & Scully, J. R. (2015). Tarnishing and Cu Ion release in Selected Copper-Base Alloys: Implications towards Antimicrobial Functionality. *Electrochimica Acta*, 169, 351–366. <https://doi.org/10.1016/j.electacta.2015.04.001>

Hrenovic, J., Milenkovic, J., Daneu, N., Kepcija, R. M., & Rajic, N. (2012). Antimicrobial activity of metal oxide nanoparticles supported onto natural clinoptilolite. *Chemosphere*, 88(9), 1103–1107. <https://doi.org/10.1016/j.chemosphere.2012.05.023>

Humphreys, H. (2014). Self-disinfecting and microbicide-impregnated surfaces and fabrics: What potential in interrupting the spread of healthcare-associated infection?

Clinical Infectious Diseases, 58(6), 848–853. <https://doi.org/10.1093/cid/cit765>

Ibáñez-Peral, R., Bergquist, P. L., Walter, M. R., Gibbs, M., Goldys, E. M., & Ferrari, B. (2008). Potential use of quantum dots in flow cytometry. *International Journal of Molecular*

Sciences, 9(12), 2622–2638. <https://doi.org/10.3390/ijms9122622>

Imlay, J. A., & Fridovich, I. (1992). Suppression of oxidative envelope damage by pseudoreversion of a superoxide dismutase-deficient mutant of *Escherichia coli*. *Journal*

of Bacteriology, 174(3), 953–961. <https://doi.org/10.1128/jb.174.3.953-961.1992>

Inspire (2012). ImageStreamX system software user's stream manual, www.amnis.com

Invitrogen. Molecular probes: The Handbook. Fluorescent indicators for Zn²⁺ and other metal ions – section 19.7

Jang, S., & Imlay, J. A. (2007). Micromolar intracellular hydrogen peroxide disrupts metabolism by damaging iron-sulfur enzymes. *Journal of Biological Chemistry*, 282(2),

929–937. <https://doi.org/10.1074/jbc.M607646200>

Jepras, R. I., Carter, J., Pearson, S. C., Paul, F. E., & Wilkinson, M. J. (1995). Development of a robust flow cytometric assay for determining numbers of viable

bacteria. *Applied and Environmental Microbiology*, 61(7), 2696–2701.

<https://doi.org/10.1128/aem.61.7.2696-2701.1995>

Johnson, S., Nguyen, V., & Coder, D. (2013). Assessment of cell viability. *Current*

Protocols in Cytometry, (SUPPL.64). <https://doi.org/10.1002/0471142956.cy0902s64>

Kalina, T., Flores-Montero, J., Van Der Velden, V. H. J., Martin-Ayuso, M., Böttcher, S., Ritgen, M., ... Orfao, A. (2012). EuroFlow standardization of flow cytometer instrument settings and immunophenotyping protocols. *Leukemia*, 26(9), 1986–2010. <https://doi.org/10.1038/leu.2012.122>

Kapoor, V., Karpov, V., Linton, C., Subach, F. V., Verkhusha, V. V., & Telford, W. G. (2008). Solid state yellow and orange lasers for flow cytometry. *Cytometry Part A*, 73(6), 570–577. <https://doi.org/10.1002/cyto.a.20563>

Karlin, K. D. (1993). Metalloenzymes, structural motifs, and inorganic models. *Science*. <https://doi.org/10.1126/science.7688141>

Kemme, M., & Heinzl-Wieland, R. (2018). Quantitative assessment of antimicrobial activity of PLGA films loaded with 4-hexylresorcinol. *Journal of Functional Biomaterials*, 9(1). <https://doi.org/10.3390/jfb9010004>

Klevens, R. M., Edwards, J. R., Richards, C. L., Horan, T. C., Gaynes, R. P., Pollock, D. A., & Cardo, D. M. (2007). *Estimating Health Care-Associated Infections and Deaths in U.S. Hospitals, 2002. Public Health Reports*, 122(2), 160–166. doi:10.1177/003335490712200205

Konen, R., & Fintov, S. (2012). Copper and Copper Alloys: Casting, Classification and Characteristic Microstructures. In *Copper Alloys - Early Applications and Current Performance - Enhancing Processes*. InTech. <https://doi.org/10.5772/39014>

Koseoglu Eser, O., Ergin, A., & Hascelik, G. (2015). Antimicrobial Activity of Copper Alloys Against Invasive Multidrug-Resistant Nosocomial Pathogens. *Current Microbiology*, 71(2), 291–295. <https://doi.org/10.1007/s00284-015-0840-8>

Kramer, A., Schwebke, I., & Kampf, G. (2006). *How long do nosocomial pathogens persist on inanimate surfaces? A systematic review. BMC Infectious Diseases*, 6(1). doi:10.1186/1471-2334-6-130

Kumar, S. S., & Ghosh, A. R. (2019, June 1). Assessment of bacterial viability: A comprehensive review on recent advances and challenges. *Microbiology (United Kingdom)*. Microbiology Society. <https://doi.org/10.1099/mic.0.000786>

Kurec, A. (2014). Flow cytometry: principles and practices. *MLO: Medical Laboratory Observer*, 46(5)

Lazary, A., Weinberg, I., Vatine, J. J., Jefidoff, A., Bardenstein, R., Borkow, G., & Ohana, N. (2014). Reduction of healthcare-associated infections in a long-term care brain injury ward by replacing regular linens with biocidal copper oxide impregnated linens. *International Journal of Infectious Diseases*, 24, 23–29. <https://doi.org/10.1016/j.ijid.2014.01.022>

Lilius, H., Hästbacka, T., & Isomaa, B. (1996). A combination of fluorescent probes for evaluation of cytotoxicity and toxic mechanisms in isolated rainbow trout hepatocytes. *Toxicology in Vitro*, 10(3), 341–348. [https://doi.org/10.1016/0887-2333\(96\)00015-X](https://doi.org/10.1016/0887-2333(96)00015-X)

Liochev, S.I. (1999), The Mechanism of “Fenton-like” reactions and their importance for biological systems. A biologist’s view. *Met. Ions Biol. Syst.* 36, 1–39.

Lizard, G. (2007, September). Flow cytometry analyses and bioinformatics: Interest in new softwares to optimize novel technologies and to favor the emergence of innovative concepts in cell research. *Cytometry Part A*. <https://doi.org/10.1002/cyto.a.20444>

Macomber, L., & Imlay, J. A. (2009). The iron-sulfur clusters of dehydratases are primary intracellular targets of copper toxicity. *Proceedings of the National Academy of Sciences of the United States of America*, 106(20), 8344–8349. <https://doi.org/10.1073/pnas.0812808106>

Macomber L., Rensing C., and Imlay J.A. (2007). Intracellular Copper does not catalyze the formation of oxidative DNA damage in Escherichia coli. *J. Bacteriol.* 189, 1616–1626. doi:10.1128/JB.01357-06

Magaldi, S., Mata-Essayag, S., Hartung De Capriles, C., Perez, C., Colella, M. T., Olaizola, C., & Ontiveros, Y. (2004). Well diffusion for antifungal susceptibility testing. *International Journal of Infectious Diseases*, 8(1), 39–45. <https://doi.org/10.1016/j.ijid.2003.03.002>

Mahmoodi, S., Elmi, A., & Hallaj Nezhadi, S. (2018). Copper Nanoparticles as Antibacterial Agents. *Journal of Molecular Pharmaceutics & Organic Process Research*, 06(01). <https://doi.org/10.4172/2329-9053.1000140>

Matocha CJ, Karathanasis AD, Rakshit S, Wagner KM. (2005), Reduction of copper (II) by iron (II). *J Environ Qual* 34:1539–1546. <http://dx.doi.org/10.2134/jeq2005.0002>

Mathews, S., Kumar, R., & Solioz, M. (2015), Copper reduction and contact killing of bacteria by iron surfaces. *Applied and Environmental Microbiology*, 81(18), 6399–6403. <https://doi.org/10.1128/AEM.01725-15>

Mauldin, P. D., Salgado, C. D., Hansen, I. S., Durup, D. T., & Bosso, J. A. (2010). Attributable hospital cost and length of stay associated with health care-associated infections caused by antibiotic-resistant gram-negative bacteria. *Antimicrobial Agents and Chemotherapy*, 54(1), 109–115. <https://doi.org/10.1128/AAC.01041-09>

Mehtar, S., Wiid, I., & Todorov, S. D. (2008). The antimicrobial activity of copper and copper alloys against nosocomial pathogens and *Mycobacterium tuberculosis* isolated from healthcare facilities in the Western Cape: an in-vitro study. *Journal of Hospital Infection*, 68(1), 45–51. <https://doi.org/10.1016/j.jhin.2007.10.009>

Michels, H. T., & Anderson, D. G. (2008). Antimicrobial regulatory efficacy testing of solid copper alloy surfaces in the USA. *Metal Ions in Biology and Medicine*, 10(2), 185–190.

Michels, H. T., Keevil, C. W., Salgado, C. D., & Schmidt, M. G. (2015). From laboratory research to a clinical trial: copper alloy surfaces kill bacteria and reduce hospital-acquired infections. *Health Environments Research and Design Journal*, 9(1), 64–79. <https://doi.org/10.1177/1937586715592650>

Mikolay, A., Huggett, S., Tikana, L., Grass, G., Braun, J., & Nies, D. H. (2010). Survival of bacteria on metallic copper surfaces in a hospital trial. *Applied Microbiology and Biotechnology*, 87(5), 1875–1879. <https://doi.org/10.1007/s00253-010-2640-1>

Molecular Probes, I. (2004). LIVE/DEAD® BacLight™ Bacterial Viability Kits. Retrieved from <https://www.thermofisher.com/order/catalog/product/L7007#/L7007>

Monk, A. B., Kanmukhla, V., Trinder, K., & Borkow, G. (2014). *Potent bactericidal efficacy of copper oxide impregnated non-porous solid surfaces*. *BMC Microbiology*, 14(1), 57. doi:10.1186/1471-2180-14-57

Montante, S., & Brinkman, R. R. (2019). Flow cytometry data analysis: Recent tools and algorithms. *International Journal of Laboratory Hematology*, 41(S1), 56–62. <https://doi.org/10.1111/ijlh.13016>

Noyce, J. O., Michels, H., & Keevil, C. W. (2006). Use of copper cast alloys to control *Escherichia coli* O157 cross-contamination during food processing. *Applied and Environmental Microbiology*, 72(6), 4239–4244. <https://doi.org/10.1128/AEM.02532-05>

O’Gorman, J., & Humphreys, H. (2012, August). Application of copper to prevent and control infection. Where are we now? *Journal of Hospital Infection*. <https://doi.org/10.1016/j.jhin.2012.05.009>

O.I.E. (2012). Laboratory Methodologies for Bacterial Antimicrobial Susceptibility Testing. *OIE Terrestrial Manual*, 1–11.

Oliver, J. D. (2005, February). The viable but nonculturable state in bacteria. *Journal of Microbiology*.

Ou, F., McGoverin, C., Swift, S., & Vanholsbeeck, F. (2017). Absolute bacterial cell enumeration using flow cytometry. *Journal of Applied Microbiology*, 123(2), 464–477. <https://doi.org/10.1111/jam.13508>

Parra, A., Toro, M., Jacob, R., Navarrete, P., Troncoso, M., Figueroa, G., & Reyes-Jara, A. (2018). Antimicrobial effect of copper surfaces on bacteria isolated from poultry meat. *Brazilian Journal of Microbiology*, 49, 113–118. <https://doi.org/10.1016/j.bjm.2018.06.008>

Payer, J. H. (1990). Corrosion processes in the development of thin tarnish films. In *Electrical Contacts, Proceedings of the Annual Holm Conference on Electrical Contacts* (pp. 203–211). Published by Illinois Inst of Technology. <https://doi.org/10.1109/holm.1990.113014>

Piddock, L. J. V. (1990). Techniques used for the determination of antimicrobial resistance and sensitivity in bacteria. *Journal of Applied Bacteriology*. <https://doi.org/10.1111/j.1365-2672.1990.tb02880.x>

Platzman, I.; Brener, R.; Haick, H.; Tannenbaum, R. Oxidation of Polycrystalline Copper Thin Films at Ambient Conditions. *J. Phys. Chem.* 2008, 1101–1108.

Pramanik, A., Laha, D., Bhattacharya, D., Pramanik, P., & Karmakar, P. (2012). A novel study of antibacterial activity of copper iodide nanoparticle mediated by DNA and membrane damage. *Colloids and Surfaces B: Biointerfaces*, 96, 50–55. <https://doi.org/10.1016/j.colsurfb.2012.03.021>

Preijers, F. W. M. B., Huys, E., Leenders, M., Nieto, L., Gautherot, E., & Moshaver, B. (2011). The new violet laser dye, Krome Orange, allows an optimal polychromatic immunophenotyping based on CD45-KO gating. *Journal of Immunological Methods*, 372(1–2), 42–51. <https://doi.org/10.1016/j.jim.2011.06.025>

Prigione, V., Lingua, G., & Filipello Marchisio, V. (2004). Development and Use of Flow Cytometry for Detection of Airborne Fungi. *Applied and Environmental Microbiology*, 70(3), 1360–1365. <https://doi.org/10.1128/AEM.70.3.1360-1365.2004>

Raffi, M., Mehrwan, S., Bhatti, T. M., Akhter, J. I., Hameed, A., Yawar, W., & Ul Hasan, M. M. (2010). Investigations into the antibacterial behavior of copper nanoparticles against *Escherichia coli*. *Annals of Microbiology*, 60(1), 75–80. <https://doi.org/10.1007/s13213-010-0015-6>

Rönquist, A., Fischmeister, H. The Oxidation of Copper - A Review of Published Data. *J. Inst. Met.* 1960, 89, 1960

Rouault, T. A. (2012, March). Biogenesis of iron-sulfur clusters in mammalian cells: New insights and relevance to human disease. *DMM Disease Models and Mechanisms*. <https://doi.org/10.1242/dmm.009019>

Rózańska, A., Chmielarczyk, A., Romaniszyn, D., Majka, G., & Bulanda, M. (2018). Antimicrobial effect of copper alloys on *Acinetobacter* species isolated from infections and hospital environment. *Antimicrobial Resistance and Infection Control*, 7(1). <https://doi.org/10.1186/s13756-018-0300-x>

Rózańska, A., Chmielarczyk, A., Romaniszyn, D., Sroka-Oleksiak, A., Bulanda, M., Walkowicz, M., ... Knych, T. (2017). Antimicrobial properties of selected copper alloys on *Staphylococcus aureus* and *Escherichia coli* in different simulations of environmental conditions: With vs. without organic contamination. *International Journal of Environmental Research and Public Health*, 14(7). <https://doi.org/10.3390/ijerph14070813>

Sanna, T., Dallolio, L., Raggi, A., Mazzetti, M., Lorusso, G., Zanni, A., ... Leoni, E. (2018). ATP bioluminescence assay for evaluating cleaning practices in operating theatres: Applicability and limitations. *BMC Infectious Diseases*, 18(1). <https://doi.org/10.1186/s12879-018-3505-y>

Santo, C. E., Quaranta, D., & Grass, G. (2012). Antimicrobial metallic copper surfaces kill *Staphylococcus haemolyticus* via membrane damage. *MicrobiologyOpen*, 1(1), 46–52. <https://doi.org/10.1002/mbo3.2>

Santo, C. E., Lam, E. W., Elowsky, C. G., Quaranta, D., Domaille, D. W., Chang, C. J., & Grass, G. (2011). Bacterial killing by dry metallic copper surfaces. *Applied and Environmental Microbiology*, 77(3), 794–802. <https://doi.org/10.1128/AEM.01599-10>

Seif El-Nasr, R., Abdelbasir, S. M., Kamel, A. H., & Hassan, S. S. M. (2020). Environmentally friendly synthesis of copper nanoparticles from waste printed circuit boards. *Separation and Purification Technology*, 230. <https://doi.org/10.1016/j.seppur.2019.115860>

Sifri, C. D., Burke, G. H., & Enfield, K. B. (2016). Reduced health care-associated infections in an acute care community hospital using a combination of self-disinfecting copper-impregnated composite hard surfaces and linens. *American Journal of Infection Control*, 44(12), 1565–1571. <https://doi.org/10.1016/j.ajic.2016.07.007>

Solioz, M. (2016). Copper Oxidation State and Mycobacterial Infection. *Mycobacterial Diseases*, 6(2). <https://doi.org/10.4172/2161-1068.1000210>

Suleiman, M. M., McGaw, L. J., Naidoo, V., & Eloff, J. N. (2010). Detection of antimicrobial compounds by bioautography of different extracts of leaves of selected south african tree species. *African Journal of Traditional, Complementary and Alternative Medicines*, 7(1), 64–78. <https://doi.org/10.4314/ajtcam.v7i1.57269>

Taylor, I. W., & Milthorpe, B. K. (1980). An evaluation of DNA fluorochromes, staining techniques, and analysis for flow cytometry. I. Unperturbed cell populations. *Journal of Histochemistry and Cytochemistry*, 28(11), 1224–1232. <https://doi.org/10.1177/28.11.6159392>

Tjioe, I., Legerton, T., Wegstein, J., Herzenberg, L. A., & Roederer, M. (2001). Phycoerythrin-allophycocyanin: A resonance energy transfer fluorochrome for immunofluorescence. *Cytometry*, 44(1), 24–29.

Theivasanthi T, Alagar M. (2011). Studies of copper nanoparticles effects on microorganisms. *Ann Bio Res*. 2011; 2:368–373.

Umer, A., Naveed, S., Ramzan, N., & Rafique, M. S. (2012, October). Selection of a suitable method for the synthesis of copper nanoparticles. *Nano*. <https://doi.org/10.1142/S1793292012300058>

US EPA (2016). Protocol for the evaluation of bactericidal activity of hard, non-porous copper containing surface products. Accessed from: <https://www.epa.gov/pesticide-registration/updated-draft-protocol-evaluation-bactericidal-activity-hard-non-porous>

Usman, M. S., El Zowalaty, M. E., Shameli, K., Zainuddin, N., Salama, M., & Ibrahim, N. A. (2013). Synthesis, characterization, and antimicrobial properties of copper

nanoparticles. *International Journal of Nanomedicine*, 8, 4467–4479.
<https://doi.org/10.2147/IJN.S50837>

Valgas, C., De Souza, S. M., Smânia, E. F. A., & Smânia, A. (2007). Screening methods to determine antibacterial activity of natural products. *Brazilian Journal of Microbiology*, 38(2), 369–380. <https://doi.org/10.1590/S1517-83822007000200034>

Vanhauteghem, D., Demeyere, K., Callaert, N., Boelaert, A., Haesaert, G., Audenaert, K., & Meyer, E. (2017), Flow cytometry is a powerful tool for assessment of the viability of fungal conidia in metalworking fluids. *Applied and Environmental Microbiology*, 83(16).
<https://doi.org/10.1128/AEM.00938-17>

Walkowicz, M., Osuch, P., Smyrak, B., Knych, T., Rudnik, E., Cieniek, Ł., ... Bulanda, M. (2018). Impact of oxidation of copper and its alloys in laboratory-simulated conditions on their antimicrobial efficiency. *Corrosion Science*, 140, 321–332.
<https://doi.org/10.1016/j.corsci.2018.05.033>

Warnes, S. L., Caves, V., & Keevil, C. W. (2012). Mechanism of copper surface toxicity in *Escherichia coli* O157:H7 and *Salmonella* involves immediate membrane depolarization followed by slower rate of DNA destruction which differs from that observed for Gram-positive bacteria. *Environmental Microbiology*, 14(7), 1730–1743.
<https://doi.org/10.1111/j.1462-2920.2011.02677.x>

Wenisch, C., Linnau, K. F., Parschalk, B., Zedtwitz-Liebenstein, K., & Georgopoulos, A. (1997). Rapid susceptibility testing of fungi by flow cytometry using vital staining. *Journal of Clinical Microbiology*, 35(1), 5–10. <https://doi.org/10.1128/jcm.35.1.5-10.1997>

Wiegand, I., Hilpert, K., & Hancock, R. E. W. (2008). Agar and broth dilution methods to determine the minimal inhibitory concentration (MIC) of antimicrobial substances. *Nature Protocols*, 3(2), 163–175. <https://doi.org/10.1038/nprot.2007.521>

Wilks, S. A., Michels, H., & Keevil, C. W. (2005). The survival of *Escherichia coli* O157 on a range of metal surfaces. *International Journal of Food Microbiology*, 105(3), 445–454. <https://doi.org/10.1016/j.ijfoodmicro.2005.04.021>

World Health Organization, Regional Office for South-East Asia. (2011). Establishment of national laboratory-based surveillance of antibiotic resistance. WHO Regional Office for South-East Asia. <https://apps.who.int/iris/handle/10665/205019>

World Health Organization. (2017), The burden of health care-associated infection worldwide. Retrieved from http://www.who.int/gpsc/country_work/burden_hcai/en/

Yasuyuki, M., Kunihiro, K., Kurissery, S., Kanavillil, N., Sato, Y., & Kikuchi, Y. (2010). Antibacterial properties of nine pure metals: A laboratory study using *Staphylococcus aureus* and *Escherichia coli*. *Biofouling*, 26(7), 851–858. <https://doi.org/10.1080/08927014.2010.527000>

Yoshida, Y., S. Furuta, and E. Niki. (1993), Effects of metal chelating agents on the oxidation of lipids induced by copper and iron. *Biochim. Biophys. Acta* 1210:81–88.

Appendix

Standard EPA Protocol

The EPA has recommended a standard protocol for the registration of hard non-porous copper containing surface products with non-food contact sanitizer claims. The test methodology for this protocol has been briefly summarized below:

- Test samples were cut into individual 1" x 1" square carriers and sample preparation was carried out as outlined in section 3.3.2
- Bacteria stains defined for this protocol are *Staphylococcus aureus* (ATCC 6538) and *Pseudomonas aeruginosa* (ATCC 15442). Bacteria cultures were prepared as outlined in section 3.3.3, using tryptic soy broth (TSB) as growth medium for both stains.
- Microbial test suspension was mixed with soil load. To obtain 500 µl of final test suspension, the following were combined:
 - 25 µl bovine serum albumin
 - 35 µl yeast extract stock
 - 100 µl mucin stock
 - 340 ul microbial test solution
- Final test suspension was then inoculated on the test surfaces (20 µl) and left for 60 minutes under ambient conditions.
- After contact time, the test surface was rinsed with PBS by placing the 1" x 1" test sample in a beaker containing 20 ml of PBS, then the beaker was placed in an ultrasonic bath for 5 minutes.

- Serial dilutions were prepared for each test sample rinse (10^1 to 10^4) and 100 μ l of each dilution were plated using appropriate agar plates.
- Agar plates were incubated for 24 hours for bacteria at 37°C.
- All colony growth observed on agar plate was counted after incubation (US EPA, 2016)

Table 6.0: Antimicrobial efficacy of samples against *E. coli* using EPA protocol

	Log Reduction				Killing Percentage (%)		
	Control	Sample A	Sample B	Copper	Sample A	Sample B	Copper
Replicate 1	0	0.130	0.033	4.732	25.925	7.407	100
Replicate 2	0	0	0	4.602	0	0	100
Replicate 3	0	0.204	0.425	4.903	37.5	62.5	100
Replicate 4	0	0.176	0.723	4.954	33.333	81.111	100
Replicate 5	0	0.087	0.087	5.041	18.182	18.182	100
Mean	0	0.119	0.254	4.847	22.988	33.840	100

Table 6.1: Antimicrobial efficacy of samples on *Pseudomonas aeruginosa* using EPA protocol

	Log Reduction				Killing Percentage		
	Control	Sample A	Sample B	Copper	Sample A	Sample B	Copper
Replicate 1	0	0.189	0.122	5.143	35.25	24.46	100
Replicate 2	0	0.051	0.051	4.954	11.11	11.11	100
Replicate 3	0	0.163	0.505	5.204	31.25	68.75	100
Replicate 4	0	0.109	0.255	4.954	22.22	44.44	100
Replicate 5	0	0.222	0.097	4.699	40	20	100
Mean	0	0.147	0.206	4.991	27.97	33.75	100

Table 6.2: Antimicrobial efficacy of samples on *E. coli* using Protocol 2

	Log Reduction				Killing Percentage (%)		
	Control	Sample A	Sample B	Copper	Sample A	Sample B	Copper
Replicate 1	0	0.091	0	4.568	18.919	0	100
Replicate 2	0	0	0	4.903	0	0	100
Replicate 3	0	0.079	0	4.778	16.667	0	100
Replicate 4	0	0.035	0.415	5.114	7.692	61.538	100
Replicate 5	0	0.125	0.301	4.602	25	50	100
Mean	0	0.066	0.143	4.793	13.656	22.307	100

Table 6.3: Antimicrobial efficacy of samples on *Pseudomonas aeruginosa* using Protocol 2

	Log Reduction				Killing Percentage		
	Control	Sample A	Sample B	Copper	Sample A	Sample B	Copper
Replicate 1	0	0.016	0.282	0.528	3.571	47.857	70.0

Replicate 2	0	0.1	0.007	0.219	20.635	1.587	39.683
Replicate 3	0	0.346	0.482	0.709	54.878	67.073	80.488
Replicate 4	0	0.097	0.076	0.076	20.0	16.0	16.0
Replicate 5	0	0.157	0.134	0.258	30.612	26.531	44.898
Mean	0	0.128	0.299	4.959	21.0	39.888	100

Table 6.4: Antimicrobial efficacy of samples on *E. coli* using Protocol 3

	Log Reduction				Killing Percentage (%)		
	Control	Sample A	Sample B	Copper	Sample A	Sample B	Copper
Replicate 1	0	0.095	0.239	0.362	19.565	42.391	56.522
Replicate 2	0	0	0	0.125	0	0	25
Replicate 3	0	0.117	0.385	0.452	23.529	58.823	64.706
Replicate 4	0	0	0.096	0.222	0	20	40
Replicate 5	0	0.029	0	0.029	6.667	0	6.667
Mean	0	0.048	0.144	0.238	9.952	24.243	38.579

Table 6.5: Antimicrobial efficacy of samples on *Pseudomonas aeruginosa* using Protocol 3

	Log Reduction				Killing Percentage		
	Control	Sample A	Sample B	Copper	Sample A	Sample B	Copper
Replicate 1	0	0.016	0.283	0.523	3.571	47.857	70.0
Replicate 2	0	0.10	0.007	0.219	20.635	1.587	39.683
Replicate 3	0	0.346	0.482	0.709	54.878	67.073	80.487
Replicate 4	0	0.097	0.076	0.076	20.0	16.0	16.0
Replicate 5	0	0.159	0.134	0.259	30.612	26.531	44.898
Mean	0	0.143	0.196	0.357	25.939	31.809	50.214

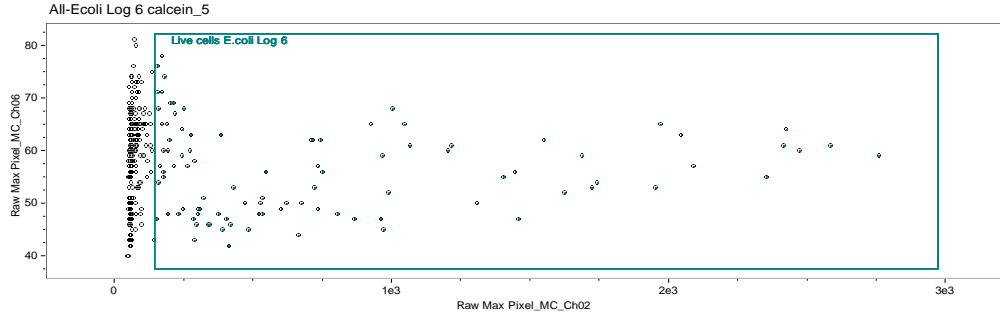
Table 6.6: Antimicrobial efficacy of samples on *E. coli* using Protocol 4

	Log Reduction				Killing Percentage (%)		
	Control	Sample A	Sample B	Copper	Sample A	Sample B	Copper
Replicate 1	0	0.047	0.269	4.892	10.256	46.154	100
Replicate 2	0	0.083	0.106	4.361	17.391	21.739	100
Replicate 3	0	0.105	0.146	4.146	21.429	28.571	100
Replicate 4	0	0.368	0.669	4.623	57.142	78.571	100
Replicate 5	0	0.073	0.073	4.114	15.385	15.385	100
Mean	0	0.135	0.253	4.427	24.321	38.084	100

Table 6.7: Antimicrobial efficacy of samples on *Pseudomonas aeruginosa* using Protocol 4

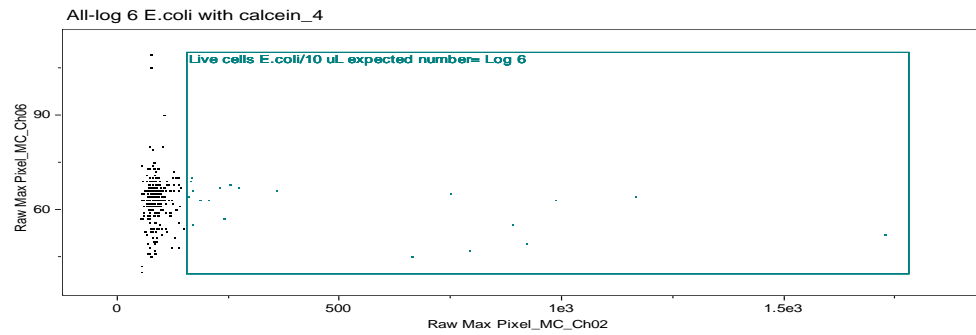
	Log Reduction				Killing Percentage		
	Control	Sample A	Sample B	Copper	Sample A	Sample B	Copper
Replicate 1	0	0.176	0.234	5.255	33.333	41.667	100
Replicate 2	0	0.236	0.412	4.491	41.935	61.29	100

Replicate 3	0	0.462	0.684	4.462	65.517	79.31	100
Replicate 4	0	0.33	0.485	5.029	53.271	67.289	100
Replicate 5	0	0.222	0	4.176	40.0	0	100
Mean	0	0.285	0.363	4.683	46.811	49.911	100



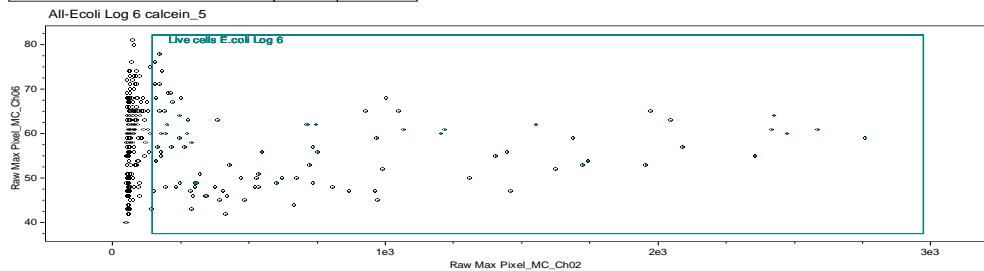
Raw Max Pixel_MC_Ch02, Raw Max Pixel_MC_Ch06

Population	Count	%Gated
All	315	100
Live cells E.coli Log 6	96	30.5



Raw Max Pixel_MC_Ch02, Raw Max Pixel_MC_Ch06

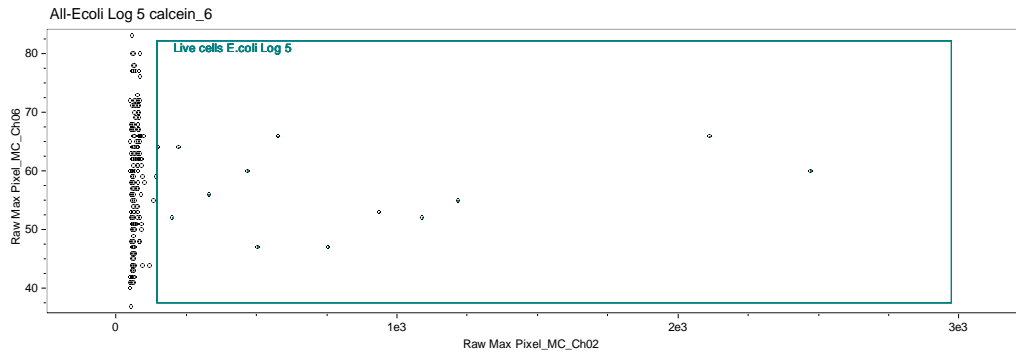
Population	Count	%Gated
All	307	100
Live cells E.coli/10 uL exp...	20	6.51



Raw Max Pixel_MC_Ch02, Raw Max Pixel_MC_Ch06

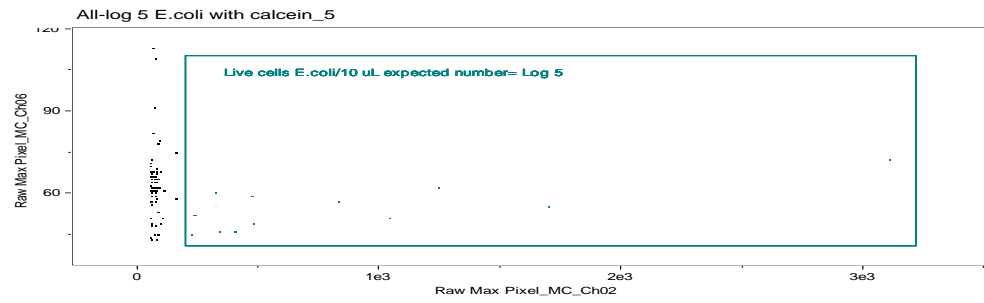
Population	Count	%Gated
All	315	100
Live cells E.coli Log 6	96	30.5

Figure 6.0: FCM results of Log 6 *E. coli* stained with calcein AM



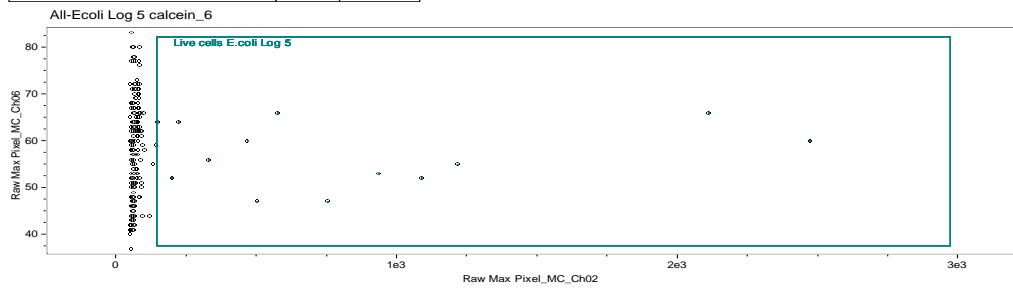
Raw Max Pixel_MC_Ch02, Raw Max Pixel_MC_Ch06

Population	Count	%Gated
All	222	100
Live cells E.coli Log 5	13	5.86



Raw Max Pixel_MC_Ch02, Raw Max Pixel_MC_Ch06

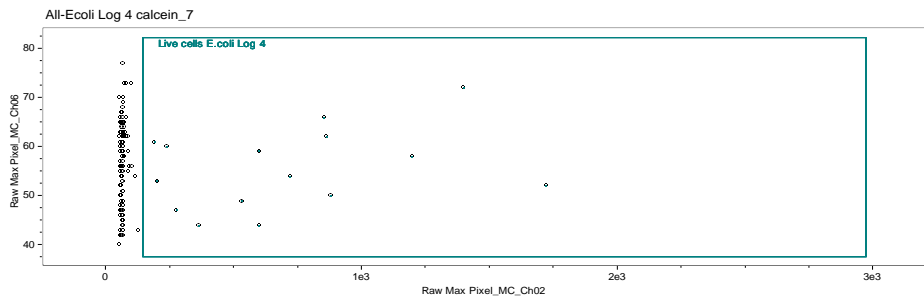
Population	Count	%Gated
All	83	100
Live cells E.coli/10 uL exp...	13	15.7



Raw Max Pixel_MC_Ch02, Raw Max Pixel_MC_Ch06

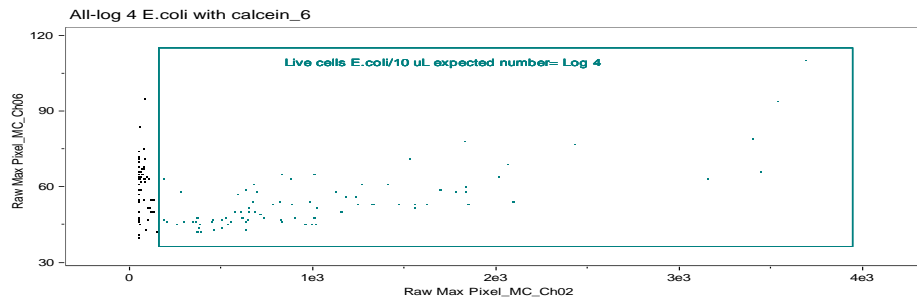
Population	Count	%Gated
All	222	100
Live cells E.coli Log 5	13	5.86

Figure 6.1: FCM results of Log 5 *E. coli* stained with calcein AM



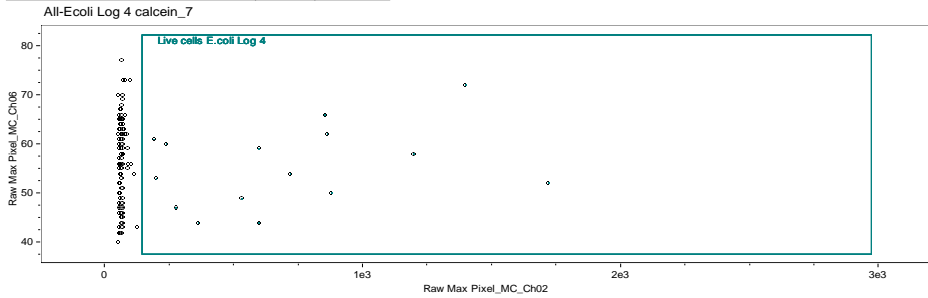
Raw Max Pixel_MC_Ch02, Raw Max Pixel_MC_Ch06

Population	Count	%Gated
All	148	100
Live cells E.coli Log 4	15	10.1



Raw Max Pixel_MC_Ch02, Raw Max Pixel_MC_Ch06

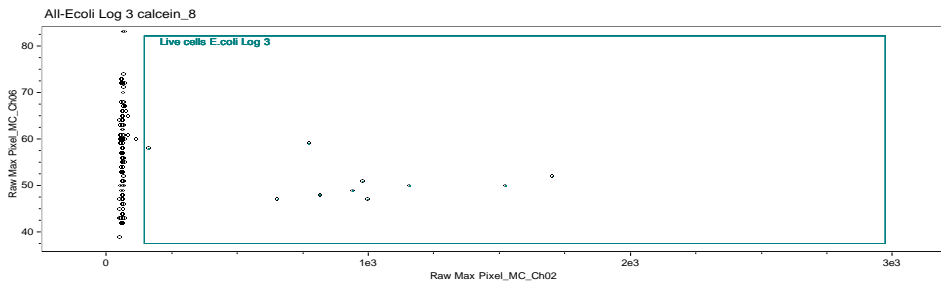
Population	Count	%Gated
All	143	100
Live cells E.coli/10 uL exp...	83	58



Raw Max Pixel_MC_Ch02, Raw Max Pixel_MC_Ch06

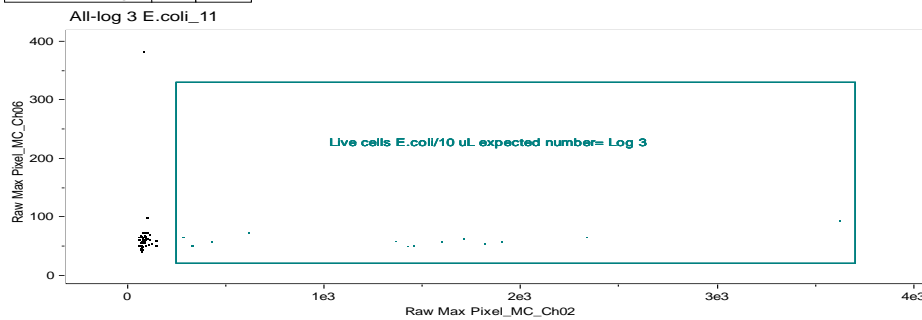
Population	Count	%Gated
All	148	100
Live cells E.coli Log 4	15	10.1

Figure 6.2: FCM results of Log 4 *E. coli* stained with calcein AM



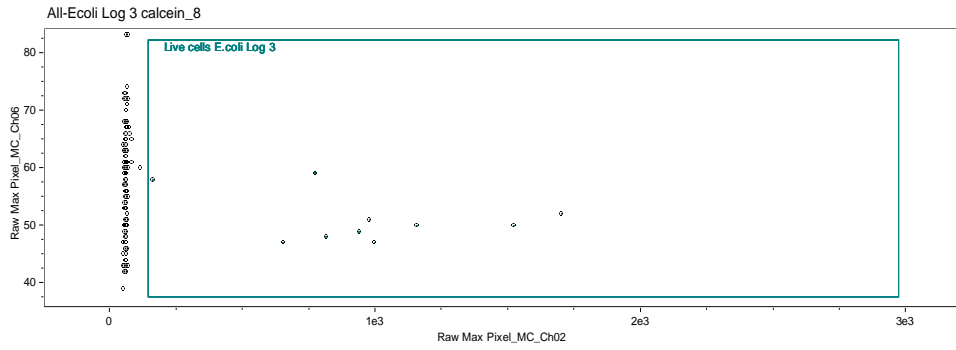
Raw Max Pixel_MC_Ch02, Raw Max Pixel_MC_Ch06

Population	Count	%Gated
All	151	100
Live cells E.coli Log 3	10	6.62



Raw Max Pixel_MC_Ch02, Raw Max Pixel_MC_Ch06

Population	Count	%Gated
All	72	100
Live cells E.coli/10 uL exp...	13	18.1



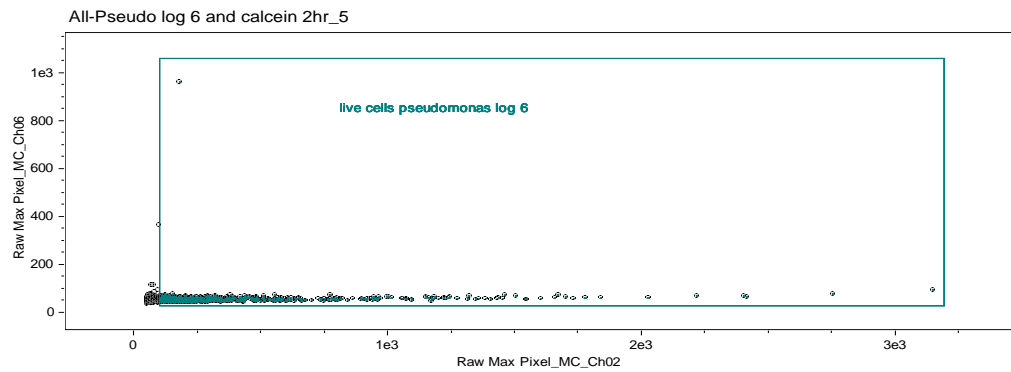
Raw Max Pixel_MC_Ch02, Raw Max Pixel_MC_Ch06

Population	Count	%Gated
All	151	100
Live cells E.coli Log 3	10	6.62

Figure 6.3: FCM results of Log 3 *E. coli* stained with calcein AM

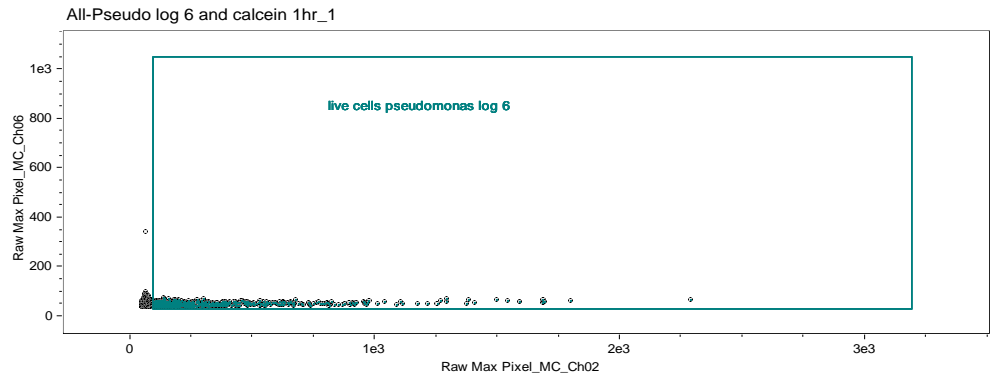
Table 6.8: Comparison between Plate count and Flow cytometry results of *E. coli* stained with calcein AM

Expected number (CFU/mL)	Log of flow cytometry number			Log plate count number		
	Replicate 1	Replicate 2	Replicate 3	Replicate 1	Replicate 2	Replicate 3
10 ⁶	5.34	3.30	3.98	5.99	5.90	5.79
10 ⁵	4.51	3.11	3.11	4.99	4.90	4.60
10 ⁴	4.06	3.92	3.18	3.99	3.83	3.87
10 ³	3.15	3.11	3.0	3.37	2.97	3.17



Raw Max Pixel_MC_Ch02, Raw Max Pixel_MC_Ch06

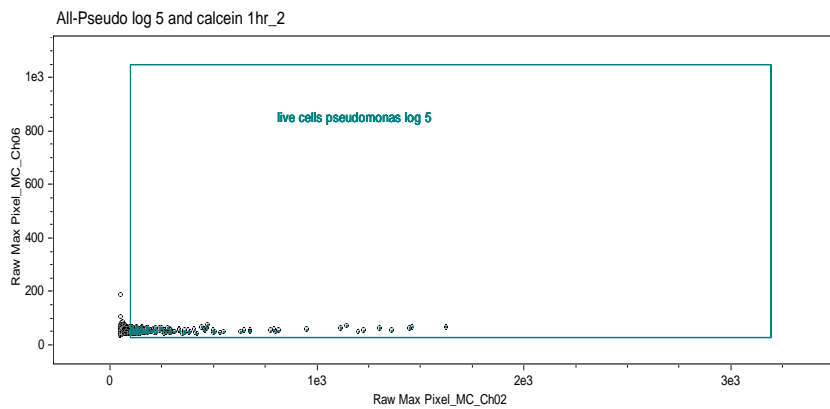
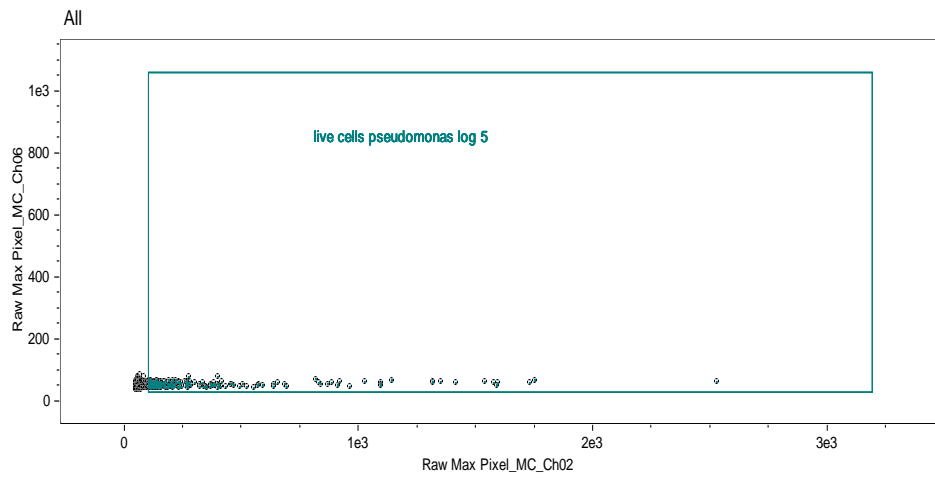
Population	Count	%Gated
All	2924	100
live cells pseudomonas log 6	1758	60.1



Raw Max Pixel_MC_Ch02, Raw Max Pixel_MC_Ch06

Population	Count	%Gated
All	1616	100
live cells pseudomonas log 6	879	54.4

Figure 6.4: FCM results of Log 6 *P. aeruginosa* stained with calcein AM

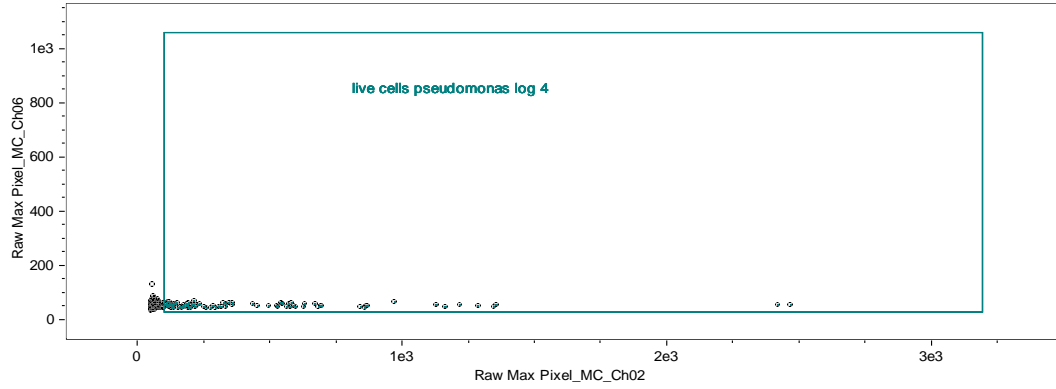


Raw Max Pixel_MC_Ch02, Raw Max Pixel_MC_Ch06

Population	Count	%Gated
All	901	100
live cells pseudomonas log 5	148	16.4

Figure 6.5: FCM results of Log 5 *P. aeruginosa* stained with calcein AM

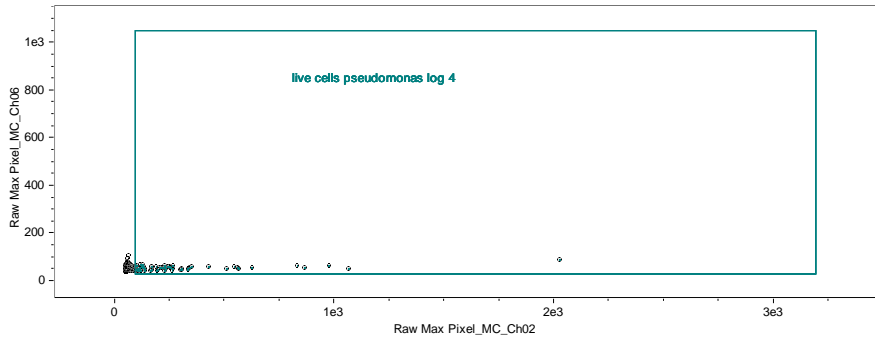
All-Pseudo log 4 and calcein 2hr_7



Raw Max Pixel_MC_Ch02, Raw Max Pixel_MC_Ch06

Population	Count	%Gated
All	669	100
live cells pseudomonas log 4	93	13.9

All-Pseudo log 4 and calcein 1hr_3

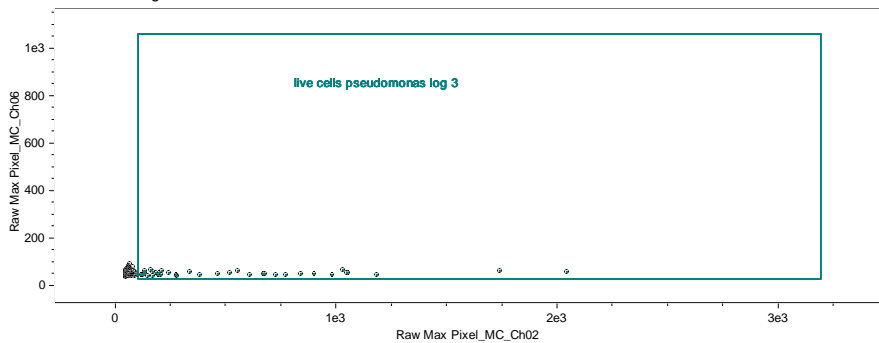


Raw Max Pixel_MC_Ch02, Raw Max Pixel_MC_Ch06

Population	Count	%Gated
All	671	100
live cells pseudomonas log 4	57	8.49

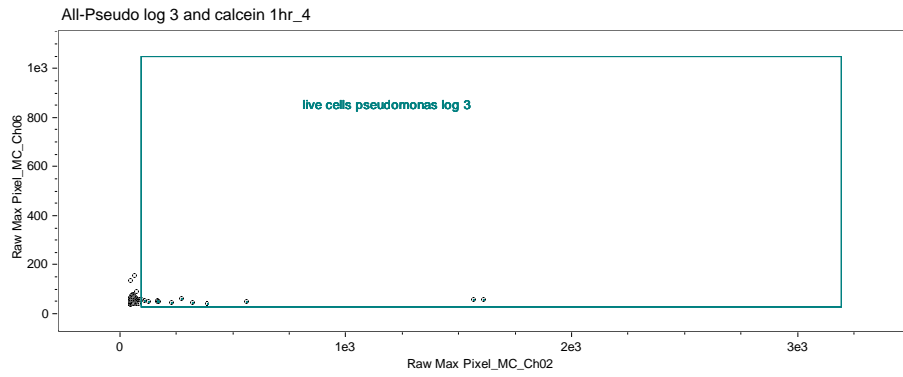
Figure 6.6: FCM results of Log 4 *P. aeruginosa* stained with calcein AM

All-Pseudo log 3 and calcein 2hr_8



Raw Max Pixel_MC_Ch02, Raw Max Pixel_MC_Ch06

Population	Count	%Gated
All	509	100
live cells pseudomonas log 3	36	7.07



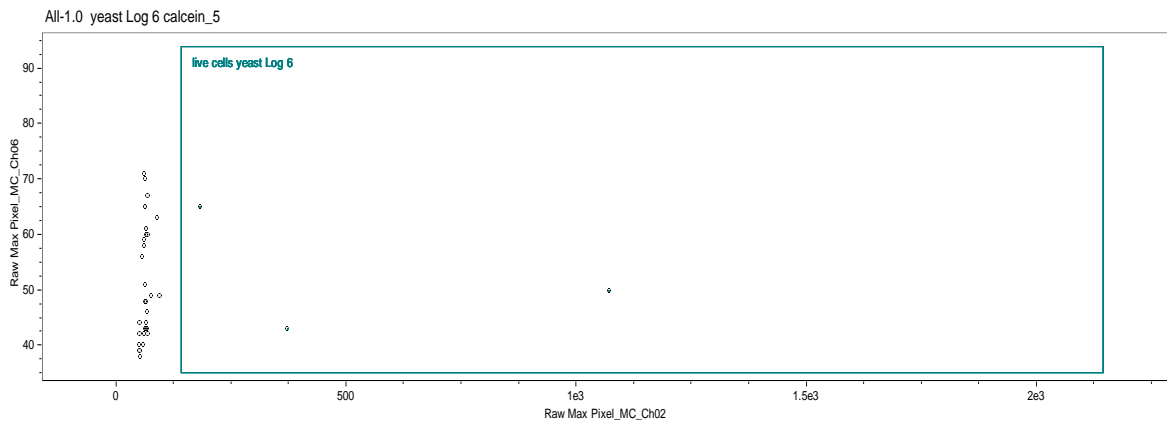
Raw Max Pixel_MC_Ch02, Raw Max Pixel_MC_Ch06

Population	Count	%Gated
All	561	100
live cells pseudomonas log 3	12	2.14

Figure 6.7: FCM results of Log 3 *P. aeruginosa* stained with calcein AM

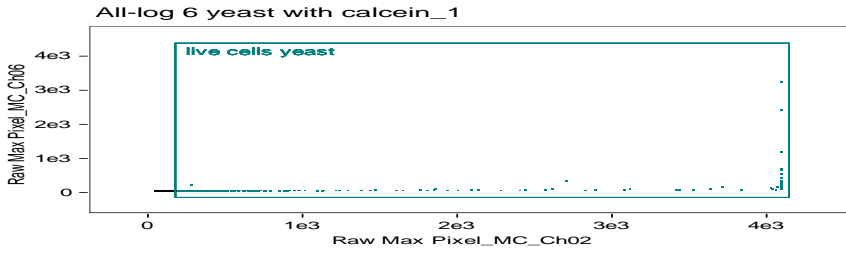
Table 6.9: Comparison between Plate count and Flow cytometry results of *P. aeruginosa* stained with calcein AM

Expected number (CFU/ml)	Log of flow cytometric number		Log plate count number	
	Replicate 1	Replicate 2	Replicate 1	Replicate 2
10 ⁶	5.25	4.94	6.27	6.14
10 ⁵	4.34	4.17	5.27	5.14
10 ⁴	3.97	3.76	4.26	4.09
10 ³	3.56	3.08	3.28	3.19



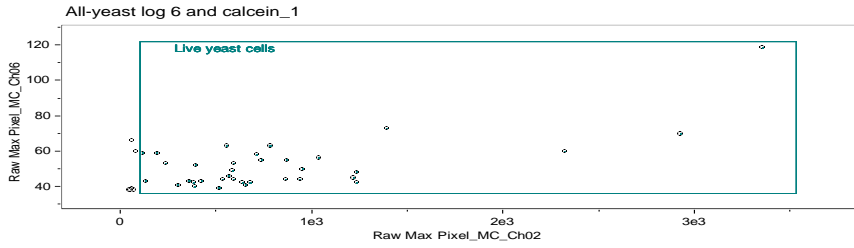
Raw Max Pixel_MC_Ch02, Raw Max Pixel_MC_Ch06

Population	Count	%Gated
All	36	100
live cells yeast Log 6	3	8.33



Raw Max Pixel_MC_Ch02, Raw Max Pixel_MC_Ch06

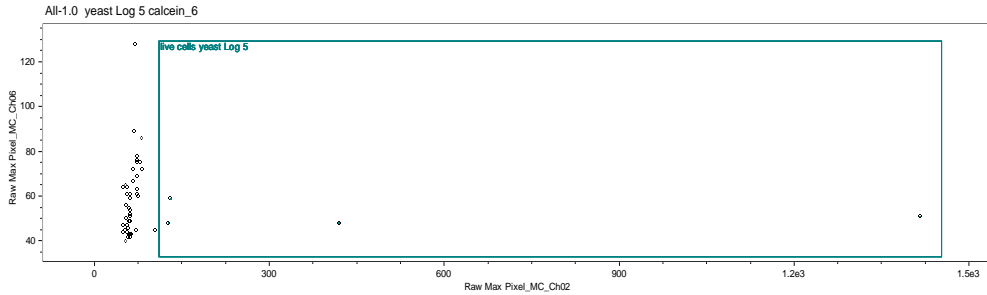
Population	Count	%Gated
All	10093	100
live cells yeast per 10 uL ...	724	7.17



Raw Max Pixel_MC_Ch02, Raw Max Pixel_MC_Ch06

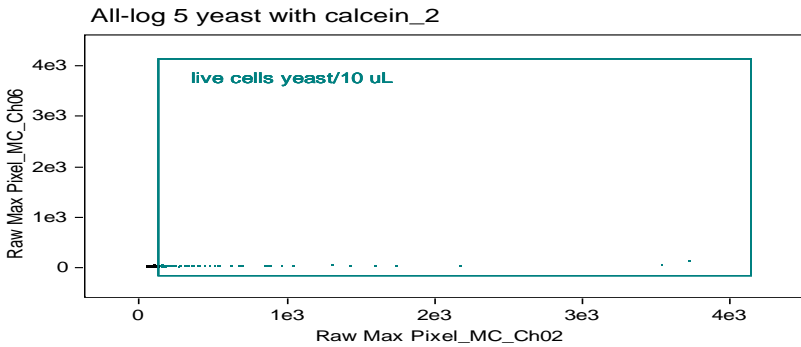
Population	Count	%Gated
All	41	100
Live yeast cells	35	85.4

Figure 6.8: FCM results of Log 6 yeast stained with calcein AM



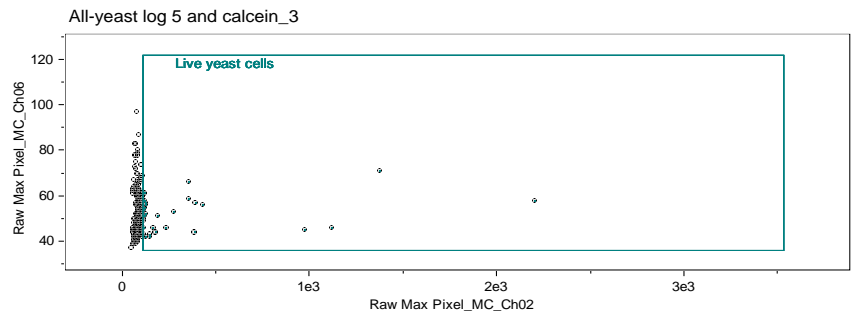
Raw Max Pixel_MC_Ch02, Raw Max Pixel_MC_Ch06

Population	Count	%Gated
All	48	100
live cells yeast Log 5	4	8.33



Raw Max Pixel_MC_Ch02, Raw Max Pixel_MC_Ch06

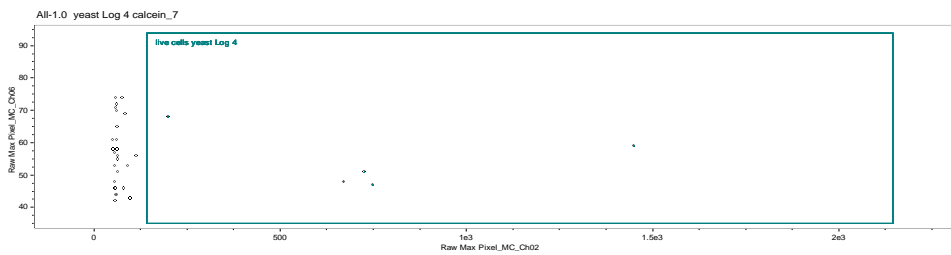
Population	Count	%Gated
All	1950	100
live cells yeast/10 uL expe...	54	2.77



Raw Max Pixel_MC_Ch02, Raw Max Pixel_MC_Ch06

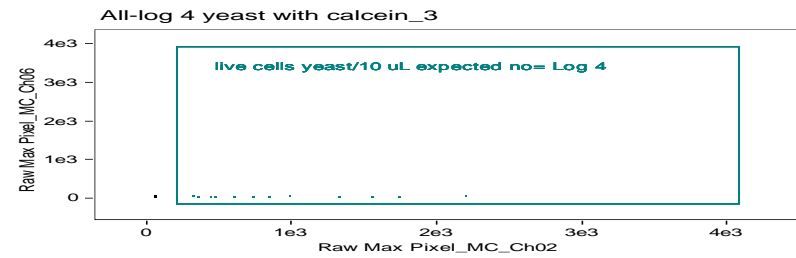
Population	Count	%Gated
All	377	100
Live yeast cells	27	7.16

Figure 6.9: FCM results of Log 5 yeast stained with calcein AM



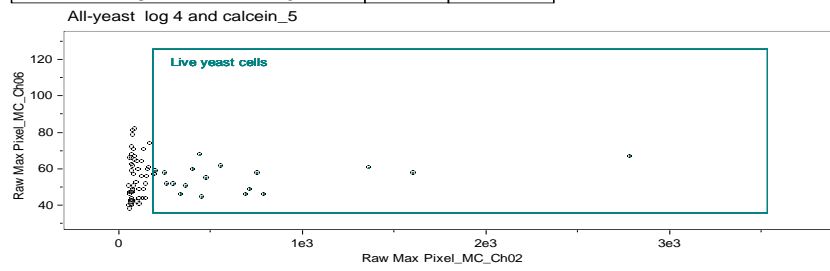
Raw Max Pixel_MC_Ch02, Raw Max Pixel_MC_Ch06

Population	Count	%Gated
All	32	100
live cells yeast Log 4	5	15.6



Raw Max Pixel_MC_Ch02, Raw Max Pixel_MC_Ch06

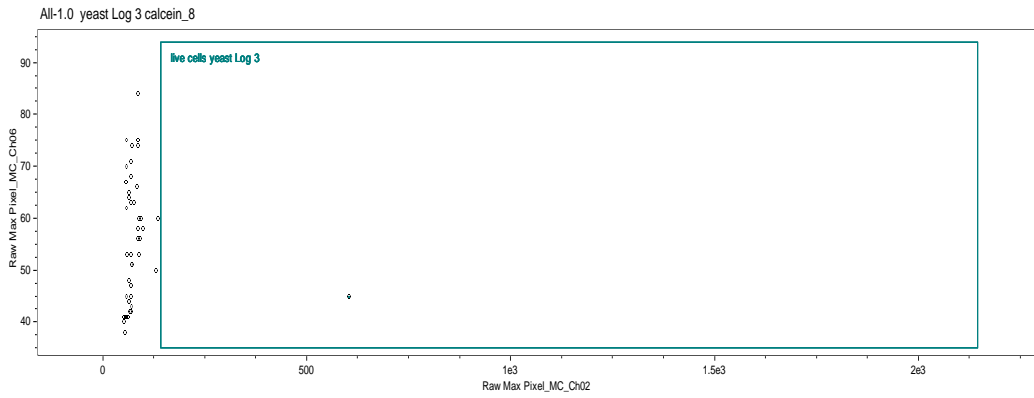
Population	Count	%Gated
All	16	100
live cells yeast/10 uL expe...	13	81.2



Raw Max Pixel_MC_Ch02, Raw Max Pixel_MC_Ch06

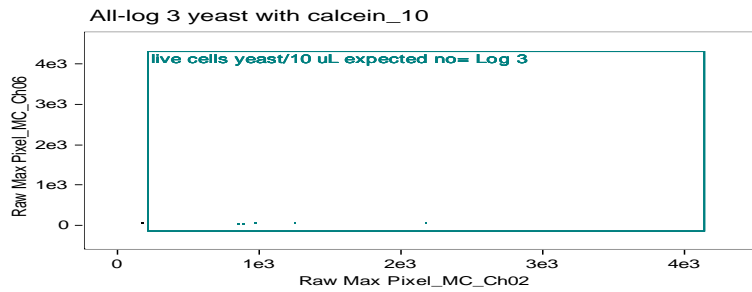
Population	Count	%Gated
All	76	100
Live yeast cells	19	25

Figure 6.10: FCM results of Log 4 yeast stained with calcein AM



Raw Max Pixel_MC_Ch02, Raw Max Pixel_MC_Ch06

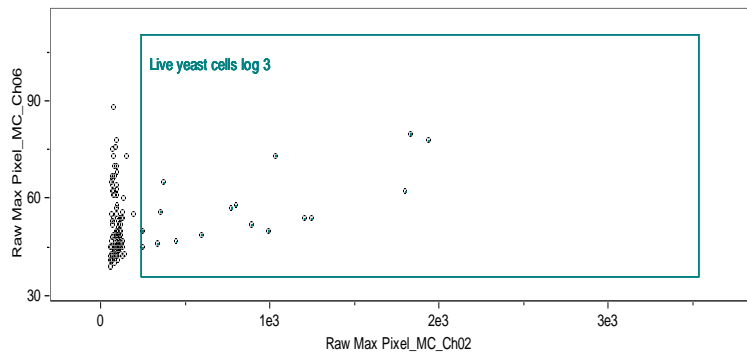
Population	Count	%Gated
All	44	100
live cells yeast Log 3	1	2.27



Raw Max Pixel_MC_Ch02, Raw Max Pixel_MC_Ch06

Population	Count	%Gated
All	6	100
live cells yeast/10 uL expe...	5	83.3

All-yeast log 3 and calcein_6



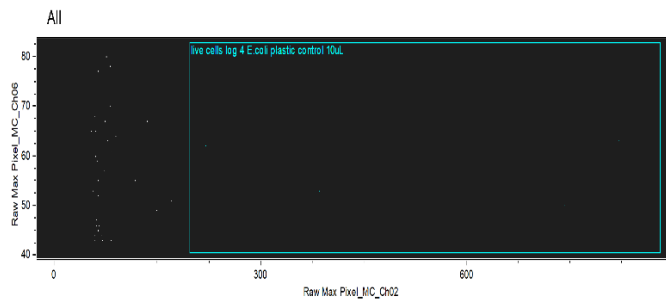
Raw Max Pixel_MC_Ch02, Raw Max Pixel_MC_Ch06

Population	Count	%Gated
All	130	100
Live yeast cells log 3	17	13.1

Figure 6.11: FCM results of Log 3 yeast stained with calcein AM

Table 6.10: Comparison between Plate count and Flow cytometry results of yeast stained with calcein AM

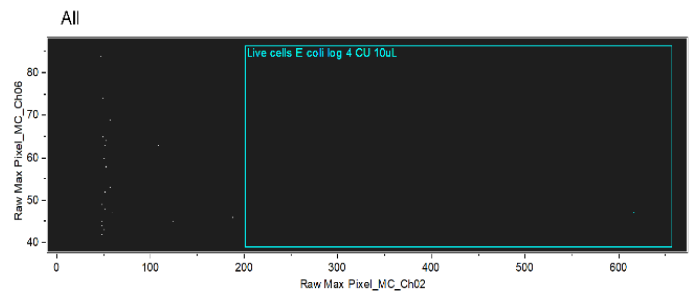
Expected number (CFU/ml)	Log of flow cytometry number			Log plate count number		
	Replicate 1	Replicate 2	Replicate 3	Replicate 1	Replicate 2	Replicate 3
10 ⁶	2.48	4.86	3.54	4.45	4.04	4.12
10 ⁵	2.60	3.73	3.43	3.60	3.04	3.45
10 ⁴	2.69	3.11	3.28	2.60	2.04	2.54
10 ³	2	2.69	3.23	1.65	1.04	1.32



Raw Max Pixel_MC_Ch02, Raw Max Pixel_MC_Ch06

Population	Count	%Gated
All	35	100
live cells log 4 E.coli pla...	4	11.4

(a)

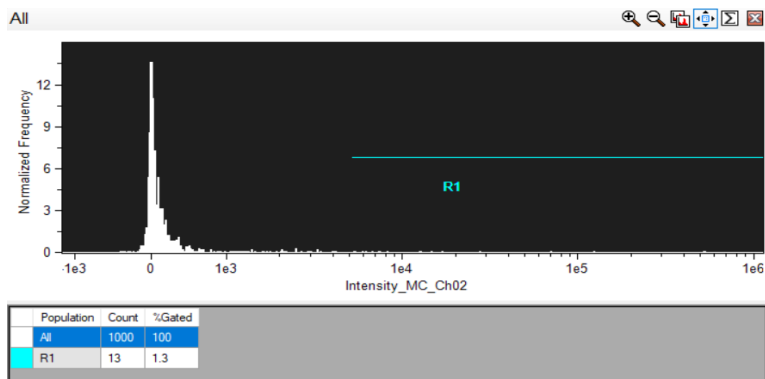


Raw Max Pixel_MC_Ch02, Raw Max Pixel_MC_Ch06

Population	Count	%Gated
All	21	100
Live cells E.coli log 4 CU ...	1	4.76

(b)

Figure 6.12: (a) FCM results of Log 4 *E. coli* applied on plastic control and stained with calcein AM
 (b) FCM results of Log 4 *E. coli* applied on copper surface and stained with calcein AM



Population	Count	%Gated
All	1000	100
R1	13	1.3

Figure 6.13: Intensity plot of Log 4 *E. coli* applied on copper surface for 5 minutes and stained with Calcein AM

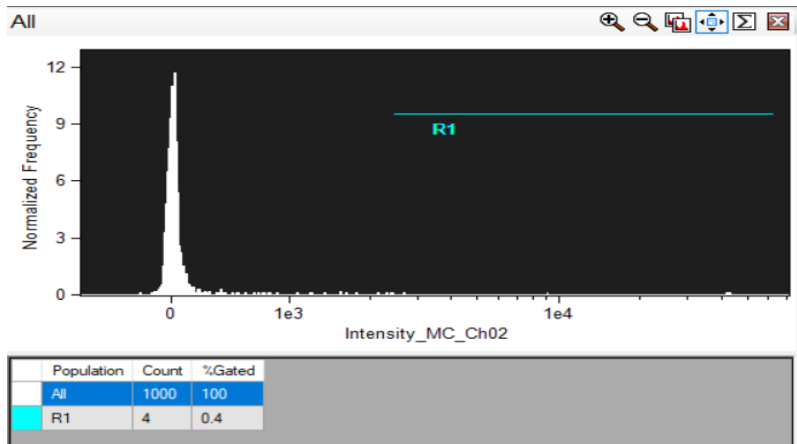
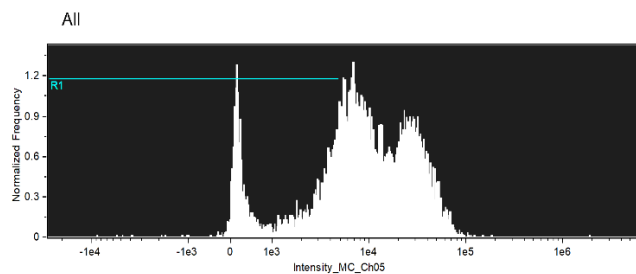
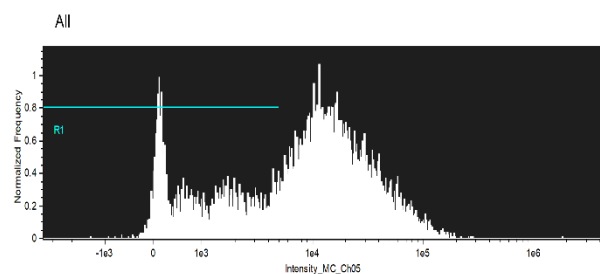


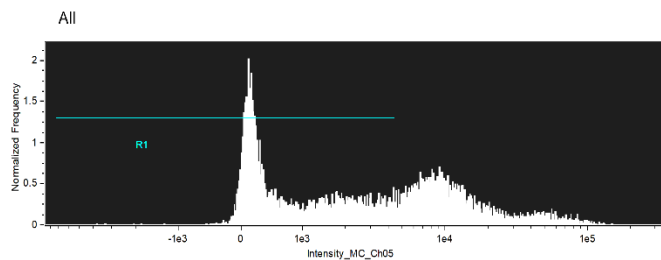
Figure 6.14: Intensity plot of Log 4 *E. coli* applied on copper surface for 120 minutes and stained with Calcein AM



Population	Count	%Gated
All	10000	100
R1	2936	29.4

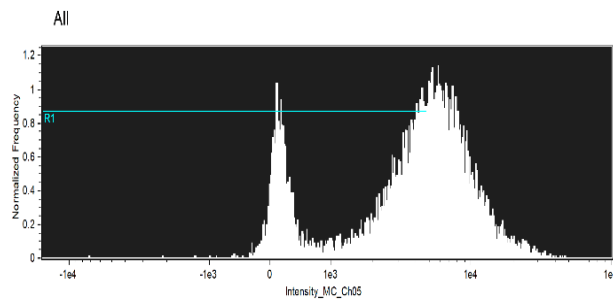


Population	Count	%Gated
All	10000	100
R1	3371	33.7



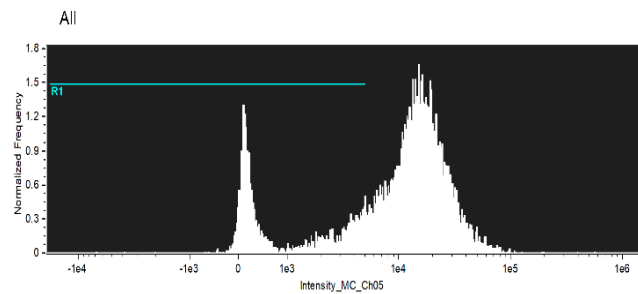
Population	Count	%Gated
All	10000	100
R1	5787	57.9

Figure 6.15: FCM results of yeast on Cu surface after 10 minutes, stained with propidium iodide



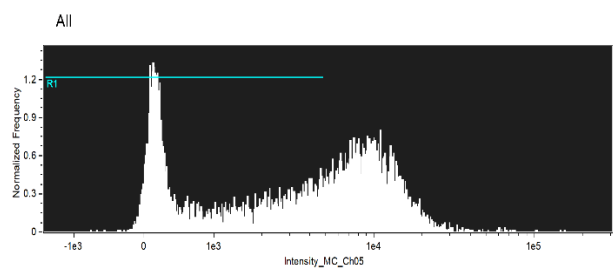
Intensity_MC_Ch05

Population	Count	%Gated
All	10000	100
R1	5271	52.7



Intensity_MC_Ch05

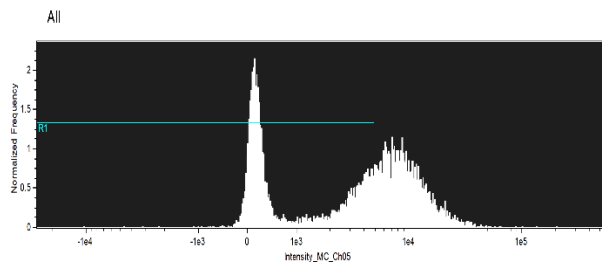
Population	Count	%Gated
All	10000	100
R1	2507	25.1



Intensity_MC_Ch05

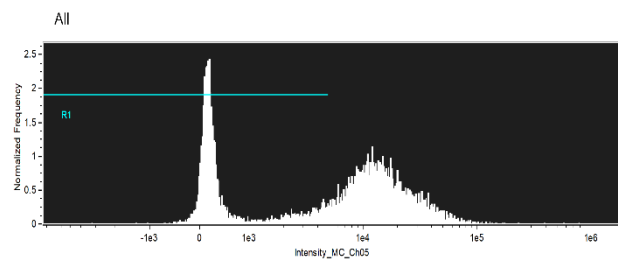
Population	Count	%Gated
All	10000	100
R1	5351	53.5

Figure 6.16: FCM results of yeast on Cu surface after 30 minutes, stained with propidium iodide



Intensity_MC_Ch05

Population	Count	%Gated
All	10000	100
R1	5323	53.2



Intensity_MC_Ch05

Population	Count	%Gated
All	10000	100
R1	4203	42

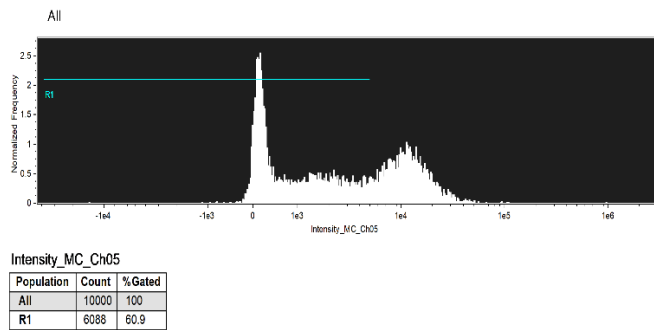


Figure 6.17: FCM results of yeast on Cu surface after 60 minutes, stained with propidium iodide

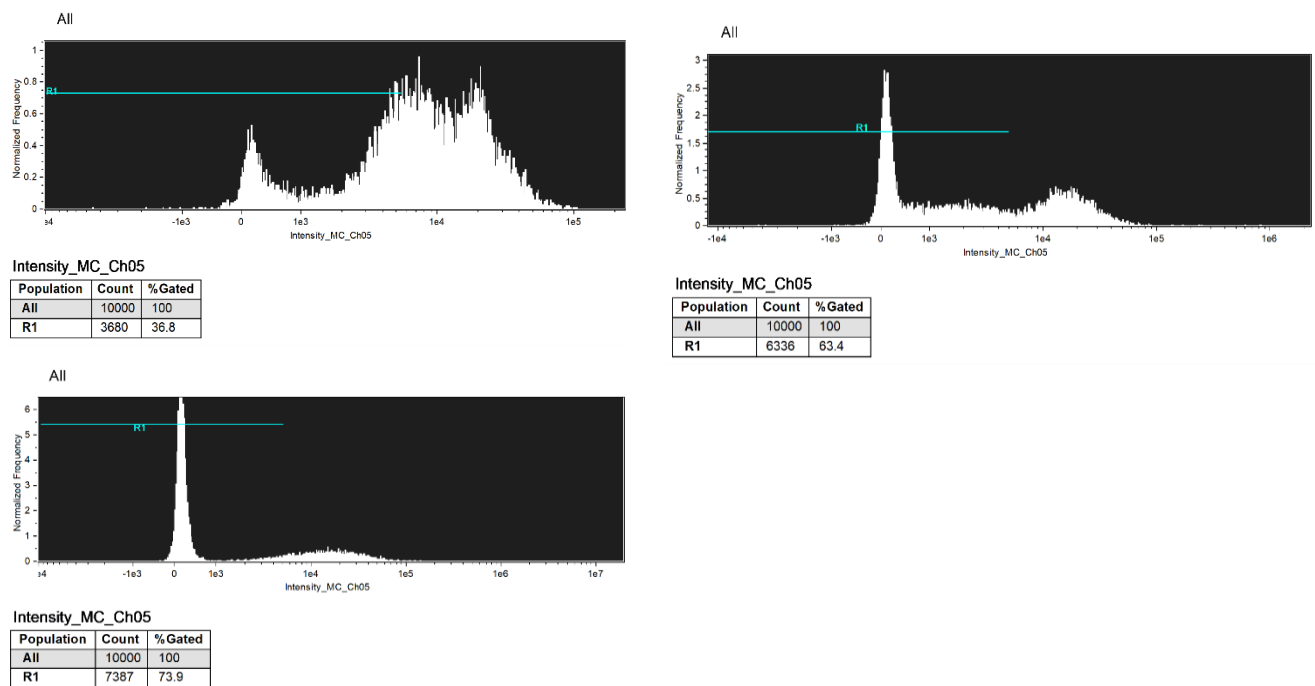
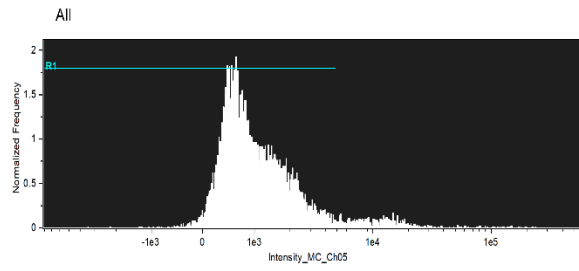


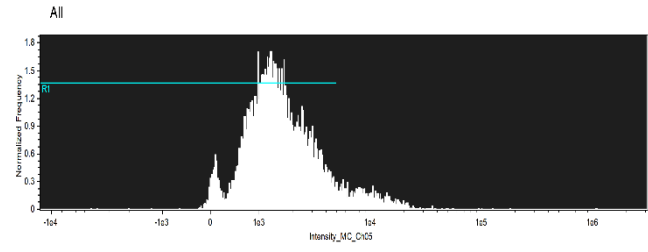
Figure 6.18: FCM results of yeast on Cu surface after 120 minutes, stained with propidium iodide



Intensity_MC_Ch05

Population	Count	%Gated
All	10000	100
R1	9374	93.7

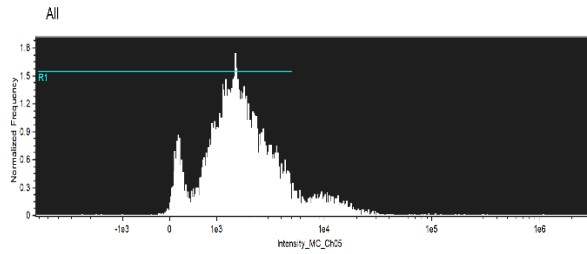
a



Intensity_MC_Ch05

Population	Count	%Gated
All	10000	100
R1	9024	90.2

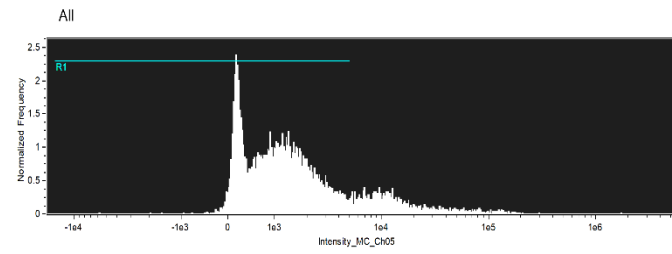
b



Intensity_MC_Ch05

Population	Count	%Gated
All	10000	100
R1	8996	89

c

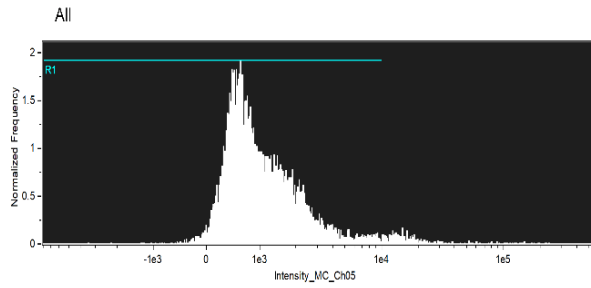


Intensity_MC_Ch05

Population	Count	%Gated
All	10000	100
R1	8226	82.3

d

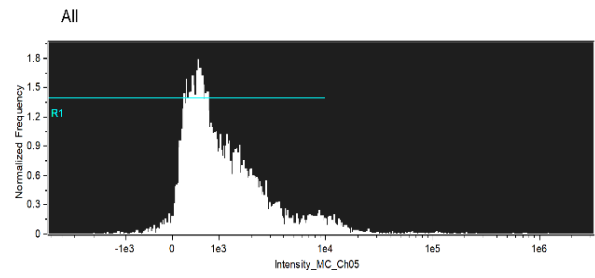
Figure 6.19: FCM results of yeast on Control after (a=120 minutes, b= 10 minutes, c= 30 minutes d= 60minutes) stained with propidium iodide



Intensity_MC_Ch05

Population	Count	%Gated
All	10000	100
R1	9646	96.5

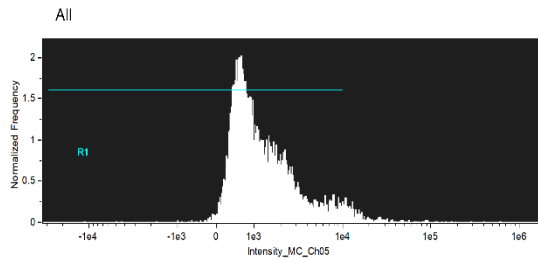
a



Intensity_MC_Ch05

Population	Count	%Gated
All	10000	100
R1	9606	96.1

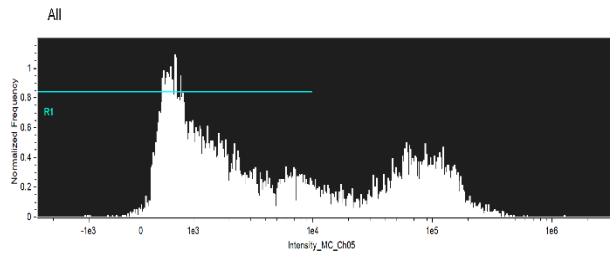
b



Intensity_MC_Ch05

Population	Count	%Gated
All	10000	100
R1	9546	95.5

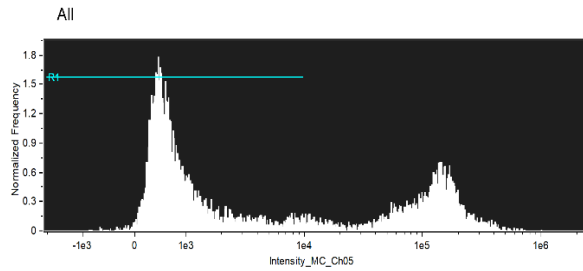
c



Intensity_MC_Ch05

Population	Count	%Gated
All	10000	100
R1	6455	64.6

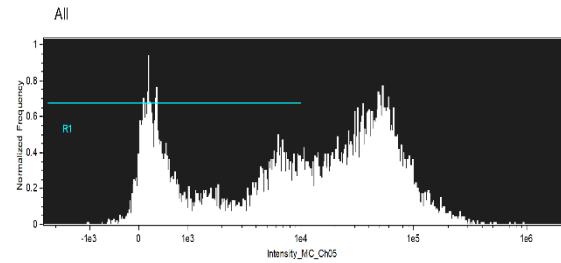
d



Intensity_MC_Ch05

Population	Count	%Gated
All	10000	100
R1	6371	63.7

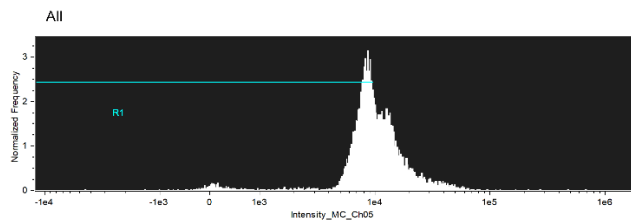
e



Intensity_MC_Ch05

Population	Count	%Gated
All	10000	100
R1	4572	45.7

f



Intensity_MC_Ch05

Population	Count	%Gated
All	10000	100
R1	5139	51.4

g

Figure 6.20: FCM results of yeast applied on surfaces for 2 hours then stained with propidium iodide (a=control, b= A1-sample, c= B1-sample d= F1-sample, e= G1-sample, f= X-sample, g= Z-sample)